Flinders UNIVERSITY
ADELAIDE · SOUTH AUSTRALIA

Patient and Surgical Variability in the Primary Stability of Cementless Acetabular Cups for Computational Pre-Clinical Testing

by

Dermot Hugh O'Rourke

Thesis
Submitted to Flinders University
for the degree of

Doctor of Philosophy

College of Science and Engineering

August 2017

Table of Contents

Abstract

The challenge in developing new acetabular cups is assessing their likely performance in a diverse population prior to clinical trials. Finite Element (FE) modelling has been used to evaluate prostheses for over 40 years but the majority of studies do not fully consider the high levels of variation among patients and during surgery. The aim of the research presented in this thesis was twofold: 1) explore the influence of patient and surgical variability in the primary stability of a cementless acetabular cup using Finite Element (FE) models of the hemipelvis and 2) develop time efficient methods to examine this variability in order to incorporate it into pre-clinical testing.

To allow a large number of models to be simulated in this work, a software pipeline with automated processes was developed to generate FE models of the implanted hemipelvis, simulate cup insertion and gait cycle loading, and post-process primary stability output metrics. The influence of patient variability on primary stability was explored with a cohort of 103 patient-specific models. Comparisons between quartile groups of patient-related factors suggested gaps between the cup and bone were larger in subjects with small acetabular diameters and depth. Meanwhile, there was evidence of higher micromotion during gait in higher bodyweight and lower bone quality quartile groups. The variability in primary stability in the cohort could be reasonably approximated with subsets of subjects that were sampled based on the extremes of patient-related factors.

To reduce the time cost of quantifying FE model sensitivity, a surrogate modelling approach was developed and illustrated with a model of the intact hemipelvis. There was a significant time and computational saving associated with a Kriging surrogate model which accurately predicted all strain output metrics based on a training set of 30 simulations. To explore the influence of surgical variability and determine influential parameters on the primary stability, the surrogate modelling approach was used with a Latin Hypercube Design on two implanted

hemipelvis models. Regression analyses indicated interference fit was the most dominant parameter in both subjects. Taken together, the elements in this thesis form the foundations for the development of a computational tool that accounts for patient and surgical variability to help provide more thorough evaluations of new cementless cups during the development phase.

Declaration

I certify that this thesis does not incorporate without acknowledgment any material previously submitted for a degree or diploma in any university; and that to the best of my knowledge and belief it does not contain any material previously published or written by another person except where due reference is made in the text.

Signed.....

Date

Acknowledgements

Undertaking this thesis so far from home has been an incredible challenge that I would not have been able to overcome without the support of many people. Firstly, I would like thank my supervisors Prof. Mark Taylor and Assoc. Prof. Murk Bottema for their guidance throughout my candidature. To Murk, thank you for always having your door open to me and for your practical advice, particularly on mathematics topics, which I found invaluable. To Mark, since the first day I (never) arrived into Adelaide, your enthusiasm, patience, and seemingly endless knowledge has inspired me to achieve my best. I have learnt a tremendous amount as your student. Thank you to Saulo for coaching me through my first journal article, to Egon for his advice on being an independent researcher, and to all staff in MDRI and Flinders University for their assistance. In particular, I would like thank Kathy Brady who not only employed me in the SLC but has nurtured me and given me great encouragement along the way. Thank you to the squad at MDRI, including Dhara, Bryant, Rami, Albert, Rowan, Mark, Laura, Maged, and Sami for making every day at Tonsley hugely enjoyable. I am also very grateful to Shane and my friends from CrossFit for all the great times I've shared with them away from my studies. A very special thank you to Megan who has lived the thesis as much as I have this past while. Above everyone, you have been the most supportive, caring, and understanding person throughout this process. Thank you for assuring me I had the grit to see this through when I needed it most. Finally, my biggest thank you goes to Mum, Dad, and Conor for all their love and support, not just in this, but in everything I do. This is for you.

List of Publications

PEER-REVIEWED JOURNAL ARTICLES

O'Rourke, D., Martelli, S., Bottema, M., and Taylor, M., 2016, *A Computational Efficient Method to Assess the Sensitivity of Finite-Element Models: An Illustration with the Hemipelvis* Journal of Biomechanical Engineering, 138(12).

O'Rourke, D., Al-Dirini, R., and Taylor, M., 2017, *Primary stability of a cementless acetabular cup in a cohort of patient-specific finite element models* Journal of Orthopaedic Research, In press.

CONFERENCE ABSTRACTS

O'Rourke D, Al-Dirini R, Taylor M *Patient and Surgical Variability in the Primary Stability of Cementless Acetabular Cups: Towards Virtual Clinical Trials* XVI International Symposium on Computer Simulation in Biomechanics, July 20 – 22, 2017, Gold Coast, Australia

O'Rourke D, Al-Dirini R, Taylor M *Determining the effect of lateral protrusion on the primary fixation of cementless acetabular cups using Finite Element methods* ISTA Congress, October 5 – 8, 2016, Boston, USA

O'Rourke D, Al-Dirini R, Taylor M *Sampling Methods for Describing Patient Variability in FE Based Studies of Acetabular Cup Fixation* 22nd Congress of European Society of Biomechanics July 10 – 13 2016, Lyon, France

O'Rourke D, Bottema M, Taylor M *Influence of Patient Variability in the Primary Stability of Cementless Acetabular Cups after Total Hip Replacement* ORS Meeting 2016, March 5 – 8 2016, Orlando, Florida

O'Rourke D, Bottema M, Taylor M *Finite Element Analysis of Press-fit Acetabular Cup Insertion* 21st Congress of European Society of Biomechanics July 5 – 8 2015, Prague, Czech Republic

O'Rourke D, Bottema M Taylor *A design of experiments approach to conducting sensitivity analyses in finite element modelling* 22nd Annual Symposium on Computational Methods in Orthopaedic Biomechanics March 14 2014, New Orleans, Louisiana

List of Figures

List of Tables

Chapter 1

Introduction

1.1 Motivation

Total hip arthroplasty is considered an effective intervention for severe osteoarthritis, reducing pain and restoring some patients to near full function (OECD, 2015). Recent data from national joint registries show that, from 2007 to 2014, procedures increased by approximately 4.0% in the UK and 4.9% in Australia year on year. Meanwhile, the rate of revision surgery remained at approximately 11% in the same period (Australian Orthopaedic Association, National Joint Replacement Registry, 2016; National Joint Registry for England and Wales, 2015). Future projections suggest the demand for hip arthroplasties will continue to climb (Culliford et al., 2015) and, based on current rates, there will be a corresponding increase in the number of required revisions.

Despite the advancements in prosthesis design and surgical technique, the acetabular cup is still considered as the weak link in total hip arthroplasty by some authors (Corten et al., 2009; Sakellariou and Sculco, 2013). The Australian Joint Registry report that revision of the acetabular component is common, with 32.7% of revisions between 1999 to 2014 involving the cup (Australian Orthopaedic Association, National Joint Replacement Registry, 2016). Meanwhile, the Canadian Joint Replacement Registry reported that acetabular components

were replaced in 56.7% of revision procedures between 2012 and 2013 (Canadian Joint Replacement Registry, 2015). It has also been reported acetabular components have higher revision rates than femoral components (McMinn et al., 2012; Smith et al., 2012).

To coincide with the increase in total hip arthroplasties performed, there has also been an increase in the number of available acetabular cup designs. Increased functional and longevity demands, particularly from younger patients, and the adoption of new technologies such as computer assisted surgery has driven innovation in the field (Taylor et al., 2013). For instance, in 2014, of the 153 cementless acetabular cup designs used in hip arthroplasties, only 14 had 10 or more years of experience. Furthermore, the cups with more than 10 years of experience were used in just 43% of arthroplasties involving a cementless cup (National Joint Registry for England and Wales, 2015). This has resulted in a large number of cups with unproven clinical track records being implanted into patients.

The orthopaedic community must rely on the results from pre-clinical tests to assess the efficacy of unproven acetabular cup designs. Traditionally, multi-centre registries provide information on the performance and incidence of complications for a design. As the difference in survivorship between hip prostheses in their initial release is becoming negligible (Viceconti et al., 2009), it requires many years of follow-up in these registries, and with that, prosthesis failures to determine whether a prosthesis design is effective (Viceconti et al., 2009). Therefore, the challenge is to develop thorough testing regimes prior to clinical trials capable of screening out poor acetabular cup designs in order to minimise risk to patients.

Pre-clinical testing evaluates acetabular cups and screens out inferior designs in the early stage of development (Huiskes, 1993). It uses a combination of test methods including experimental studies on cadaver specimens and computational studies to investigate potential clinical failure scenarios. Once design objectives of a new prosthesis are set, possible failure modes and the associated failure scenarios are identified to establish a testing protocol (Viceconti et al., 2009). Measurable and quantifiable parameters are identified for each failure

mode (Martelli et al., 2011). Each test method used in a protocol provides reliable information of the risk associated with a different failure mode (Huiskes, 1993).

Finite Element (FE) modelling is a computational tool used in pre-clinical testing. It was introduced to orthopaedics in 1972, soon after Sir John Charnley's low friction arthroplasty, in order to "acquire a sound understanding of the mechanical behaviour of skeletal parts under physiological loads" (Brekelmans et al., 1972). Since then, the size and sophistication of FE models have increased. A range of techniques within FE are now available to examine failure scenarios including failed bone ingrowth, stress shielding, damage accumulation and wear (Huiskes, 1993; Taylor et al., 2013). Before a prototype prosthesis is made, it can allow the effect of minor changes in a design to be explored in order to refine key design concepts (Viceconti et al., 2009). The key advantage of FE modelling in pre-clinical testing is the ability to alter input parameters easily in a model or set of models. This means that, in contrast to *in vitro* testing, multiple prosthesis designs can be compared in the same set of subjects.

Despite these advantages, the majority of FE models do not fully consider the high levels of variability present within patients and during surgery. There are significant variations in geometry and bone quality between patients that are influenced by a wide range of factors such as gender, age and underlying pathologies (Taylor et al., 2013). The accompanied variation in the placement and orientation during surgery increases the range of environments to which a prosthesis is subjected. However, models are, often, based on a single representative subject and assume average deterministic values for surgical parameters (Viceconti et al., 2005). Many FE studies perform simple parametric studies under a limited set of ideal conditions to assess changes in prosthesis performance (Taylor et al., 2013). As a result, only the average performance of a prosthesis design is assessed and the extremes, where failure is more likely to occur, are ignored. The assumption that results from such models can be extrapolated to represent the performance in the general population is inappropriate in pre-clinical testing and should be reconsidered.

Pre-clinical FE testing of acetabular cups requires methods that are capable of accounting for variability in anatomy, bone quality and surgical technique. However, there is a large time and computational cost associated with comprehensively examining such variability. A large volume of FE analyses is required to simulate a large cohort of subject-specific bone models and explore multiple surgical parameters that may contribute to the risk of failure. Moreover, the time taken to manually develop a new model for each subject or surgical scenario is prohibitive for scaling to larger sample sizes. Therefore, not only is examining patient and surgical variability important but determining methods to reduce the time and computational cost of examining the variability will help pre-clinical FE studies evaluate acetabular cups more thoroughly.

1.2 Research Aims

The overall aim of the research presented in this thesis is to explore the influence of patient and surgical variability in the primary stability of cementless acetabular cups in FE models of the hemipelvis and subsequently determine time efficient methods to examine this variability so that it can be incorporated into pre-clinical testing of prospective acetabular cup designs.

Aim I Develop a pipeline with automated processes that is capable of running the large volume of FE analyses required to assess patient and surgical variability in pre-clinical testing.

Aim II Explore the variability in primary stability of a cementless acetabular cup in a cohort of patient-specific FE models and investigate the association between patient-related factors and the observed variability.

Aim III Explore the surgical variability in the primary stability of a cementless acetabular cup and determine which surgical variables have the greatest influence.

Aim IV Develop methods and identify influential variables that allow pre-clinical testing to take a more computationally efficient approach to simultaneously exploring patient and surgical variability in the primary stability of a cementless acetabular cup.

1.3 Thesis Outline

To achieve the research aims set out, the thesis is organised into the following chapters:

Chapter 2 provides a review of the literature. It includes descriptions of the native hemipelvis, the aspects of cementless acetabular cup design and the performance of cups in the population. Moreover, it evaluates the experimental and computational studies of primary stability of cementless acetabular cups to provide a basis for the research in this thesis.

Chapter 3 presents the pipeline for automatically generating and running FE models of the implanted hemipelvis. It details how acetabular cups are automatically sized, aligned and inserted into subject-specific FE models, as well as applying the boundary and loading conditions. It also describes the output metrics used to assess the primary stability of a cup.

Chapter 4 explores the variability in primary stability of a cementless acetabular cup design in a cohort of subjects and examine the relationship between patient-related factors and primary stability. Consequently, it investigates using a subset of subjects based on influential factors to represent the distribution of primary stability output metrics in the cohort.

Chapter 5 examines the use of a surrogate modelling approach as a time-efficient method for quantifying FE model sensitivity. As an illustration, the method is applied to an FE model of the intact hemipelvis to investigate the sensitivity of strain outputs uncertainties in geometrical parameters and material properties.

Chapter 6 uses the time-efficient method developed in Chapter 5 to explore the surgical variability in the primary stability of a cementless acetabular cup design and identify influential parameters on the primary stability.

Chapter 7 presents an amalgamation of the major findings from this research. It discusses how the elements from this thesis can be incorporated to simultaneously explore patient and surgical variability in pre-clinical testing of cementless acetabular cups. The limitations of this work and potential future research directions are also discussed.

Chapter 2

Literature Review

2.1 Anatomy

2.1.1 Hemipelvis

The hemipelvis[1] is formed by the fusion of the ilium, ischium and pubis bone that meet in the acetabulum (Figure 2.1). Anteriorly, the site of articulation of the two pubis bones is called the pubic symphysis and at this site the pubic bones are attached to a pad of fibrocartilage. Posteriorly, the ilium articulates with the sacrum to form the sacroiliac joint (Martini et al., 2012). There are geometric differences between a male and female hemipelvis. Some of the differences are the result of variations in body size and muscle mass but other skeletal differences for females are for childbearing. In general, the female hemipelvis is lighter and smoother with less prominent landmarks. The ilium in the female pelvis projects farther laterally than in the male pelvis but does not extend as far superior to the sacrum. The male pelvis has a more acute angle between the pubic bones at the pubic symphysis. These geometric differences allow the female pelvis to support the weight of a developing foetus within the uterus and passage of a newborn during delivery (Martini et al., 2012).

[1] In anatomy nomenclature, the hemipelvis is also referred to as the os coxa or hip bone.

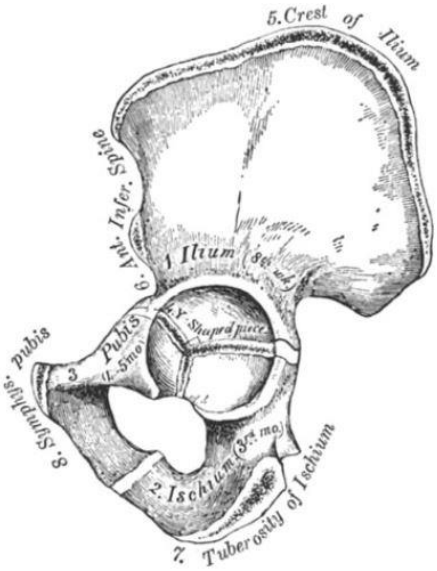

Figure 2.1 The fusion of the ilium, ischium, and pubis bones meeting in the acetabulum of the hemipelvis (Williams and Warwick, 1973)

The acetabulum is the concave socket on the lateral surface of the hemipelvis and articulates with the head of the femur to form the hip joint (Figure 2.2). The articular surface of the acetabulum, called the lunate surface, extends like a horseshoe around the acetabular fossa which is the depressed area in the floor of the acetabulum containing a fat pad. The acetabular notch is the gap in the anterior and inferior portion of the acetabulum where a ridge of bone is incomplete.

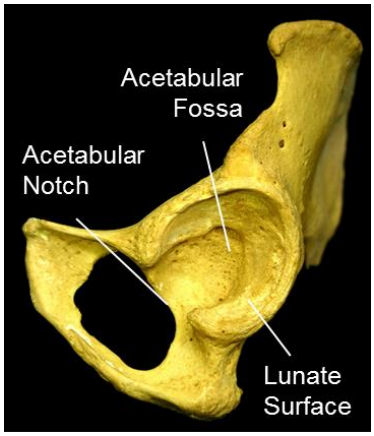

Figure 2.2 A closer view of the bony acetabulum on the lateral surface of the hemipelvis. Displayed is the horseshoe shaped articular surface (lunate surface), the depressed area (acetabular fossa), and notch at the inferior aspect of the acetabulum (acetabular notch). (Modified from (Schwartz, 2006))

2.1.2 The Hip Joint

The hip joint is a ball and socket joint that articulates the hemipelvis to the femur (Figure 2.3). The acetabulum (socket) accommodates the head of the femur (ball). The joint contains a dense and strong articular capsule that consists of the iliofemoral, pubofemoral and ischiofemoral ligaments. It attaches to the transverse acetabular ligament at the inferior aspect of the acetabulum. The combination of a bony socket, a strong articular capsule and surrounding musculature makes the hip joint a very stable joint (Martini et al., 2012).

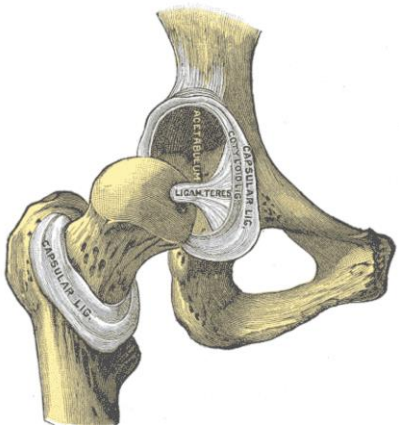

Figure 2.3 The hip joint (Drake et al., 2014)

2.1.3 Forces at the Hip Joint

The intact and prosthetic hip joint experience contact forces between the femoral head and acetabulum during daily activities. Walking is the most frequent dynamic movement for total hip arthroplasty patients and they take an estimated 4988 to 6324 steps per day (Morlock et al., 2001; Schmalzried et al., 1998). The walking gait cycle is the sequence of motion from heel strike to heel strike of a given foot and is divided into the stance and swing phases (Figure 2.4). The stance phase represents 60% of the gait cycle and is when the foot is in contact with the ground. The remaining 40% is the swing phase which describes when the leg is not weight bearing (Esquenazi and Talaty, 2011).

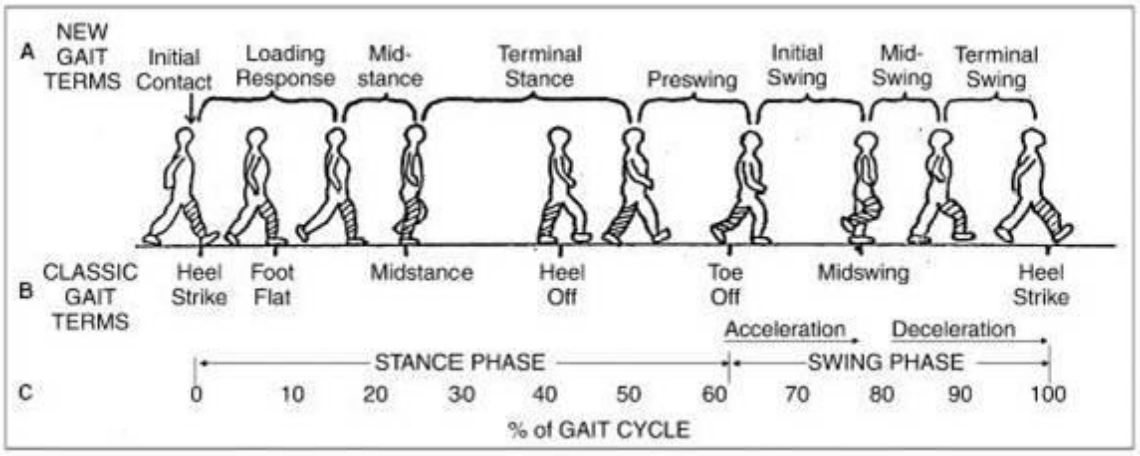

Figure 2.4 Diagram of the gait cycle (Esquenazi and Talaty, 2011)

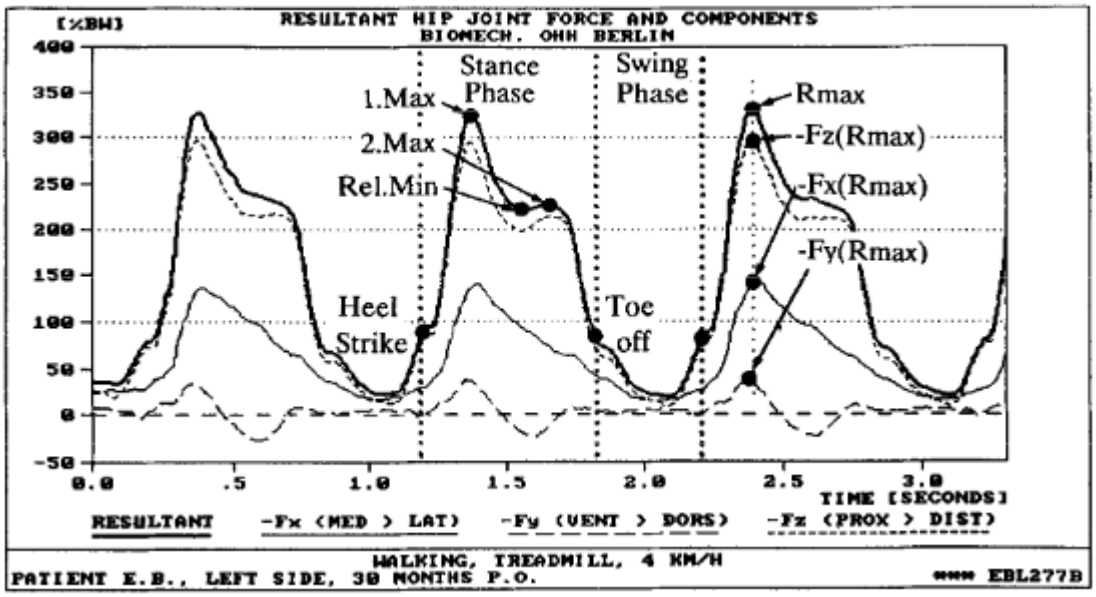

Figure 2.5 Hip joint contact forces of a subject (thick line) during the key events of normal walking (Bergmann et al., 1993).

The hip joint force curve characteristically has two peaks which occur immediately before or after the transition from single to double leg support and vice versa (Paul, 1976) but there can be large inter-subject differences in the pattern (Bergmann, 2001) (Figure 2.5). In general, the first peak occurs during the loading response phase just before the leg passes through the vertical. This peak force increases with walking speed (Bergmann et al., 1993). The second peak occurs at end of the terminal stance phase when the opposite limb is advancing into the swing phase. This second peak often varies in magnitude and has been found to decrease at higher walking speeds (Bergmann et al., 1993).

Peak magnitudes of contact forces during walking are typically 2.1 – 3.3 bodyweights (BW) but can reach to 2.3 – 5.5 BW during stair-climb and as high as 8.7 BW for accidental stumbling (Bergmann, 2001). Peak contact forces as high as 4.1 BWs have been found in patients with disturbed gait patterns (Bergmann et al., 1993). This suggests dysfunction of one muscle increases the joint contact force as part of the required joint moment is taken over by other muscles with shorter lever arms and therefore higher forces (Bergmann et al., 2001). Patients with hip osteoarthritis (OA) exhibit altered joint mechanics during gait compared to healthy individuals. Patients with mild-to-moderate hip OA have been found to experience less net hip joint loading over a reduced range of hip motion for a longer proportion of the gait cycle when walking at their preferred gait speed (Constantinou et al., 2017). These gait alterations may represent compensatory strategies that attempt to reduce joint pain or joint instability.

In order to have realistic testing scenarios for hip prostheses, knowledge of the contact forces in the hip joint during the walking gait cycle is required. Data on the contact forces can be collected using inverse dynamic analysis or direct measurement. Inverse dynamics analysis is a non-invasive method that takes measurements of body segment kinematics and external forces as inputs in equations of motion to calculate muscle and internal joint forces (Pandy and Berme, 1988). As the number of muscles at the joint exceeds the number of degrees of freedom describing joint movement, static optimisation algorithms are applied to predict muscle and

internal joint forces. Direct measurement of hip joint contact forces during gait has been carried out in vivo with prostheses instrumented with strain gauges (Bergmann et al., 1993). In vivo forces at the hip joint during many daily and sporting activities recorded by Bergmann et al. has been collated in a database (Orthoload) to provide data for researchers to test prostheses (Figure 2.6) (Bergmann, 2001).

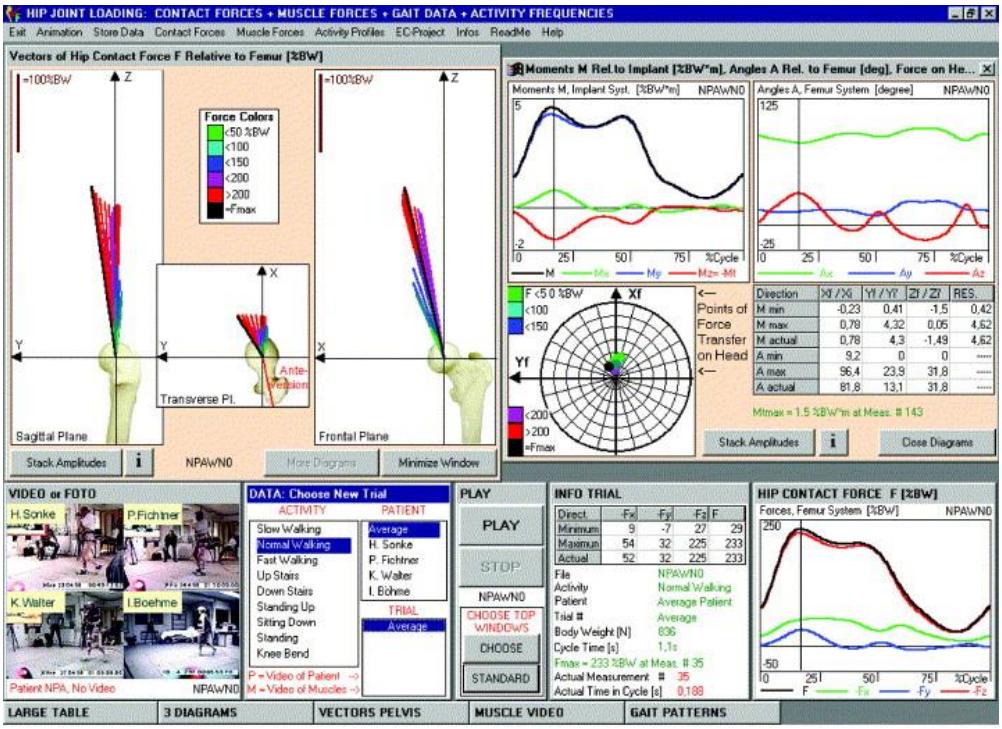

Figure 2.6 Screenshot from Orthoload database showing data on hip contact force measurement and gait analysis (Bergmann, 2001)

2.1.4 Hip Osteoarthritis

Hip osteoarthritis (OA) is a leading cause of joint pain and disability. It is estimated that 2 - 3% of the worldwide adult population suffer from OA (Brown, 2007). The prevalence of hip OA is strongly age-related and is more common in females than males (Dieppe and Lohmander, 2005). In 2015, national health system costs on osteoarthritis in Australia were estimated to exceed $2.1 billion, with nearly 75% being spent on patients admitted to hospital. OA can arise occur in any synovial joint in the body but, in addition to the hip, is most common in the knee, foot

and hand. It is characterised by damage to articular cartilage, new bone formation on the joint margins, changes in the subchondral bone and thickening of the joint capsule (Dieppe and Lohmander, 2005). The main problems associated with the pathological changes in the joint include pain and stiffness. Pain is generally related to use and post-activity pain or pain during movement with a reduced range often occurs (Dieppe and Lohmander, 2005). The joint pain and stiffness associated with OA has a substantial impact on the health-related quality of life of individuals (Picavet and Hoeymans, 2004).

The goal of hip OA management is to control pain and improve function in the joint. Lifestyle alterations such as exercise and weight loss are important components of non-operative management of mild OA to help increase in strength around the joint, reduce stiffness and improve range of motion (Dieppe and Lohmander, 2005). Simple analgesics such as paracetamol or non-steroidal anti-inflammatory drugs (NSAIDS) can be used in conjunction with the educational and exercise-based interventions for relieving pain (Felson et al., 2000). Surgical treatments of OA are considered for patients who do not obtain sufficient symptom reduction with nonsurgical interventions. Total hip arthroplasty is the preeminent surgical intervention for the osteoarthritic hip (Figure 2.7). It represents the most significant advancement treatment of OA and among the most effective of all medical interventions (Felson et al., 2000). Over one million total hip arthroplasties are performed worldwide (OECD, 2015) and 40,000 performed in Australia each year (Australian Orthopaedic Association, National Joint Replacement Registry, 2016). Eight-eight percent of total hip arthroplasties are performed in patients diagnosed with OA (Australian Orthopaedic Association, National Joint Replacement Registry, 2016). For patients with severe OA, it is highly successful in eliminating joint pain and disability and restoring them to near full function.

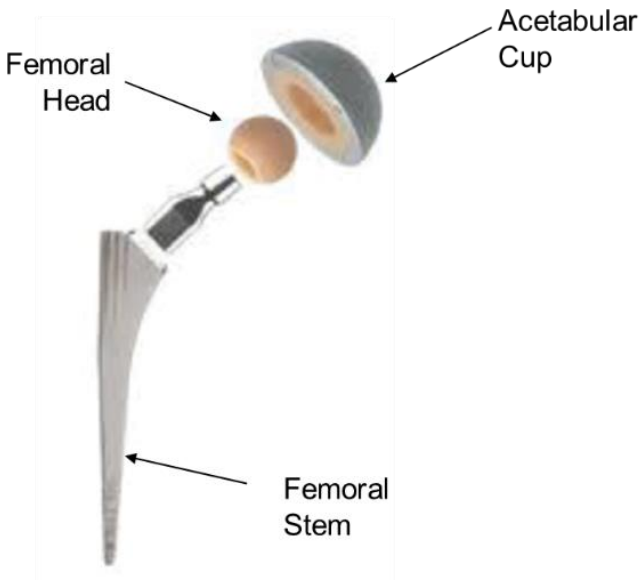

Figure 2.7 The individual components of a total hip prosthesis (Modified from (Knight et al., 2011))

2.2 Acetabular Cup Design

The history of technological advancements in total hip arthroplasty has led it to be a safe and cost-effective intervention to restore hip joint functionality and allow pain-free mobility in patients. Sir John Charnley's pioneering work lay the foundations for innovation in total hip arthroplasty. He developed the concept of low friction arthroplasty by articulating a stainless steel femoral component with a polyethylene acetabular cup and fixing them with polymethylmethacrylate (PMMA) cement (Charnley, 1979). Since then, research has led to rapidly evolving designs that have drawn on the performances of prostheses from preceding years to try to reduce the risk of failure (Holzwarth and Cotogno, 2012). The continuous research has produced a wide variety of prosthesis designs that differ in fixation mode, geometry and materials used.

2.2.1 Methods of Fixation

Fixation of the acetabular cup can be achieved using PMMA bone cement in a cemented prosthesis or via bone ingrowth into the porous surface in a cementless prosthesis (Figure 2.8).

The first acetabular cups were cemented polyethylene cups with grooves on the surface to increase stability within the cement mantle. However, follow-up studies at ten years or more revealed that mechanical failure due to aseptic loosening was the most frequent and significant problem (Johnston and Crowninshield, 1983; Salvati et al., 1981; Stauffer, 1982; Sutherland et al., 1982). While the rate of loosening of the femoral stem appeared to be high during the early follow-up period and decrease with time (Stauffer, 1982), the rate of acetabular cup was lower in the early follow-up period but increased with time (Sutherland et al., 1982). Modern cemented cup designs include metal-backed cups and modifications that ensure a uniform cement mantle (Canale and Beaty, 2012). Despite such technical advancements, the long-term fixation of cemented cups has not improved significantly (Mulroy Jr and Harris, 1990).

Figure 2.8 A Charnley polyethylene cemented cup (Wroblewski et al., 2016) and a titanium cementless cup with a polyethylene liner (Knight et al., 2011)

Cementless cups were introduced due to the high incidence of late aseptic loosening with cemented prostheses. They eliminated the need for cement and instead relied on biologic fixation, through bone ingrowth, to achieve and maintain a strong mechanical bond between the cup and bone (Morscher and Masar, 1988). Bone ingrowth refers to bone formation within the porous surface of a prosthesis and the interconnection of ingrown bone into the pores (Jasty et al., 2007). The physiologic response to a cup after bone reaming resembles the healing of cancellous bone defects, with newly formed tissue occupying the voids of the porous surface (Jasty et al., 2007). In the time that follows surgery, endochondral or intramembranous bone

formation is evident around the porous surface within a week of surgery and woven bone is seen in the porous surface by 3 weeks. Lamellar bone modelling occurs thereafter and bone marrow is usually re-established by around 6 weeks (Jasty et al., 2007).

Cementless fixation is currently the most commonly used fixation method for acetabular cups in total hip arthroplasty. The National Joint Registry for England and Wales has reported that cementless cups were used in 64% of primary total hip arthroplasties in 2014 (National Joint Registry for England and Wales, 2015). This is an increase of 30% since 2004. Meanwhile, use of cemented fixation has decreased from 55% in 2004 to 35% in 2014 (National Joint Registry for England and Wales, 2015). In Australia, 96% of cups were cementless in 2014 (Australian Orthopaedic Association National Joint Replacement, 2015). Similar to the UK, the use of cemented cups has steadily declined in the past decade, from 14% in 2003 to 4% in 2014 (Australian Orthopaedic Association National Joint Replacement, 2015). In Scandinavian countries, cemented fixation remains the preferred method of fixation but the use of cementless cups has been gradually increasing in recent years (Mäkelä et al., 2008; Malchau et al., 2005).

The threaded cup design is a derivative of cementless acetabular cups that relies on threaded rings around the cup to provide fixation. First introduced in 1974, early threaded designs relied solely on the mechanical interlocking between the bone and the prosthesis threads for primary stability and long-term fixation. While these designs had initial satisfactory results, longer-term follow ups demonstrated high rates of migration and early revisions for aseptic loosening from 4% to 31% at 3.5 to 10 years (Bruijn et al., 1995; Fox et al., 1994; Lord and Bancel, 1983). The second generation of threaded cups added porous coatings to provide for bone ingrowth. These designs relied on threads to provide initial mechanical stability and bone ingrowth to provide long-term fixation. The addition of the porous coating improved the performance of the threaded cup. Pupparo et al. reported that a second generation porous-coated threaded cup design had a 0% loosening rate, compared with a 29% loosening rate for the non-porous design at 2 to 4 years follow up (Pupparo and Engh, 1991).

2.2.2 Supplemental Fixation

Achieving adequate primary stability immediately after surgery is a crucial factor in allowing bone ingrowth within the porous surface of a cementless cup. In an effort to improve stability at the time of surgery, the use of supplemental fixation including cancellous bone screws and anchoring pegs or spikes attached to the back of the cup have been investigated (Figure 2.9). Cook et al. demonstrated bone ingrowth in cups with pegs and spikes (Cook et al., 1992). However, larger gaps and less bone ingrowth were seen in cups with pegs and spikes than in cups with screw fixation. The authors conclude that the presence of pegs or spikes may prevent complete seating of the acetabular cup, thus reducing the contact area between the cup and bone (Cook et al., 1992). This is supported by Schwartz et al. who found incomplete seating of cups with spikes when the subchondral bone was retained during acetabulum preparation (Schwartz Jr et al., 1993). In addition, there is some difficulty in repositioning a spiked cup if it is initially malpositioned (Peters and Miller, 2007). For long-term outcomes, Engh et al. found spiked cups had slightly lower 15-year survivorship when using revision for aseptic loosening as an end point among 4289 hip arthroplasties in the same institution (94.7% vs. 98.4% for cups with screws and 100% for press-fit cups) (Engh et al., 2004).

Figure 2.9 An RM acetabular cup (Mathys) with two fixation pegs (Ihle et al., 2008) and the Tri-Spike acetabular cup (Biomet) (Klaassen et al., 2009).

Inserting screws with the cup may be required for patients with osteoporotic bone, patients with dysplastic hip that do not permit complete coverage of the cup or if the surgeon is aware of

instability at the time of surgery (Udomkiat et al., 2002). Clohisy et al. reported that screw fixation provides adequate primary stability and good clinical results for most patients at an average of 10 years follow up (Clohisy and Harris, 1999). Retrieval studies have observed higher bone ingrowth adjacent to screws than in other regions and it has been demonstrated that cups with screw fixation required greater torque to fail than cups with spike or pegs (Stiehl et al., 1991).

The insertion of cups with screws can be difficult and is not without risk. Although the trauma to neural and vascular structures is rare with screw placement, there is potential for severe complications if damaged. The iliac artery and vein and neurovascular structures are at risk with the placement of screws in the anterosuperior and anteroinferior aspects of the acetabulum (Figure 2.10) (Keating et al., 1990). The posterior aspect is considered safer for screws but is located near the gluteal and internal pudenal neurovascular structures which are endangered if screws greater than 25 mm are used (Keating et al., 1990). Further, fretting corrosion between the screws and acetabular shell may occur (Peters and Miller, 2007) and screws and screw holes can provide pathways for particulate wear debris which may lead to osteolysis (Schmalzried et al., 1992a). Therefore, the benefit of supplemental screw fixation for bone ingrowth is weighed against the concerns regarding risk of particulate debris movement and neurovascular injury.

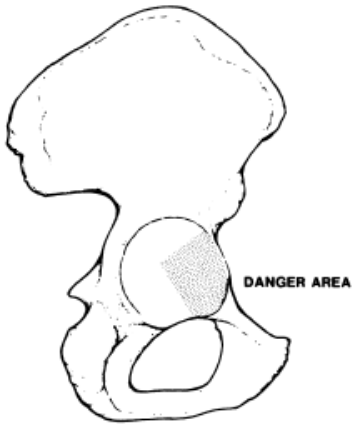

Figure 2.10 The shaded area of the hemipelvis represents the danger area for the pentration of intrapelvic structures by screws (Keating et al., 1990)

2.2.3 Press-Fit Fixation

Press-fit fixation became popular for cementless acetabular cups in order to address the concerns about fixation with bone screws. Press-fit cups eliminate the wear of the polyethylene liner against bone screws and decrease the risk of neurovascular injury (Peters and Miller, 2007). Press-fit also maximises the contact of the acetabular cup against the bone at the periphery which provides a large surface area for bone ingrowth to occur (Adler et al., 1992). Press-fit has been shown to reduce the incidence and extent of peripheral radiolucencies compared to cups with screw fixation (Schmalzried et al., 1994). However, initial gaps at the pole of the cup are more frequent (Kwong et al., 1994). Full seating of the press-fit cup is recommended during insertion in order to obtain dome contact (Schmalzried et al., 1994). Studies have found no difference in the rate of revision between cups with screws and press-fit cups (Morscher, 1992; Udomkiat et al., 2002). Several authors have concluded that supplemental screw fixation is not necessary for optimum primary stability of cementless cups (Kwong et al., 1994; Morscher, 1992; Roth et al., 2006) and recommend press-fit fixation (Schmalzried et al., 1994).

The optimal press-fit produces a tight peripheral fit and minimises the extent of gaps in the polar region. When the cup is inserted, the bone deforms and then recoils to grip it firmly. Compressive forces act on the periphery to restrict micromotion of the cup after surgery (Curtis et al., 1992). To achieve primary stability with press-fit, cups are typically 1 to 3 mm larger in diameter than the last reamer used to prepare the acetabulum. Oversizing the cup by 1 mm, referred to as a 1 mm interference fit, provides the optimum combination of seating and stability (Adler et al., 1992; Kwong et al., 1994). Meanwhile, Curtis et al. found 2 mm and 3 mm interference fits provide better stability when testing torsional lever-out tests (Curtis et al., 1992). However, while a greater interference fits will increase the hoop stress around the prosthesis, thereby tightening the grip, it may prevent the cup from fully seating and may fracture the rim of the acetabulum. With 2 mm interference fits, incomplete seating has been consistently found, resulting in thick and extensive gaps between the bone and pole of the cup

(Kwong et al., 1994; MacKenzie et al., 1994). Cup insertion with 4 mm interference fit can cause acetabular fracture (Curtis et al., 1992; Kim et al., 1995).

2.2.4 Cup Geometry

To date, five main cup geometries have been used in cementless fixation: cylindrical (Griss and Heimke, 1981), square (Griss and Heimke, 1981), conical (Ring, 1983), elliptical and hemispherical cups (Figure 2.11). Early prostheses were designed to achieve mechanical fixation to the hemipelvis, generally through cup geometry with large pegs or threaded rings. Ring and Freeman et al. introduced all polyethylene conical acetabular cups that required pegs for fixation (Freeman et al., 1983; Ring, 1983). Although short-term results were good for the designs, there were high failure rates due to inadequate fixation, cup migration, wear and severe bone resorption (Bertin et al., 1985; Wilson-MacDonald et al., 1990).

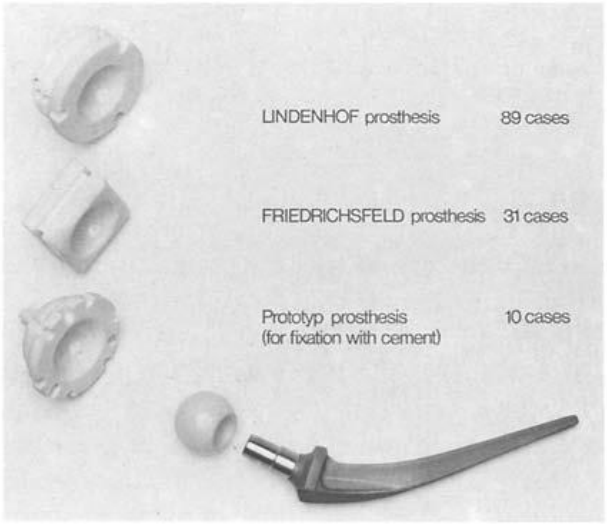

Figure 2.11 Top to bottom, cylindrical, square, and conical geometries of early acetabular cup designs (Griss and Heimke, 1981)

Hemispherical cups have proven to be the most successful design (Harris, 2003). In an investigation of hemispheric porous-coated cups, Udomkiat et al. reported that among 110 cups in patients who were followed up for a mean 10 years, one was revised for aseptic loosening and

four had osteolysis (Udomkiat et al., 2002). Hemispherical cups closely match the geometry of the acetabulum and allow for the least resection of bone during surgery. The contact surface provided by hemispherical cups allows physiologic transmission of forces from hemipelvis to cup (Morscher, 1992). Additionally, the hemispherical shape reduces stress concentrations that occur with cement fixation or other cup geometries (Peters and Miller, 2007). Elliptical cups have either hemispherical designs that are slightly flared to an ellipse at the periphery or dual-geometry cups that have a larger radius at the equator than at the dome. Elliptical cups were developed to improve cup stability by enhancing the peripheral contact between the cup and acetabulum. However, a smaller radius at the dome of elliptical cups creates gaps in the polar region and elliptical cups are more likely to cause fracture of the acetabulum during insertion than hemispherical cups (Haidukewych et al., 2006).

2.2.5 Porous Coatings

A porous coating is a three-dimensional surface with interconnected porous networks that acts as scaffold on the acetabular shell to facilitate the osseointegration. Bone trabeculae and osteons are approximately tens of micrometres thick and pores in the coating must be of an appropriate size in order for bone to infiltrate. The effect of pore size has been investigated in canine models, using pore sizes ranging from 50 to 800 μm. While studies investigating pore size between 150 and 400 μm have shown no relationship between pore size and fixation strength (Bobyn et al., 1980; Cook et al., 1985), a canine acetabular model demonstrated more bone ingrowth in prostheses with pores sizes of 450 μm and 200 μm than in prostheses with 140 μm (Jasty et al., 1989). Based on data from canine studies, Kienapfel et al. concluded that the optimal range for pore size was 100 – 400 μm (Kienapfel et al., 1999). Bobyn et al. found a pore size range of 50 – 400 μm provided the highest fixation strength in the shortest period (Bobyn et al., 1980). Smaller size porous systems have pores that are too small to allow for uniform tissue calcification within. Meanwhile, larger size pores are too large to be consistently and uniformly infiltrated with mature bone. Pore systems within the optimum range become more quickly

filled with bone than the larger pore systems. Therefore, the maximum fixation strength develops more rapidly (Bobyn et al., 1980).

The porous coatings most widely available for press-fit acetabular cups are fibremesh, sintered beads, and porous metal (Figure 2.12) (Swarts et al., 2015). The titanium fibremesh surface has the longest follow-up of available surfaces. It is fabricated using a diffusion bonding process to attach fibre metal pads to a titanium substrate (Klika et al., 2007). The porosity of the mesh is 30 – 40% and is controlled by the arrangement of the wire in the metal pads and the temperature and pressure of the diffusion bonding process (Klika et al., 2007). Follow-up data at minimum of 20 years has demonstrated a 4% failure rate of cups with the titanium fibremesh surface when failure was defined as revision for loosening or radiographic evidence of loosening (Della Valle et al., 2009).

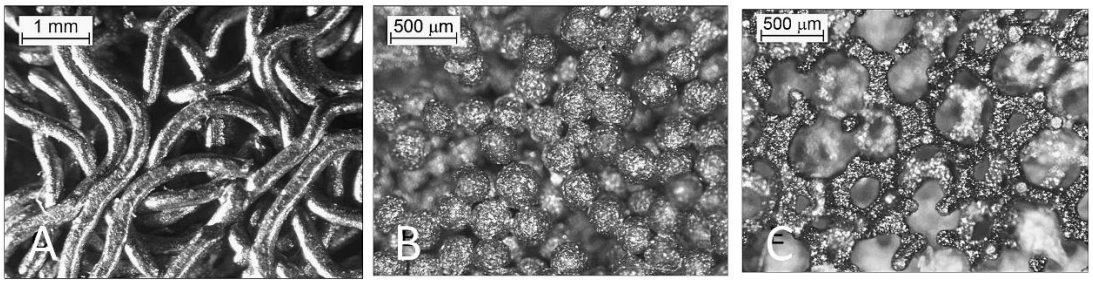

Figure 2.12 Porous coatings. A) fibremesh coating from a Harris-Galante II cup (Zimmer-Biomet), B) sintered beads (250 µm), and C) porous ("trabecular") metal surface (Zimmer-Biomet) (Swarts et al., 2015).

Sintered bead and plasma-spray coated prostheses represent the most common cementless acetabular cups in current clinical use. The sintered bead fixation surface is a porous coating consisting of various sizes of spherical beads that are bonded to a Co-Cr or titanium substrate through a sintering process. Engh et al. reported that of 427 cups with sintered bead surface and screw fixation, 3 were revised for aseptic loosening at a mean follow-up of 9.5 years (Engh et al., 2004). In a retrieval study, Swarts found greater bone ingrowth had occurred in acetabular cups with the smaller bead size, with an optimum bead size being 250 µm (Swarts

et al., 2015). For the plasma-spray deposition of a titanium coating onto a substrate, powders are applied with a high-energy arc created within a nozzle (Klika et al., 2007). While there have been shorter follow-up periods for the titanium plasma-spray surface, clinical results have been comparable to other porous surfaces. Reina et al. reported none of the hemispherical, titanium plasma-sprayed cups required revision for any reason in 145 total hip arthroplasties in an average 8-year follow-up (Reina et al., 2007). Additionally, a study by Manley et al. also found no revisions after a minimum 5-year follow-up in 101 total hip arthroplasties with titanium plasma-sprayed acetabular cup (Manley et al., 1998).

More recently, highly porous, or "trabecular" metal surfaces (Zimmer Biomet) have been used in an effort to maximise bone ingrowth (Klika et al., 2007). For instance, porous tantalum metal surfaces have higher porosity (70 – 80%), lower elastic modulus, and a higher coefficient of friction as other titanium surfaces (Cohen, 2002) which potentially help greater ingrowth (Klika et al., 2007). Animal models have demonstrated 2 times greater bone ingrowth than sintered bead fixation surfaces (Bobyn et al., 1999). Additionally, porous tantalum prostheses have demonstrated good early clinical results. In a minimum 2-year follow-up multi-centre study of 414 total hip arthroplasties, Gruen et al. found no evidence of lysis or revisions for loosening of porous tantalum acetabular cups (Gruen et al., 2005).

2.2.6 Hydroxyapatite

Hydroxyapatite (HA) is a bioactive material that is applied as a coating to improve osseointegration of cementless prostheses within bone. HA is a form of calcium phosphate with an apatitic structure that resembles the inorganic mineral phase of bone (Sun et al., 2001). HA is plasma sprayed onto the surface of the prosthesis by driving HA particles at high velocity from a plasma gun against the surface of the substrate. It creates a local osteoinductive and conductive local environment of calcium and phosphate ions with a calcium phosphate precipitate on the prosthesis surface (Klika et al., 2007) that helps induce a faster rate of osseointegration than other porous surfaces (Cook et al., 1992).

HA-coated prostheses require less intimate initial contact with bone at the time of surgery (Jaffe and Scott, 1996). In a canine model, new formation of bone found at gaps were 400 μm from the HA surface (Soballe et al., 1993). Furthermore, a HA coating prevents the formation of fibrous tissue due to excessive micromotion that would occur in an uncoated titanium prosthesis (Soballe et al., 1993). Initially, the overall success of the HA-coated acetabular cup did not match those for the HA-coated femoral stem because the smooth surfaces of cups could not sustain the tensile stresses between the cup and bone during patient activity (Manley et al., 1998). Since then, many clinical studies have demonstrated that the subsequent acetabular cup design with an arc-deposited titanium surface beneath the plasma-spayed HA performs well. In the short term, D'Antonio reported 1 cup was revised for aseptic loosening in a series of 169 total hip arthroplasties at 2 to 4 years (D'Antonio et al., 2002). Meanwhile, John et al. reported no cups revised for osteolysis or aseptic loosening in 223 total hip arthroplasties at 6-year follow-up (John et al., 2015).

2.2.7 Bearing Surfaces

Total hip arthroplasty has used a variety of femoral head and acetabulum articulation surface materials in many combinations. The articulation of a metal femoral head onto a polyethylene acetabular liner is the most commonly used bearing surface. The National Joint Registry for England and Wales reported that, in 2015, the metal-on-polyethylene bearing was used in 59% of all total hip arthroplasties (National Joint Registry for England and Wales, 2015). The alloys primarily used for the femoral component are stainless steels, cobalt- and titanium-based alloys (Gilbert, 2007). The material choice for cementless acetabular cups is ultra-high molecular weight polyethylene (UHMWPE), typically combined with a titanium- or cobalt- based alloy shell.

Operative management with constrained acetabular liners are required in patients with recurrent dislocations. Constrained liners use a locking mechanism to hold the femoral head captive within the cup. The two prevailing designs of constrained liner are the Trident

constrained tripolar liners (Stryker) and the S-ROM (DePuy-Synthes) (Lachiewicz and Kelley, 2002). The constrained tripolar design is composed of an inner polyethylene liner, with a locking ring, that accepts the femoral head. This liner is covered with a polished Cobalt-Chrome shell. The polished shell then articulates with another polyethylene liner that can be inserted into the acetabular shell. The S-ROM constrains the femoral head using extra polyethylene about the rim, which deforms upon location of the head within the liner. A rim ring is then subsequently locked about the periphery.

The higher fracture toughness, biocompatibility and improved wear resistance UHMWPE has over other polymers (McKellop et al., 1999) makes it the preferred acetabular bearing material in total hip arthroplasty. However, the bone resorption and eventual loosening associated with polyethylene wear debris remains one of the primary factors limiting the lifespan of prostheses (McKellop et al., 1999). Efforts to improve the wear resistance of UHMWPE have included cross-linking by irradiation and heat treatment. Cross-linking reduces free radicals in polyethylene by allowing the formation of covalent bonds between adjacent molecules (Kurtz et al., 1999). It has been demonstrated to significantly increase the resistance of polyethylene to abrasive and adhesive wear by improving its resistance to crossing-path motion, as occurs in an acetabular cup (McKellop et al., 1999).

Early hip prostheses adopted metal-on-metal articulation (McKee and Watson-Farrar, 1966) but were rejected soon afterwards in favour of Charnley's technique for low friction total hip arthroplasty using metal-on-polyethylene bearings. Recently, a second generation of metal-on-metal bearings for hip prostheses were manufactured with improved methods and materials. These high carbon, cobalt-chromium-molybdenum alloy bearing surfaces have lower wear rates than cross-linked polyethylene (Fisher et al., 2006). However, the deposition of cobalt-chrome wear debris induces a variety of necrotic and inflammatory changes to periprosthetic soft tissue. It has been suggested that these changes are attributed to cytotoxicity and a delayed hypersensitivity reaction (Haddad et al., 2011). Adverse reactions to metal debris include

metallosis, lymphocytic vasculitis-associated lesions, and pseudotumours (Langton et al., 2010). Pseudotumours are cystic masses that develop in the periarticular region (Pandit et al., 2008). The use of metal-on-metal bearing surfaces has virtually ceased (National Joint Registry for England and Wales, 2015).

Alumina (Al_2O_3) and zirconia (ZrO_2) are bioinert ceramics with excellent hardness and tribological properties for the femoral head and acetabular cup articulation regions. Ceramic-on-ceramic bearings have the lowest wear rate of any bearing combination (Fisher et al., 2006). In addition, ceramics are biocompatible with low risk for adverse soft tissue reactions for any wear debris that is produced (Greenwald and Garino, 2001). Despite the excellent material and properties, early ceramic-on-ceramic bearings had a relatively high risk of fracture due to impurities, poor prosthesis design, and fabrication processes that resulted in reduced strength and wear resistance (Lee and Bistolfi, 2015). Since then, processing methodologies have significantly improved and the fracture toughness properties of ceramics have been enhanced by partially stabilising them with materials such as yttrium and magnesium oxide additions (Deville et al., 2003). The current generation of ceramic-on-ceramic total hip arthroplasties have demonstrated survivorship of 92 – 100% at an average of 10 years follow up (Lee and Bistolfi, 2015) and fracture rate of ceramic liners have ranged between 0.6 – 1.6% (Traina et al., 2013).

2.3 Failure Scenarios

A thorough pre-clinical evaluation of a prosthetic design starts with the identification of possible indications for revision surgery and their associated failure mechanisms (Martelli et al., 2011). Prosthetic failure is a process with multiple contributing mechanisms, both mechanical and biological, that produces clinical and radiological signs along the way. Excessive pain and impaired function are clinical indications of failure in a patient. Meanwhile, loosening and migration of a prosthesis can be identified on radiographs. Huiskes defined failure mechanisms in terms of particular courses of events, called failure scenarios (Huiskes, 1993). Pre-clinical

testing protocols are established for separate failure scenarios to investigate how likely a prosthesis design instigates failure according to a particular failure scenario.

Aseptic loosening is the most common reason for revision of acetabular cups (Australian Orthopaedic Association National Joint Replacement, 2015; Canadian Joint Replacement Registry, 2015; National Joint Registry for England and Wales, 2015). The Canadian Joint Replacement Registry reported that aseptic loosening was the reason for 23.9% of revisions in 2013 – 2014 (Canadian Joint Replacement Registry, 2015). The Australian Joint Registry has reported that the combined reasons of aseptic loosening and osteolysis were the reported reason for 32.5% of revisions between 1999 and 2014 (Australian Orthopaedic Association National Joint Replacement, 2015). The national joint registries for England and Wales and Australia report that the revision rate for aseptic loosening is initially low but increases after 7 years (Australian Orthopaedic Association National Joint Replacement, 2015; National Joint Registry for England and Wales, 2015).

2.3.1 Accumulated Damage

Mechanical damage in materials and interfaces can gradually accumulate due to repetitive dynamic loading (Huiskes, 1993). This scenario has been indicated as a loosening mechanism of cemented prostheses. Interface stresses may locally exceed the strength of the cement bond and initiate a disruption. Cracks may then propagate under dynamic loading to produce micromotion, bone resorption, and, eventually, loosening. As there is no cement link and prosthesis-bone interfaces can be relatively strong in cementless prostheses, the accumulated damage scenario is less likely to be initiated but it is conceivable that there may be a disruption of the prosthetic coating. Prostheses can be tested pre-clinically for this failure scenario with computational simulation or laboratory endurance tests. Simulations are used iteratively to determine the stresses of materials during a simulated cyclic loading process. Where the stresses are greater than the material fatigue strength, damage is allocated in the FE model

and the next iteration is simulated. The process is repeated until an adequate number of loading cycles are simulated (Verdonschot and Huiskes, 1997).

2.3.2 Particulate Reaction

Wear particles from bearing surfaces or modular connections collect in the prosthetic joint and can migrate into the cement-bone or prosthesis-bone interfaces (Huiskes, 1993). The small particles that enter the periprosthetic space, such as polyethylene from the acetabular bearing surface, are phagocytosed by macrophages. The macrophages then release cytokines and other mediators of inflammation that lead to inflamed tissue adjacent to the bone. Eventually, osteoclasts are recruited or activated to resorb the local bone leading to osteolysis and, in turn, the loosening of the prosthesis (Ingham and Fisher, 2005). The characteristics of wear particles can be assessed pre-clinically using hip simulators (Maher and Prendergast, 2002).

2.3.3 Destructive Wear

The bearing surfaces or modular connections wear out, to the extent that the mechanical integrity can no longer be maintained (Huiskes, 1993). All the articulating surfaces in a prosthesis are subject to micromotion, however small, which leads to wear and abrasion. For younger patients receiving a cemented or cementless hip prosthesis, the destructive wear scenario may arise with heavy use and more than 20 years at approximately one million cycles per year (Saikko et al., 1993). The sensitivity of a prosthesis design to this scenario can be pre-clinically tested in hip simulators (Maher and Prendergast, 2002).

2.3.4 Stress Shielding

The bone in an intact joint carries the external joint and muscle loads by itself. When a prosthesis is in place, it shares the load-carrying with the prosthesis. Thus, the bone is shielded from the stress to which it would normally be subjected. This strain-adaptive bone remodelling process reduces the support the bone provides to the prosthesis and may cause fracture or fatigue failure of the prosthesis-bone bond (Huiskes, 1993). The potential for excessive bone

remodelling can be predicted in pre-clinical testing with computational methods. The strain energy in the bone around the prosthesis as result of an applied load is compared to the strain energy in the same locations in the intact joint for the same applied load (Huiskes et al., 1987). *In vitro* experiments measuring bone strain can also be used (Cristofolini et al., 2010a).

2.3.5 Failed Bonding

The success of bone ingrowth in cementless prostheses depends on the primary stability of the bone-cup interface. Good primary stability allows the patient to bear weight until permanent secondary stability is achieved as a result of bone ingrowth into the porous surface (Ochsner and Schweizer, 2003). Primary stability is provided by press-fit fixation where an oversized cup is inserted into an acetabulum (Ries et al., 1997; Spears et al., 1999), or by supplemental fixation with screws, spikes, and pegs. However, motion and gaps at the prosthesis-bone interface may delay, inhibit, or prevent bone ingrowth. If there is excessive micromotion, fibrous connective tissue can form around the cup rather than bone (Lee et al., 1984). Reported values on allowable micromotion range between 20 μm (Jasty et al., 1997), 28 μm (Pilliar et al., 1986), 40 μm (Jasty et al., 1997) and 50 μm (Szmukler-Moncler et al., 1998) but *in vivo* studies have consistently demonstrated that micromotion above 150 μm only allows for the attachment of fibrous tissue (Jasty et al., 1997; Pilliar et al., 1986; Soballe et al., 1993). A fibrous tissue interface can be stable for a while (Huiskes, 1993) but it is not as reliable or predictable as a cementless prosthesis with bone ingrowth (Engh et al., 1987) and can lead to eventual loosening (Pilliar et al., 1986).

The lack of direct and continuous contact at the cup-bone interface is a secondary factor responsible for failed bone ingrowth (Schmalzried et al., 1992a). Experiments using canine models have shown that gaps greater than 500 μm between the bone and porous surface adversely affected bone ingrowth (Jasty et al., 1989; Sandborn et al., 1988). Other canine studies have demonstrated that bone can grow with gaps up to 2 mm but there was a decrease in the degree of bone ingrowth and attachment strength (Bobyn et al., 1981; Sandborn et al., 1988). In

a study on human cancellous bone, Bloebaum et al. observed the absence of bone ingrowth in retrieved implants of 14 patients when gaps greater than 50 μm were present between the bone and porous surface (Bloebaum et al., 1994).

Interfacial gaps can allow joint fluid and particulate debris to penetrate the periprosthetic joint space (Schmalzried et al., 1992a). The extent of intimate contact between bone and prosthesis and how this contact varies determines the access for particulate debris dispersed within the joint fluid to the periprosthetic joint space. Joint fluid flows into and out of the joint space according to pressure gradients. When a sufficient number of debris particles accumulate, macrophages can be activated which results in bone resorption. As bone is resorbed, a bigger pit is produced which encourages more fluid flow into that area, hence more particles and more bone resorption (Schmalzried et al., 1992a).

2.4 Aseptic Loosening of the Cup in the Population

Different patient-related factors affect aseptic loosening to varying degrees (Young et al., 1998) and variability in loosening rates exist in patient groups implanted with the same prosthesis and within the same institution (Udomkiat et al., 2002). A prospective prosthesis design must be robust to the variations in geometric features and material properties which exist between individuals and are influenced by a range of patient-related factors such as gender, age and obesity level (Galloway, 2012).

2.4.1 Gender

Total hip arthroplasties are more commonly performed on females than males. According to the national joint registries, between 58% (Canadian Joint Replacement Registry, 2015) and 66% (National Joint Registry for England and Wales, 2015) of total hip arthroplasties in 2014 were performed in females in Canada and England and Wales respectively. The Australian Joint Registry similarly reported females account for 55% of primary total hip arthroplasties in 2014

and that this proportion had remained stable since 2003 (Australian Orthopaedic Association National Joint Replacement, 2015).

Gender differences in anatomy of the hemipelvis may be important to consider for prosthesis design in total hip arthroplasty but whether gender is influential on failure is unclear. Males are generally reported to have a higher rate of revision for failure of one or more components for any reason (Santaguida et al., 2008; Schurman et al., 1989). In a systematic review examining just aseptic loosening, Cherian et al. reported that males were associated with an increased risk of loosening when considering all components in total hip arthroplasty (Cherian et al., 2015). In contrast, Inacio reported that at a median follow-up of 3 years females had a higher risk of revision for any reason than males (Inacio et al., 2013). Other studies have found no differences in failure rates between genders (Cornell et al., 1985; Kim and Kim, 1993).

As with overall prostheses failure in total hip arthroplasty, there is little consensus as to the association between gender and aseptic loosening of cementless cups. Röder et al. found that the risks of cup failure including loosening, migration and cup fracture was 37% lower for females (Röder et al., 2010). However, an earlier study by the same authors found that there were no differences in risk between males and females when cup loosening was considered on its own (Röder et al., 2008). In contrast, Manley et al. found that within a group of 168 patients with HA-coated cementless cups, 58% of the patients who had a revision were female but included aseptic loosening and mechanical failure of the cup as reason for revision (Manley et al., 1998). Havelin et al. reported inferior cup survival until revision for aseptic loosening in females based on 11 cup designs and over a 6-year period (Havelin et al., 1995). Other studies did not demonstrate a correlation between acetabular component instability and gender (Engh et al., 1990; Incavo et al., 1993).

Conflicting findings on prosthesis failure among studies may be attributed to other patient-related factors which confound the effect of gender. There is a greater decrease in cancellous volumetric bone mineral density (vBMD) with age for females than males (Riggs et al., 2004)

and female patients tend to be older at the time of surgery (Canadian Joint Replacement Registry, 2015). Differences in the definition of failure, follow-up times and component type among studies can further complicate matters (Inacio et al., 2013). Studies often adjust for potential confounders in their analysis. Surin et al. found a statistically significant association between male gender and aseptic loosening but the differences were not present after an adjustment for bodyweight (Surin and Sundholm, 1983).

2.4.2 Age

The majority of total hip arthroplasty recipients are age 55 – 84 years (Australian Orthopaedic Association National Joint Replacement, 2015; Canadian Joint Replacement Registry, 2015) and those patients at either end of this age range have a worse prognosis for functional outcomes and prosthesis survival (Young et al., 1998). While some studies have found that older age is associated with poorer functional outcomes (Espehaug et al., 1998; Santaguida et al., 2008; Young et al., 1998), it appears to have a protective factor against failure (Röder et al., 2010). Patients in the age groups 70-80 years old and >80 years were reported to have a significantly lower risk of failure when compared to < 60 years old (Röder et al., 2010). The Australian Registry report that patient group aged ≥ 75 yrs had the lowest rate of revision for all reasons after six months (Australian Orthopaedic Association National Joint Replacement, 2015).

Younger patients are at a greater risk for revision due to their increased physical demands on their prostheses (Young et al., 1998). Havelin et al. found that patients < 65 years had a higher risk of revision for cementless prostheses at 4.5 years (Havelin et al., 1994). However, this study included all indications for revision on femoral and acetabular components. Younger patients may benefit from a higher degree of regained mobility after a total hip arthroplasty but placing higher physical demands on the prosthesis may lead to higher failure rates (Röder et al., 2010; Young et al., 1998). Cherian et al. found a higher activity level increased the risk of aseptic loosening of hip prostheses (Cherian et al., 2015).

2.4.3 Bone Quality

The long-term success of cementless prostheses is provided by adequate primary stability and bone ingrowth and, as such, is dependent on bone quality. Although no long-term clinical study has been conducted on the effect of bone quality and aseptic loosening of cementless prostheses, surgeons are reluctant to implant them in patients with poorer bone quality, such as those with osteoporosis, for risk of failure (Meneghini et al., 2011). Previously, Aro et al. evaluated how low bone mineral density (BMD) affected primary stability and bone ingrowth in cementless total hip arthroplasties in 39 female patients with primary hip osteoarthritis. The study found delayed osseointegration of the femoral stem in patients with low BMD (Aro et al., 2012).

In vitro testing has demonstrated the adverse effect of poor bone quality on the primary stability of cementless cups. In polyurethane foam blocks, stability of cups has been lower in low density (0.2 g cm^{-3}) compared to high density (0.5 g cm^{-3}) substrate (Baleani et al., 2001; Crosnier et al., 2014). During cup insertion, Crosnier et al. found greater foam deformation in low density substrate which resulted in lower compressive stresses acting on the cup. Adler et al. found slight lower strength for some cup designs in higher density blocks due to increased resistance to compression which sometimes prevented complete seating (Adler et al., 1992).

2.4.4 Obesity

Increased bodyweight is considered a risk factor for the failure of total hip arthroplasty components. Higher stresses exerted by heavier patients may compromise primary stability and lead to delayed bone ingrowth and increased risk of failure (Röder et al., 2010). Despite this widely-held belief, many studies have not found a clear association between increased bodyweight and prosthetic failure (Engh et al., 1990; Manley et al., 1998; Röder et al., 2010).

The apparent lack of association between a patient's weight and cup failure may be because studies have not considered the difference between mass and obesity (Young et al., 1998). BMI is a classification of obesity that divides adults into categories of underweight, normal and overweight (A Workgroup of the American Association of Hip and Knee Surgeons Evidence

Based Committee, 2013). In total hip arthroplasty, increased BMI has been previously associated with a reduced prosthesis survival time before a revision and an adverse effect on the functional outcomes (Stickles et al., 2001), infection rate (Haverkamp et al., 2011) and dislocation (Lübbeke et al., 2007).

BMI has not been found to affect the long-term success of cementless cups (Lehman et al., 1994; McLaughlin and Lee, 2006) but there is some evidence to suggest it is a risk factor for early loosening. McLaughlin et al. compared an obese cohort (BMI > 30) and non-obese (BMI < 30) patients at 10 to 18 years follow-up and found no significant differences between the groups in regards to aseptic loosening of the cementless cup. However, in a case-control study on cementless cup failure with mean follow-up of 3.8 years, Röder et al. found the risk of failure increased by 1.03 for each additional unit of BMI over 25 kg/m^2. Additionally, patients with a BMI > 30 kg/m^2 had a 40% greater risk of cup failure compared to patients of normal weight (25 kg/m^2) (Röder et al., 2010).

2.4.5 Bone Geometry

Geometry of the acetabulum varies between individuals and may affect cup loosening. Previously, Wilson-Macdonald et al. found a higher rate of aseptic loosening for cups with diameters of 52 mm and smaller was 8% compared to 5.4% for cups 54 mm and larger at five to ten years (Wilson-MacDonald et al., 1990). In experimental studies, Adler et al. found cups that were implanted in deeply reamed cavities had greater stability than those that sat flush or proud (Adler et al., 1992). Moreover, the surface of the acetabulum available for contact with the cup is dependent on geometry. Schwartz et al. found the acetabulum may not be deep enough to completely contain the cup and limited the surface apposition of the bone-implant interface (Schwartz Jr et al., 1993).

2.5 Acetabular Cup Implantation

The goal in replacing the acetabulum with a cementless cup is to provide stability that allows weight-bearing until bone ingrowth into the porous surface occurs (Ochsner and Schweizer, 2003). A cementless cup must fit as accurately as possible into the reamed acetabulum for this to occur. A poor match, due to a shape mismatch between a cup and reamed acetabulum, results in an unstable cup and gives rise to inconsistent bone ingrowth (Macdonald et al., 1999). Therefore, preparation of the acetabulum and implantation of the cup are crucial for the long-term success of cementless acetabular cups.

2.5.1 Preparation of the Acetabulum

Good acetabular preparation during surgery allows intimate bone-prosthesis contact and primary stability of the cup (Callaghan et al., 1995). In order to prepare the acetabulum to receive the cup, existing bone is removed so the cup will be oversized with respect to the reamed cavity. A reamer 6 – 10 mm smaller than the anticipated size of the acetabular cup is used to initiate reaming. The reamer is used to ream medially towards the floor of the acetabular fossa until the medial wall of the acetabular fossa is exposed. Reaming then proceeds in the direction of the final cup position (Peters and Miller, 2007). The acetabulum is then expanded using sequentially larger reamers in either 1 or 2 mm increments.

The size difference between the cup and final acetabulum diameter provides the cup with stability upon implantation (Ries and Harbaugh, 1997). The majority of studies in the literature report the interference fit as the nominal oversizing of the cup with respect to the last-reamer used. However, despite the intentions of the surgeon to obtain an optimal nominal interference fit, the exact dimensions of the reamed acetabulum have been found to be different from the dimensions of the last-reamer used (Kim et al., 1995; Macdonald et al., 1999; MacKenzie et al., 1994). Previously, *in vitro* studies have reported the reamed cavity diameter was, on average, 0.56 ± 0.504 mm larger than the last-reamer used in five cadaveric acetabula (MacKenzie et al., 1994) and 0.41 mm larger (standard deviation, 0.32 mm) in 38 specimens (Kim et al., 1995).

Macdonald et al. found greater differences under surgical conditions. Cavities were found to be larger than the last-reamer used by a mean of 2.1% and the differences ranged from -0.2% to 5.7% in ten patients presenting for a total hip arthroplasty (Macdonald et al., 1999).

While the reamed acetabulum should be close to being a true hemispherical shape to achieve optimal contact upon implantation (Kim et al., 1995), achieving an ideal shape is challenging due to the imprecision of the reaming process (Kim et al., 1995). Uneven elasticity in the bone may distort the cavity and result in a departure from a hemispherical shape (Macdonald et al., 1999; Schwartz Jr et al., 1993). Previous studies measuring reamed cavity dimensions have reported lower root mean square errors (RMSEs) for best-fit ellipsoids than best-fit spheres (Kim et al., 1995; MacKenzie et al., 1994). Kim et al. found the ratio of the ellipsoid principal axes transverse to longitudinal axis of the cavity to the best-fit sphere diameter to be 0.99 ± 0.01 and 1.00 ± 0.02 (Kim et al., 1995). MacKenzie et al. found the transverse axes were 0.85% larger than the best-fit sphere (MacKenzie et al., 1994).

The extent to which a surgeon reams medially affects cup stability but there are contrasting views in the literature as to the optimal reaming depth. Several authors advocate removing the subchondral plate and reaming to the floor of the acetabular fossa in order to provide intimate bone-implant contact (Callaghan et al., 1995; Schmalzried et al., 1992a; Schwartz Jr et al., 1993) and reduce the risk of prosthetic overhang (Bonnin et al., 2012). However, reaming the subchondral plate weakens the bone and can increase micromotion (Morscher et al., 1989). Therefore, some surgeons are more conservative in their reaming and preserve the subchondral plate (Bonnin et al., 2012; Morscher et al., 1989). This technique leaves a space between the cup and the acetabular fossa and creates large interfacial gaps (Bonnin et al., 2012).

The orientation of an acetabular cup is described by its inclination and anteversion (Figure 2.13). The anteversion angle, as observed at operation, is the angle between the longitudinal axis of the patient and the acetabular axis projected onto the sagittal plane. The acetabular axis is the axis that passes through the centre of the cup and is perpendicular to the plane of the cup

mouth. The inclination angle is the angle between the acetabular axis and the transverse axis (Murray, 1993). The acetabular cup is normally orientated with a mechanical alignment guide which has two rods perpendicular to each other. The inclination of the cup is set by placing the vertical rod of the guide perpendicular to the theatre floor and the horizontal rod in a perpendicular position. Anteversion is achieved by rotating the guide until the horizontal rod is in line with the longitudinal axis of the patient. Mean inclination and anteversion angles of 40 - 48° and 5 - 30° respectively have been reported in non-dislocation patients (Seagrave et al., 2017).

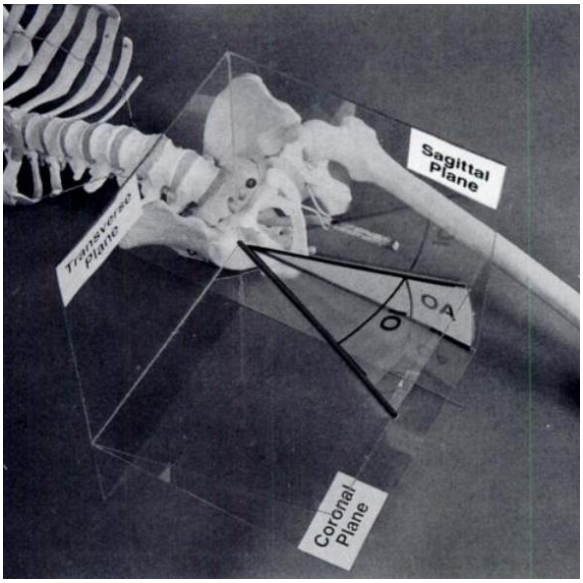

Figure 2.13 Anteversion (OA) and inclination (IO) as observed at operation (Murray, 1993).

There is no consensus on the optimal orientation of the acetabular cup in total hip arthroplasty (Seagrave et al., 2017). Lewinnek et al. proposed a "safe zone" as inclination of 40 ± 10° and anteversion as 15 ± 10° that has become a standardised range for acetabular cup orientation (Figure 2.14) (Lewinnek et al., 1978). However, several authors have criticised the Lewinnek safe zone for being derived from 9 cases of dislocation in a series of 300 total hip arthroplasties, 3 of which occurred within the safe zone (Biedermann et al., 2005; Moskal et al., 2013). A previous study examining the cup orientation in 127 total hip arthroplasties with dislocation found 60% were within the safe zone (Biedermann et al., 2005).

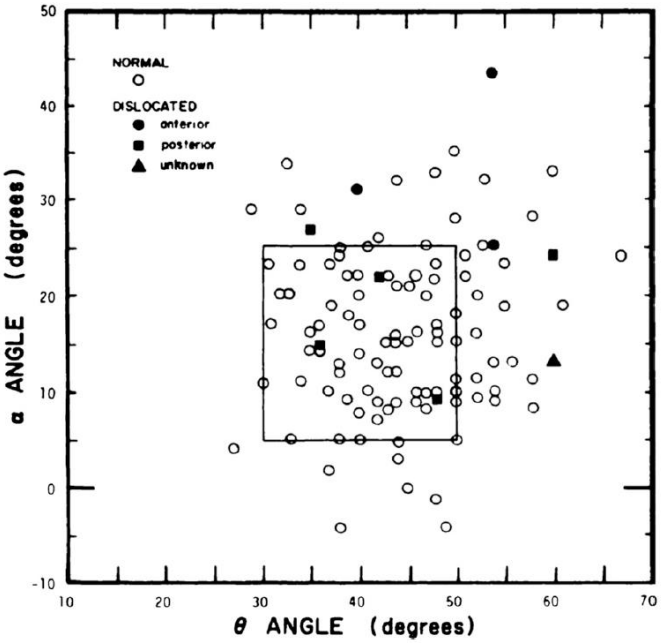

Figure 2.14 The "safe zone" (shown as a box) for acetabular cup orientation (Lewinnek et al., 1978)

Improper acetabular cup orientation contributes to dislocation (Lewinnek et al., 1978), osteolysis and cup migration (Kennedy et al., 1998). Poor visualisation, inaccuracies of mechanical alignment guides (Kalteis et al., 2009) and intraoperative pelvic motions (Asayama et al., 2004) can negatively influence acetabular cup orientation. Most conventional alignment guides do not account for the tilt of the bony pelvis and assume a neutral pelvic position which can have a significant influence on cup orientation (Kalteis et al., 2009). Intraoperative motions of the pelvis can be caused by fixation of the pelvis on the operating table, leg position during surgery, and movement generated by the surgical procedure itself (Asayama et al., 2004). If the patient is in the lateral decubitus position, a forward roll can result in a decrease in acetabular component anteversion relative to external landmarks (Schmalzried, 2009). Image-guided surgical navigation systems and robotic assistive devices have been developed to provide intraoperative measurement of pelvic location and relative cup alignment to try to overcome the limitations of conventional alignment guides (DiGioia et al., 1998)

Orientating the cup based on anatomical landmarks is an alternative method for cup positioning (Moskal et al., 2013). A commonly used method described by Archbold et al. takes the transverse acetabular ligament as a reference to orientate the cup (Archbold et al., 2006). The transverse acetabular ligament is a ligament that crosses the acetabular notch and fills the gap in the inferior aspect of the acetabulum (Martini et al., 2012). To prepare the acetabulum with this technique, the patient's natural anteversion is matched by aligning the reamer parallel to the ligament (Archbold et al., 2006). This technique does not require any external guides and the orientation is independent of the patient's position on the table (Moskal et al., 2013). In a series of 1000 total hip arthroplasties using this technique, the reported dislocation rate was 0.6% (Archbold et al., 2006).

2.5.2 Insertion of Press-Fit Cementless Cups

The acetabular shell is firmly impacted into position using several blows to the insertion device. Advancing the cup into the acetabulum expands the peripheral acetabular bone and generates high compressive forces that act on the cup periphery to provide stability (Mathieu et al., 2013). Elastic spring back of the cup occurs due to elastic recoil of the acetabulum which leaves a gap at the pole of the cup immediately after implantation. When inserted, the acetabulum squeezes the cup which creates additional radial compression superiorly and inferiorly (Morscher, 1992).

Primary stability of cementless cups can be maintained with the press-fit mechanism but perfect apposition with the bone following implantation remains difficult. Udomkiat et al. reported 37 of 105 hips had a gap around the cup on initial postoperative radiographs (Udomkiat et al., 2002). In an *in vitro* study, Schwartz reported imperfect contact in all 12 cadaveric specimens studied. Contact distributions varied from a small area to almost complete contact on the surface of the cup (Schwartz Jr et al., 1993). MacKenzie et al. found contact of up to 20% of the entire cup surface for 2 mm oversized cups, while 12.3% contact area for cups with 0 mm interference fit (also called exact-fit) (MacKenzie et al., 1994).

Due to the mechanism for achieving primary stability with press-fit, the bone-implant contact distribution exhibits preferential contact at the periphery of the cup and little or no contact at the pole (Kim et al., 1995; MacKenzie et al., 1994). For hemispherical cups with interference fits of 0 to 2 mm, fractional microcontact of 0.5 to 9% has been reported in the polar and middle regions of the cup, while the microcontact at the peripheral region has been 10 to 41%. MacKenzie et al. reported the average gap at the polar region was 1.37 mm with 2 mm oversized cups and less than 1 mm with exact-fit cups in cadaveric specimens (MacKenzie et al., 1994). Kim et al. reported higher magnitude polar gaps in 38 specimens with 2.7 ± 1.1 mm (Kim et al., 1995).

2.6 Pre-Clinical *In Vitro* Testing

Pre-clinical testing aims to evaluate of acetabular cups in order to screen out poor designs. Historically, prostheses have been tested *in vitro* to assess possible failure scenarios. Excluding the tests required for a prosthesis to meet regulatory standards, *in vitro* tests focus on the biomechanical function of a cup by applying loads when it is implanted in synthetic bone and cadaver specimens (Cristofolini, 2015). Due to the concern of aseptic loosening, i*n vitro* measurements are commonly used to assess the primary stability of cementless acetabular cups.

In experiments with cadavers, hemipelvis specimens are securely mounted into a loading apparatus before a load is applied (Figure 2.15). Perona et al. embedded each pelvis in gypsum dental stone prior to mounting them into the apparatus to minimise rigid body motion (Perona et al., 1992). Won et al. firmly clamped their pelvis specimens at the iliac crests to the baseplate of an apparatus (Won et al., 1995). These typical restraints on the hemipelvis *in vitro* do not match the physiological support at the sacroiliac joint and pubic symphysis and may over-constrain the hemipelvis compared to *in vivo*. Loading conditions *in vitro* can vary from simple loads like pure axial force or torsional moments to more complex ones replicating physiological loading. Most studies apply loads cyclically to a maximum load representing peak hip contact force during an activity (Clarke et al., 2012a; Won et al., 1995; Perona et al., 1992) such as

single-stance phase of gait (Perona et al., 1992). However, these loading regimes applied do not encompass the complete gait cycle loading. Moreover, while some studies orient the hemipelvis into a position relative to the applied load to shift the axis of the load (Won et al., 1995; Kwong et al., 1994), the load directions may not reflect the direction of hip joint loading that occurs *in vivo*.

Figure 2.15 A pelvis specimen positioned in a loading apparatus to provide a force similar to anatomic forces produced during the stance phase of gait (Perona et al., 1992)

In vitro studies have previously quantified the primary stability of cementless acetabular cups with different methods (Table 2.1). Several studies have assessed primary stability with the peak failure load during uniaxial pull-out, push-out, or tangential lever-out tests (Antoniades et al., 2013; Baleani et al., 2001; Crosnier et al., 2014; Curtis et al., 1992; Fehring et al., 2014; Lachiewicz et al., 1989; Markel et al., 2002). Other studies have measured micromotion of the cup under physiological loads with linear variable differential transformers (LVDTs) connected through the screw hole at the dome of the cup (Crosnier et al., 2014; Kwong et al., 1994) or secured to the periacetabular bone at locations corresponding to the ilium,

ischium, and pubis (Perona et al., 1992; Stiehl et al., 1991; Won et al., 1995). However, measuring micromotion at a small number of sites fails to provide information on micromotion over the entire cup-bone interface. Measurements at additional locations require using more transducers which is associated with an increase in cost and complexity of the testing set-up (Cristofolini et al., 2010b).

Researchers have taken *in vitro* measurements of areas of contact and the extent of interfacial gaps following cup implantation with moulds and pressure-sensitive films. Studies found less than complete contact at the interface between the cup and bone (Kim et al., 1995; MacKenzie et al., 1994; Schwartz Jr et al., 1993). Little or no contact has been demonstrated in the polar region of cup and more preferential engagement at the periphery (Kim et al., 1995; MacKenzie et al., 1994). However, Kim et al. did find that for exact-fit hemispherical cups had better contact in the polar region and less dense contact at the periphery (Kim et al., 1995). Polar gaps have been consistently found *in vitro* with oversized cups, with a reported range of < 1 mm to 3.85 mm (Kim et al., 1995; MacKenzie et al., 1994). However, moulds and pressure-sensitive film can only record contact at the instant of maximum contact. Thus, interfacial gaps formed as a result of cup rebounding during implantation are difficult to measure with *in vitro* methods. As cup-bone apposition remaining after rebounding is important for bone ingrowth (Chen et al., 1983), this limitation may affect observations.

Pre-clinical *in vitro* studies are typically conducted to compare the primary stability of two or more different prosthesis designs (Adler et al., 1992; Antoniades et al., 2013; Baleani et al., 2001; Lachiewicz et al., 1989; Stiehl et al., 1991), porous-coatings (Markel et al., 2002), or fixation methods (Adler et al., 1992; Kwong et al., 1994; Perona et al., 1992; Won et al., 1995). Results from studies comparing press-fit and screw fixation suggest that the inclusion of screws can reduce local micromotion near the screw but may not significantly enhance the overall primary stability of the cup (Kwong et al., 1994; Won et al., 1995). However, due to limited availability of human tissue specimens, the sample size for each design tested may be

statistically underpowered in many studies. This prevents drawing of statistically meaningful conclusions, unless a large effect exists that can be statistically detected even with a small sample size (Cristofolini et al., 2010b). Therefore, *in vitro* testing is not ideal for performing comparative studies where a large number of subjects need to be explored (Cristofolini et al., 2010b).

Several studies have attempted to determine the effects of patient or surgical related parameters on the primary stability of cementless cups. When investigating bone quality, stability of cups has been found to be lower in low density (0.2 g cm^{-3}) foam blocks compared to high density (0.5 g cm^{-3}) blocks (Baleani et al., 2001; Crosnier et al., 2014). Results from studies examining the effect of interference press-fit cups suggest 1 mm interference fit provides optimal stability *in vitro* (Adler et al., 1992; Kwong et al., 1994). Adler et al. found cup sizing and depth of the acetabular cavity in surgical preparation were important for primary stability of the cup. However, *in vitro* studies only provide a limited description of the behaviour of the bone-implant construct in different patients or after surgery. Even the most extensive experimental studies can only explore a small subset of all possible surgical scenarios that occur *in vivo* (Viceconti et al., 2006).

Table 2.1 Summary of *in vitro* studies examining the primary stability of cementless acetabular cups.

Author	Model	N	Aims	Primary Stability Metrics	Main Findings
Lachiewicz (1989)	Cadaver	20	Assess the primary stability of three porous-coated cup designs	Cup Motion: 570 - 970 μm. Max Torque: approx. 32 - 46 Nm	Superior stability in three screws compared to two-peg or three-spike fixation
Stiehl (1991)	Cadaver	33	Compare five different porous-coated designs	Average mean micromotions were 89 μm and 86 μm for anteromedial and posterolateral transducers. No cup had average mean > 125 μm and 4 had > 150 μm	Good primary stability for all designs but best configuration was 1 mm interference fit with 2 screws
Adler (1992)	Foam Blocks and Bovine Bone	24	Investigate the effect of 6 cup designs, bone density and surgical preparation on primary stability.	Tangential Stability: Low Density 30 - 110 N High Density 40 - 100 N Bovine Bone 10 - 150 N	Cup Geometry, sizing, and depth of the acetabular cavity are important in determining primary stability
Perona (1992)	Cadaver	11	Compare primary stability of press-fit, screw fixation and spikes	Press-fit: 54 - 162, One screw: 51 - 134, two screws: 52 - 126, spikes: 39 - 143	One screw does not significantly affect primary stability. Two screws provide added support at ilium but fails to decrease micromotion at the pubis or ischium. Spiked fixation does not restrict motion to the same extent as screws
Curtis (1992)	Cadaver	40	Assess the effect of interference fit on primary stability of a cementless hemispherical cup	Torque to produce rotation of 2°: 1 mm = 13.7 Nm, 2 mm = 2.8 Nm 3 mm = 29 Nm 4 mm = 35 Nm	2 - 3 mm interference fit gave better stability than 1 mm. 4 mm interference fit caused some fractures.
Schwartz (1993)	Cadaver	12	Determine the cup-bone apposition of press-fit, spiked and threaded hemispherical cups	Less than complete interface contact was achieved in most cases	Retention of the subchondral plate causes incomplete seating of cups with spikes or threads.

Table 2.1 Continued

Author	Model	N	Aims	Primary Stability Metrics	Main Findings
Kwong (1994)	Cadaver	6	Compare the primary stability of press-fit and screw fixation of Titanium cup	2 mm: Polar Gap 0.5 - 1.5 mm Micromotion = 35 μm (Press-fit), 38 – 23 μm (1 to 4 screws). 1mm: Micromotion = 22 μm (Press-fit), 20 – 15 μm (1 to 4 screws) Exact-fit: Micromotion = 62 – 40 μm (1 to 4 screws). Lateral Tilt micromotion displayed.	1mm with or without screws provided optimum combination to reduce micromotion and avoid discernible gaps. Incomplete seating with 2 mm press-fit. Addition of screws did not significantly enhance stability of prosthesis.
MacKenzie (1994)	Cadaver	28	Examine the effect of interference fit on contact area and extent of gaps of press-fit cups	Contact: Exact-fit = 12% 2 mm interference fit = 19.6%, 1 mm interference fit = 16.4% Interfacial Gap (5 mm from pole): Exact-fit = < 1 mm 2 mm interference = 1.37 mm 4 mm interference = 3.85 mm	Extensive peripheral cup contact but minimal polar area contact. Less peripheral contact on exact-fit. Consistent finding of extensive polar gaps for over-sized cups.
Won (1995)	Cadaver	12	Compare primary stability of press-fit and screw fixation	Average Micromotion: Press-fit = 34 μm 2 Screws = 34 μm 3 Screws = 30 μm 4 Screws = 30 μm	Adding screws decreased micromotion at the site of the screw but sometimes increased it at the opposite side. The addition of screws does not necessarily increase primary stability.

Table 2.1 Continued

Author	Model	N	Aims	Primary Stability Metrics	Main Findings
Kim (1995)	Cadaver	38	Examine areas of contact and extent of polar gaps created with exact-fit and oversized hemispherical and elliptical hemispherical cups	Polar Gap: Hemispherical = 1.3 mm 2 mm interference hemispherical = 2.1 mm Exact-fit elliptical = 2.7 mm 1 mm interference elliptical = 3.1 mm	Seating of exact-fit hemispherical was best near the pole and poorest nearest the rim. The exact-fit elliptical cup had better compromise between polar and rim contact than 2 mm oversized hemispherical cups.
Baleani (2001)	Foam Block	6	Investigate the effect of fins on the primary stability for 2mm and 0mm in high and low density	Frontal Stability Torque: 2 mm interference: (high density) 40 - 41 Nm (low density) 9 - 11 Nm, 0 mm interference: (high density) 0 - 14.5 Nm (low density) 0 - 2.9 Nm	The addition of fins enhanced stability, especially for low density and 0 mm interference.
Markel (2002)	Foam Block	11	Examine the primary stability of hemispherical cementless cups with fibre mesh, beaded and plasma-sprayed surface treatments	Mean lever-out loads to create 150 μm maximum rim rotation: Beaded = 504 N Fiber Mesh = 455 N Plasma-sprayed = 1157 N	Plasma-sprayed withstood stood greatest tangential load within the 150 μm range of motion
Antoniades (2013)	Foam Block	10	Compare the primary stability of two cups by the same manufacturer that differed by geometry	Peak pull-out force: 1. 579 - 820 N 2. 626 - 814 N Peak lever-out moment: 1. 9.7 - 17.5 Nm 2. 12.2 - 18.3 Nm	Primary stability of both cups was similar

Table 2.1 Continued

Author	Model	N	Aims	Primary Stability Metrics	Main Findings
Crosnier (2014)	Foam Block	12	Compare spherical and physiological acetabular geometries. Assess the effect of density on the micromotion of the cup.	Spherical = 137 μm Physiological = 161 μm High density = 161 μm Low density = 90 μm (Max in Z-direction only shown)	Spherical cavity may overestimate the micromotion of the cup. Micromotion in low density blocks higher compared to high density block.
Fehring (2014)	Cadaver	17	Determine range of primary stability in cementless cups. Assess the effect of 1 mm vs 2 mm interference fit	Mean bending moment to cause > 150 μm: 1 mm interference fit = 17.3 Nm, 2 mm interference fit = 18.9 Nm	High variability in bending moments to create > 150 μm. No significant differences found between 1 mm and 2 mm interference fit.

2.7 Pre-Clinical Finite Element Modelling

Finite Element (FE) modelling was introduced to orthopaedics in 1972 as a method for analysing the mechanical behaviour of skeletal parts (Brekelmans et al., 1972). It was traditionally used to investigate the stress and strain in bones and the relationship between architecture and joint loading (Huiskes and Chao, 1983). Since then, technologic advances in computer processing have allowed FE models to be applied in the design and pre-clinical testing of hip prostheses (Prendergast, 1997).

2.7.1 FE Models of the Hemipelvis

The hemipelvis is an important weight-bearing structure in the human body with a complex geometry and structure. Early FE models of the hip joint were either two dimensional (Rapperport et al., 1985; Vasu et al., 1982) or axisymmetric (Pedersen et al., 1982) approximations of the hemipelvis anatomy. Neither of these approaches adequately represented the mechanical environment of the acetabulum and predictions were far from the actual conditions. Two dimensional models could not account for the out-of-plane aspect of the acetabulum wall (Dalstra et al., 1995), leading it to have a low stiffness and, in turn, an overestimation of stresses in the acetabular region (120 MPa) (Vasu et al., 1982). Axisymmetric models assume the acetabular wall is present around 360° (Dalstra et al., 1995) which requires the material properties and geometry of the acetabulum around the axis to be adequately described by a single two-dimensional section. The representative section has been previously taken at the superior region of the acetabulum (Pedersen et al., 1982; Ries et al., 1997; Spears et al., 1999) where the bone-mineral density is high, leading models to have a high stiffness and, in turn, an underestimation of stresses (0.5 MPa) (Pedersen et al., 1982).

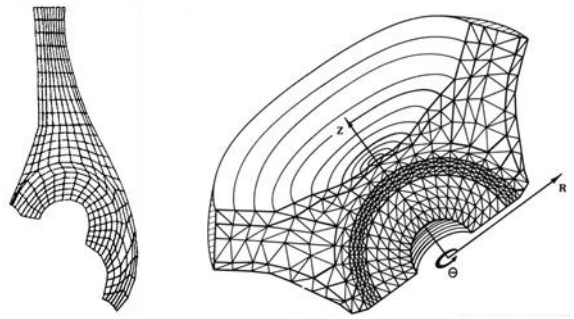

Figure 2.16 Two dimensional (left) and axisymmetric (right) models of the implanted hemipelvis (Pedersen et al., 1982; Vasu et al., 1982)

More realistic descriptions of the shape and architecture of the hemipelvis were developed with the introduction of three dimensional models. To produce a three-dimensional geometry, Dalstra et al. sectioned a hemipelvis submerged in polyester resin by cutting 6 mm slices. The contour of each sectioned bones was digitised, divided into 4-node elements and then connected to the elements of the subsequent contours to form an FE mesh (Dalstra et al., 1995). As increased computational power has become more widely available, high-fidelity models are being constructed from three-dimensional imaging modalities (Young et al., 2008).

Extraction begins with image segmentation of the bone voxels on individual slices of the CT image (Anderson et al., 2005; Leung et al., 2009; Thompson et al., 2002). Following segmentation, there are several techniques available for generating volumetric meshes from the boundaries defined by the segmented data. Traditional meshing techniques generate three-dimensional volume meshes from image data with an intermediary step of surface reconstruction followed by an application of CAD-based meshing algorithms. The two most common tetrahedral mesh generation approaches are the advancing front approach and Delaunay tetrahedralization (Young et al., 2008). These techniques require reconstructing a suitably smooth surface mesh prior to the application of meshing algorithms. One surface reconstruction approach is to extract contours of the segmentation for the different slices of the

CT image and combine them form a three-dimensional surface. An alternative approach is based on marching cubes algorithm (Young et al., 2008). This algorithm considers the centre points of voxels in the image to be the vertices of a grid of cubes. Based on whether a vertex is considered inside or outside the volume of interest, the edges bridging vertices inside and outside the object can be bisected and a configuration of triangular patches is assigned to each cube.

The resultant surface extracted is used as the starting point for triangulated bounding surfaces to be used for meshing with advancing front or Delaunay meshing techniques. In the advancing front approach, additional nodes are added on the inside of the initial surface triangular discretization to generate a first layer of tetrahedra. This is followed by another set of nodes forming another layer of tetrahedra on top of the first and continues until the volume is generated. Delaunay meshing starts from a distribution of points within a convex hull. A Dirichlet tessellation of the domain consisting of polyhedral cells enclosing each distributed point is generated. Connecting the generated points across the polyhedral boundaries results in a Delaunay tetrahedralization of the volume. Alternatively, grid-based methods, such as the voxel method, can simplify and make robust the meshing process by bypassing the surface generation stage. The voxel method combines geometric detection and mesh creation stages into one process (Keyak et al., 1990). As this meshing process is carried out directly from the imaging data there is a one-to-one correspondence between parent image sample values and elements it is easy to assign inhomogeneous material properties to the elements. However, the approach does not allow element size to adapt to features or allow for localized mesh refinement (Young et al., 2008).

The majority of current studies extract the geometry of the hemipelvis from Computed Tomography (CT) scans. Extraction begins by is based on image segmentation of the bone contours on individual slices of the CT image (Anderson et al., 2005; Leung et al., 2009; Thompson et al., 2002). The contours are combined and smoothed to form a solid three-

dimensional model of the hemipelvis. Finally, a volumetric finite element mesh is then created from the three-dimensional model.

Unlike long bones such as the femur, the hemipelvis resembles a 'sandwich' structure, where the low density cancellous bone is surrounded by a thin layer of cortical bone (Dalstra and Huiskes, 1991). To replicate this structure, Dalstra et al. applied membrane elements on the free surface of hemipelvis mesh (Dalstra et al., 1995; Thompson et al., 2002). However, membrane elements only have in-plane stiffness and cannot be subjected to loads perpendicular to the element. Alternatively, the cortical bone layer has been represented with shell elements (Anderson et al., 2005). Shell elements are quadrilateral or triangular elements with three translational and two rotational degrees of freedom per node (Ahmad et al., 1970). Previous studies have assigned elements representing the cortical bone a constant thickness of 0.9 – 2 mm (Manley et al., 2006; Phillips et al., 2007; Spears et al., 2001; Zou et al., 2013). Meanwhile, some studies have subject-specific models with variable cortical bone thickness derived from CT images (Anderson et al., 2005). These studies have found a range of approximately 0.45 to 4 mm for cortical bone thickness (Anderson et al., 2005; Dalstra et al., 1995; Ghosh et al., 2015; Majumder et al., 2007). Anderson et al. found no statistically significant differences in predicted strain in the cortical bone between a model with average cortical layer thickness and a subject-specific model with variable cortical layer thickness (Anderson et al., 2005).

The behaviour of the hemipelvis in an FE model depends its shape and size, as well as on the material properties assigned to the elements. CT scans provide information on bone density which can be related to the material properties (Marom and Linden, 1990). CT can measure the linear attenuation of tissue and the relationship between the greyvalues, in Hounsfiled Units (HU), and the apparent density of bone tissue is approximately linear (Rho et al., 1995). The elastic modulus can be determined from the apparent density with an empirical power relation. Density-modulus relationships vary significantly between anatomical sites due to differences in trabecular architecture and tissue modulus (Helgason et al., 2008). Dalstra et al. (1993)

developed a relationship for pelvic cancellous bone based on mechanical testing which is typically used in FE studies of the hemipelvis:

$$\mathrm{E} = 2017.3\rho_{app}^{2.46} \qquad (1)$$

where E is the elastic modulus and ρ_{app} is the apparent density (Dalstra et al., 1993). Studies using this relationship have reported cancellous bone moduli that lie within the range of approximately 2 to 3800 MPa (Anderson et al., 2005; Majumder et al., 2007; Zhang et al., 2010). In addition to the relationship, Dalstra et al. found that pelvic cancellous bone was not highly anisotropic and had a Poisson's ratio close to 0.2 (Dalstra et al., 1993).

The hemipelvis is supported at the sacroiliac joint and pubic symphysis. The sacroiliac joint has very strong ligamentous support and an interlocking surface with the sacrum which allows very little movement. The pubic symphysis is a cartilaginous joint consisting of a pad of fibrocartilage that separates the hemipelvis bones. For models not fixed to correspond to the boundary conditions of an experimental set-up (Anderson et al., 2005; Dalstra et al., 1995), rigid fixation is typically applied to the sacroiliac joint and pubic symphysis (Clarke et al., 2013; Ghosh et al., 2015; Ong et al., 2006). Other studies have joined the pubic symphysis of two pelvic bones with ligaments represented by linear spring elements or rigid links (Janssen et al., 2010; Pakvis et al., 2014). Clarke et al. developed a model that included the sacrum fixed at the L5S1 joint and pelvic ligaments which crossed between the pelvic bones and sacrum, and at the pubic symphysis. However, no differences in acetabular stress and strain were found between the model and a model in which the sacroiliac joint and pubic symphysis were rigidly fixed (Clarke et al., 2013). Phillips et al. applied complex muscular and ligamentous boundary conditions using spring elements distributed over muscle attachment points and found they reduced the stress concentrations in the cortical bone compared with a model with fixed boundary conditions applied at the sacroiliac joints (Phillips et al., 2007).

2.7.2 FE Models of Press-Fit Cup Insertion

Simulating the residual strain in the bone and the extent of interfacial gaps following insertion allows FE models to more accurately simulate the press-fit fixation that occurs clinically. Previously, studies have modelled the peripheral compression associated with press-fit fixation with a contact algorithm (Janssen et al., 2010; Pakvis et al., 2014; Udofia et al., 2007). The oversized cup is placed in the acetabulum with its elements overlapping bone elements. Subsequently, the nodes on the surface of the bone are pulled back to the cup. While this method permits compression of the acetabulum, the hemispherical cup is assumed to be perfectly seated. The absence of gaps may lead to overestimating the level of primary stability of the cup. Spears et al. found the cup rebounded a certain amount when applying the contact algorithm and there were polar gaps of 0.12 mm and 0.27 mm when full seating was assumed. A polar gap of 0.58 mm was found with a 0.5 mm initial polar gap representing incomplete penetration (Spears et al., 2001).

Attempts to represent a more realistic press-fit surgical procedure have modelled repeated hammering on an insertion device to seat the cup. Studies have used incremental static loads (Spears et al., 1999; Yew et al., 2006) or successive impactors with the same initial velocity (Hothi et al., 2011; Michel et al., 2016) to drive the cup into the acetabulum on each impact and then allow it to rebound when the load is removed. The insertion simulation is ended when further impactions have negligible effect on the residual cup seating. Spears et al. and Yew reported using 4 load cycles to seat the cup, while Michel reported using 18 impacts and Hothi et al. required a range of 1 to 23 impacts for different configurations of interference fit and impact velocities (Hothi et al., 2011; Michel et al., 2016; Spears et al., 1999; Yew et al., 2006). However, these studies performed cup insertion using two-dimensional axisymmetric models and there would be a drastic increase in computational cost for three-dimensional models of the hemipelvis with contact surfaces (Yew et al., 2006).

Displacement-control insertion of the cup is an alternative method to simulate the press-fit procedure without a high computational cost. Yew et al. demonstrated reasonably good agreement in predicted cup deformation between a finite element model of cup inserted into a polyurethane foam block by displacement and a previous experiment (Jin et al., 2006; Yew et al., 2006). While considerably higher press-fit forces were found with displacement-controlled insertion compared to load-controlled, similar predictions were made for polar gap with a shorter simulation time. Previous studies investigating the primary stability of cementless cups in three-dimensional models of the hemipelvis have inserted the cup into the acetabular cavity by displacing it along a path perpendicular to the cup rim (Clarke et al., 2012b; Ong et al., 2006; Ong et al., 2008). While this generated compression at the cup periphery, none of these studies reported on the strain in the acetabulum. Moreover, Clarke et al. had pre-determined polar gaps which prevented the effects of parameters on their size being investigated (Clarke et al., 2012b).

2.7.3 Primary Stability of Cementless Cups

Patient and surgical variability has the potential to affect the primary stability of a cementless acetabular cup. Anatomical, material property, and obesity level variations exist between patients as a result of a range of factors including gender, age, and underlying pathologies. Moreover, uncertainty in cup positioning and geometry of the reamed acetabular cavity achieved by the surgeon means the prosthesis can be subject to a broad spectrum of environments that may affect primary stability. Studies use FE models to examine the effects of patient- and surgical-related parameters on the primary stability (Table 2.2). Once models are created, FE allows input parameters to be easily adjusted so that variability can be included.

A decrease in bone quality, as defined by elastic modulus, has been previously found to increase micromotion of the cup. Janssen et al. found peak micromotion of 381 μm for a hemispherical cup in a model with 'poor bone quality' in which the elastic moduli of the local subchondral quality was reduced by half compared to a peak of 179 μm for the 'good bone quality' model (Janssen et al., 2010). Meanwhile, Hsu et al. reported that peak micromotion had a non-

linear increase from 80 to 160 μm and decrease of 55% to 33% of the cup region with micromotion < 28 μm when the homogeneous elastic moduli of bone (Cortical bone: 5.6 GPa, subchondral bone: 500 MPa, cancellous bone 100 MPa) were uniformly decreased in 10% increments to 50% (Hsu et al., 2007). Similar trends have been observed in other studies (Amirouche et al., 2015).

Among surgical parameters, varying the interference fit has been found to affect primary stability of the cup. Spears et al. found larger polar gaps and smaller contact areas in models with 0.5 mm interference fit compared to 0.25 mm interference fit (Spears et al., 1999). Similarly, Hothi et al. and Michel et al. found incrementally larger polar gaps for all impact velocities when interference fits were examined at 0.25, 0.5, 1, and 2 mm (Hothi et al., 2011; Michel et al., 2016). For micromotion, Spears et al. found the lower micromotion in a model with a 0.5 mm interference fit compared to an exact-fit but highest micromotion in a cup with a 1.5 mm interference fit (Spears et al., 2001). Udofia et al. predicted little difference in peak micromotion for interference fits of 1 mm (6.8 μm) and 2 mm (5.9 μm), while highest micromotion was predicted for an exact-fit (60 μm) (Udofia et al., 2007).

The main limitation of studies investigating patient and surgical variability in the primary stability of cementless cups is that only one subject has been modelled. By examining one hemipelvis model, variations in bone geometry and material property distribution that exist between individuals cannot be fully considered. Clarke et al. demonstrated that bone anatomy was highly influential on the micromotion of metal-on-metal cementless cups with a small sample size (N = 4) (Clarke et al., 2012b). While this is indicative of the need to include multiple subjects, all FE meshes in the study were uniformly scaled so they had a reamed cavity with diameter of 52 mm (Clarke et al., 2012b). Furthermore, the sample size was smaller than would be expected in an equivalent clinical study. Therefore, there is a limit as to how much findings can be extrapolated to the target population (Radcliffe et al., 2007).

Larger sample sizes may be required in order to account for patient variability when assessing the primary stability of cementless cups in pre-clinical FE studies. Studies comprising

of large cohorts of FE models have investigated load transfer in a femoral resurfacing prosthesis (Bryan et al., 2012) and the primary stability of cementless tibial trays (Galloway et al., 2013) and short femoral stems (Bah et al., 2015). By using a large number of subjects, the spread of primary stability of a cup in a population can be predicted and allow statistically meaningful analysis to be performed on the influence of patient-related factors (Taylor et al., 2013).

Significant time and computational costs are associated with generating and running populations of subjects. Therefore, techniques to reduce the computational cost of accounting for patient variability may help make pre-clinical testing more feasible. To circumvent the need for collecting and manually generating FE models from large CT datasets, studies have used shape and intensity statistical models to examine large populations of femurs whilst incorporating geometry and material property variation (Bah et al., 2015; Bryan et al., 2012; Galloway et al., 2013). Alternatively, if a population of CT images is not available, a few subjects that are representative of the extremes of variability of that population could be investigated to give a gross estimation of variability in primary stability (Viceconti et al., 2005).

In addition to patient- and surgical-related parameters, the primary stability of the cementless cup depends on the magnitude and direction of the external forces transmitted by the daily activities that a patient performs. FE studies have applied a single load representing the peak load of an activity under the assumption that it produces the peak micromotion. The peak gait load from normal walking is commonly applied with magnitudes varying from 1500 N (Amirouche et al., 2014), to 2835 N (Clarke et al., 2012), and 3200 N (Udofia et al., 2007) representing different bodyweights of the patients. However, Ong et al. demonstrated that micromotion, as well as the change in volume between the cup and bone were sensitive to the direction of the applied load (Ong et al., 2008).

Other studies have applied the stance phase and the full cycle of level gait in a number of phases ranging from 5 to 10 (Spears et al., 2000; Hsu et al., 2007; Janssen et al., 2010; Pakvis et al., 2014). Among the FE studies applying gait cycle loading conditions in models, there has

been variation where the peak micromotion occurs. Spears et al. and Hsu et al. found the highest micromotion occurred in the terminal stance phase of gait, prior to toe-off (at approximately 40% of gait) (Hsu et al., 2007; Spears et al., 2001), whereas Pakvis et al. found the highest micromotions at the beginning of the swing phase (phase 6 of 8) (Pakvis et al., 2014). Spears et al. found that increasing gait speed caused an increase in the magnitude of micromotion and that maximum values occurred earlier in the cycle. The greatest micromotion for slow walking (> 100 μm) occurred at toe-off, while for normal and fast gait speeds the greatest micromotion were highest at heel-strike (Spears et al., 2000).

Table 2.2 Summary of FE studies examining the effect of patient, surgical, and design parameters on the primary stability of cementless acetabular cups.

Author	N	Parameters Investigated			Polar Gap	Micromotion	Other Metrics	Main Findings
		Surgical	*Patient*	*Design*				
Spears (1999)	1	Interference fit	-	Friction coefficient	0.25 mm: 0.17-0.24 mm 0.5 mm: 0.35 - 0.7 mm (friction 0.1-0.5)	-	Contact Area: 1. 20-44% 2.13-26%	Better seating with intermediate coefficient of friction and lower interference fit.
Spears (2000)	1	-	Activities of daily living	-	0.5 mm (set prior to analysis)	0 - 200 µm	-	Highest micromotion for climbing upstairs.
Spears (2001)	1	Interference fit Penetration	-	Screw fixation	0.12mm 0.58mm 0.27mm	1. 1mm interference: 0 - 6 µm 2. 2mm interference fit: 20-50 µm	-	Increased interference fit increased micromotion. Higher penetration decreased micromotion. Influence of screw fixation difficult to isolate.
Yew (2006)	1	Impaction procedure	-	-	1. 0.164 mm 2. 0.172 mm	-	-	Displacement control had considerably higher press-fit force. Polar gap predictions were similar.

Table 2.2 Continued

Author	N	Parameters Investigated			Polar Gap	Micromotion	Other Metrics	Main Findings
		Surgical	*Patient*	*Design*				
Ong (2006)	1	Cup penetration distance	Peak gait load mag. Peak gait load direction	Cup equatorial diameter Cup eccentricity	Max Polar Gap = 0.4 mm	-	Total Contact Area: 1465 – 3869 mm^2 Rim Contact Area: 575 – 1019 mm^2 Chang in gap volume: 32 - 161 mm^3	Design parameters explained most of the variations in the change in gap volume, rim contact area and total contact area.
Udofia (2007)	1	Interference fit	-	-	-	1mm interference fit: max=6.8 µm 2mm interference fit: max=5.9 µm	Contact area < 50 µm: over 70% for 1mm and 2mm interference	Reduction in micromotion with increase in interference fit

Table 2.2 Continued

Author	N	Parameters Investigated			Polar Gap	Micromotion	Other Metrics	Main Findings
		Surgical	*Patient*	*Design*				
Hsu (2007)	1	-	Bone quality	Number of screws Friction coefficient	-	Peak micromotion for one screw: 7.5 - 126.3 μm. Peak micromotion for decreasing bone quality 80 - 160 μm	Stable Region (< 28 μm): 55% - 33% approx.	Increasing number of screws reduced peak micromotion and increased size of region < 28 μm. Non-linear increase in peak micromotion and decrease in region < 28 μm bone stiffness decreased. The influence of friction was less significant than bone quality.
Ong (2008)	1	Cup penetration Nominal reaming deviations at equator/pole. Frequency of reamer undulations (cross and transverse sections) Peak amplitude and decay rate of amplitude of undulation	Peak gait load mag. Peak gait load direction Density-modulus relation	Cup equatorial diameter Cup eccentricity	-	Mean: 30-45 μm 95th Percentile: 100-200 μm	Mean Potential Ingrowth Area: 25 - 30%	Design variables did not contribute as much to variation as patient and surgical variables.

Table 2.2 Continued

Author	N	Parameters Investigated			Polar Gap	Micromotion	Other Metrics	Main Findings
		Surgical	*Patient*	*Design*				
Janssen (2010)	1	Interference fit	Bone quality	Cup Geometry Friction coefficient Cup Elastic Modulus	-	All Cup Geometries: max = 174-1620 µm Hemispherical Cups: max = 179 - 381m	Lever-out moment: 1.5 - 13.5 Nm	Poor bone quality resulted in larger micromotion. Decreasing interference fit increased micromotion. Lower friction coefficient increased micromotion. Lower cup elastic modulus led to slight increase in micromotion
Zivkovic (2010)	1	Interference fit	Bone quality	-	-	0-550 µm	-	Higher interference fits increased polar gap. Higher interference fit decreased micromotion. Increasing bone density decreased micromotion.
Hothi (2011)	1	Interference fit Impact velocity	-	Friction coefficient	0.16 - 1.9 mm	-	-	Increasing interference and friction coefficient resulted in more impacts and higher impact velocity needed to seat the cup.

Table 2.2 Continued

Author	N	Parameters Investigated			Polar Gap	Micromotion	Other Metrics	Main Findings
		Surgical	*Patient*	*Design*				
Clarke (2012)	4	Cup inclination angle Cup version angle Interference fit Polar gap	Bone anatomy	-	0 - 3 mm (set prior to analysis)	Max micromotion from 8 load cases: 110 – 370 µm	-	Micromotion depended on the level of seating achieved and patient anatomy
Amirouche (2014)	1	Interference fit Cup penetration distance	-	-	0.681 mm	1mm interference fit: 430-455 µm 2mm interference fit: 378-313 µm	Contact Area: 1mm interference fit: 12.9-18.13% 2mm interference fit: 15.8-19.35%	Insertion force had greater influence on surface conformity than interference fit.
Pakvis (2014)	1	-	-	Cup Elastic Modulus	-	Maximum: 400 µm 165 µm 218 µm	Potential Ingrowth Area (% micromotion < 40 or 150) 1. 39%, 89%. 2. 58%, 99% 3. 56%, 99%	Increased cup stiffness resulted in decreased micromotion

Table 2.2 Continued

Author	N	Parameters Investigated			Polar Gap	Micromotion	Other Metrics	Main Findings
		Surgical	*Patient*	*Design*				
Amirouche (2015)	1	-	Bone quality	-	-	-	Max Displacement: Healthy bone: 78um Mild osteoporosis 111 μm Severe osteoporosis 177 μm	Decrease in bone density resulted in increased cup displacement
Michel (2016)	1	Impact velocity Interference fit	-	-	0.35 - 1 mm	-	-	Polar gap decreased with velocity and increased with interference fit

2.7.4 Experiment Designs

Low 5-year revision rates have made it increasingly difficult to differentiate between prosthesis designs after a few years of follow-up in the national joint registries (Cristofolini et al., 2003). This has meant a greater emphasis is placed on pre-clinical testing methods to screen out poor designs (Viceconti et al., 2009). FE is applied early in the pre-clinical stage to predict how a failure process initiates or progresses and identify the effect of different parameters on performance (Taylor and Prendergast, 2015). Pre-clinical experiment designs must be able to thoroughly demonstrate whether prospective cementless cup designs are robust to patient and surgical variability.

Aside from the studies of Ong et al. (Ong et al., 2006; Ong et al., 2008), patient- and surgical-related parameters have been varied in parametric studies. However, varying one parameter at a time in such parametric studies limits how a study can account for interactions which potentially occur between factors and does not consider the probability that a particular value of a parameter will occur (Taylor and Prendergast, 2015). Comparative study designs have been used to compare the primary stability of two or more prosthesis designs (Janssen et al., 2010; Pakvis et al., 2014). However, these studies were performed using a single model of a joint and under deterministic conditions, where perfect cup seating and average bodyweight were assumed. As a result, the studies only provide a limited understanding of prosthesis behaviour in the general population.

Design of Experiment (DoE) methods can assess multiple parameters at a fixed number of levels. By testing all possible combinations of the input parameters, a full factorial design can explore the influence of individual input parameters and their possible interactions. However, the number of simulations required by the design increases exponentially with the number of input parameters and can result in an impractically large study design. Clarke et al. used a full factorial design to assess the influence of 5 input parameters, at various levels, on acetabular cup failure. After the authors removed “unrealistic” cases, their experiment required 112 FE

models, 8 load cases each, resulting in a total of 896 simulations (Clarke et al., 2012b). Therefore, the adoption of full factorial designs in pre-clinical FE assessment is limited by the computational time rapidly increasing with the number of factors to be investigated, model size and complexity.

In order to reduce the computation time associated with a full factorial design analysis, other studies have used fractional factorial designs (Isaksson et al., 2008; Malandrino et al., 2009; Yao et al., 2005). Fractional factorial designs reduce the experimental effort by comprising of a subset of all possible combinations to investigate input parameters (Isaksson et al., 2009; Mason et al., 2003). While fractional factorial designs can investigate the effects of individual input variation, they have limited capability for studying interactions between input parameters and may cause misleading results (aliasing) (Mason et al., 2003).

Probabilistic analysis represents input parameters with the generation of random values from a specified range according to a distribution instead of using deterministic values or fixed levels. Computational studies have used probabilistic analysis to explore the effect of bone geometry, loading and component alignment variations on implanted joint mechanics (Fitzpatrick et al., 2012) and risk of failure (Dopico-González et al., 2010; Martelli et al., 2012). A Monte Carlo simulation is a commonly adopted probabilistic approach in which the parameter space is randomly sampled according to a desired probability distribution (Kroese et al., 2011). While Monte Carlo simulation is considered a gold standard, the number of simulations exponentially increases with the number of parameters and the accuracy of the Monte Carlo approach depends on the number of simulations. Therefore, a large sample size may be required to reach a sufficient level of accuracy. The Monte Carlo method has a stopping criterion at convergence but the square-root convergence rate is slow (Glasserman, 2003). As an example, to achieve a ten-fold increase in accuracy, the Monte Carlo method needs a hundred-fold increase in the number of data points.

Alternatively, a Latin Hypercube design samples more uniformly over the parameter space by partitioning it such that the probability of each partition is equal (McKay et al., 1979). Larger partitions at the tails of the probability distribution and more partitions near the mean ensure a smaller number of samples and a more even spread compared to Monte Carlo sampling which is prone to clustering (Fitzpatrick et al., 2011). Good agreement between the Latin Hypercube design with 50 samples and a Monte Carlo simulation with 500 samples in an examination of prosthesis alignment and loading on knee joint mechanics demonstrates it is an efficient approach that can be performed without significant loss of information (Fitzpatrick et al., 2011). Overall, by being a stochastic process, probabilistic approaches are better equipped to account for variability when examining the risk of failure and the relative contribution of parameters to performance metrics.

2.8 Summary

Total hip arthroplasty is an effective surgical intervention for relieving hip pain and disability and restoring the joint to near full function. Cementless fixation was introduced to eliminate the need for bone cement and is now the most popular option for acetabular component fixation. Cementless prostheses rely on biologic fixation, through bone ingrowth, to achieve and maintain a strong mechanical bond with the bone. Adequate primary stability is necessary to achieve bone ingrowth into the porous surface and, in turn, the long-term success of a cup. Press-fit cups achieve stability by compressive forces that act on oversized cups when they are implanted into to an undersized reamed acetabular cavity. However, excessive micromotion and large gaps at the cup-bone interface may prevent bone ingrowth. Despite rapid technological evolutions in the field, aseptic loosening remains the most common indication for revision of the cementless acetabular cup and depends on many factors including component design, patient selection and surgical technique.

With concerns about aseptic loosening and a wide variety of cementless acetabular cup design possibilities, thorough computational and experimental pre-clinical tests are required to

screen out inferior designs. To be thorough, tests must demonstrate whether a prospective design is robust to patient and surgical variability (Taylor et al., 2013). *In vitro* studies are commonly used to assess the primary stability of cementless cups in synthetic bone blocks or cadaver specimens. However, due to the limited availability of tissue specimens, even the most extensive experimental studies can only explore a small proportion of all possible combinations (Viceconti et al., 2006). Therefore, *in vitro* is unsuitable for exploring a large number of patients and surgical scenarios.

Computational studies, particularly, Finite Element (FE) modelling, allows for input parameters to be easily adjusted and tested in hemipelvis models generated from Computed Tomography (CT) images. In pre-clinical testing, this advantage allows the effect of multiple surgical scenarios on the primary stability of different press-fit acetabular cups to be assessed in the same set of subjects. However, models of the hemipelvis in FE studies have not simulated either the peripheral compression associated with press-fit fixation or the elastic spring back of the cup which occurs during insertion and creates a polar gap. Moreover, FE studies have mostly concentrated on one subject and simple parametric studies to assess the primary stability of a cup. While these studies begin to capture some aspects of patient and surgical variability, they do not consider the full spectrum of anatomical and material variation found in the population or large uncertainty in the surgical preparation and positioning of cups.

A paradigm shift in pre-clinical FE modelling is required to account for patient and surgical variability when assessing acetabular cups. Using a larger sample size of subjects, the spread of primary stability in a cup can be predicted and allow statistically meaningful analysis to be performed on the influence of patient-related factors. Moreover, designs of computer experiment allow for exploration of the surgical parameter space. However, there is a large time and computational cost associated with examining cohorts of patients and multiple surgical scenarios. Therefore, techniques which can reduce the cost of simulating this variability must also be sought. Combining the exploration of patient and surgical variability and

computationally efficient techniques to do so can help work toward more thorough computational assessment of cementless acetabular cups before they enter the market.

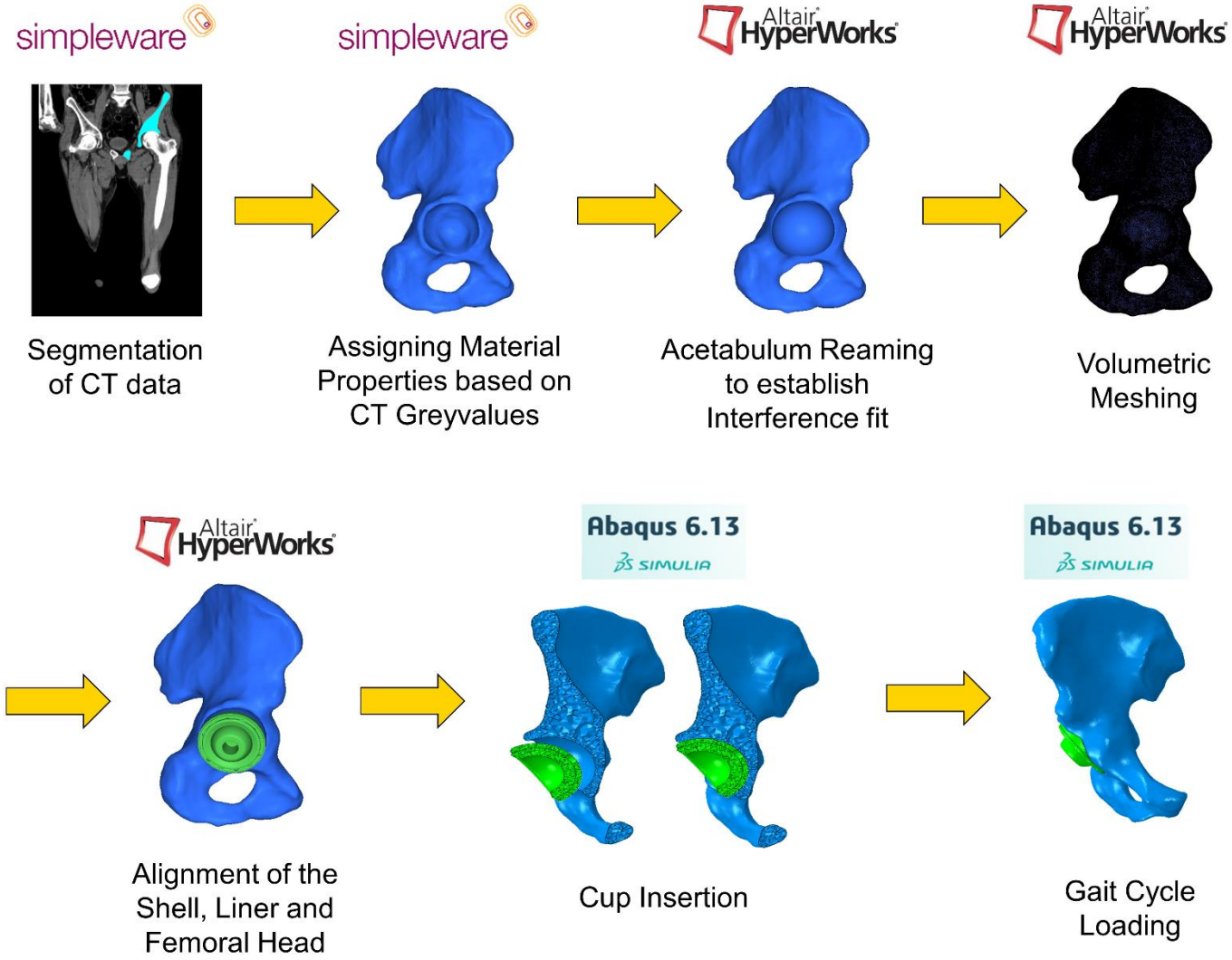

Figure Overview of the FE model development methodology

Chapter 3

Automated Methodology for Finite Element Models of the Implanted Hemipelvis

3.1 Introduction

Assessing patient and surgical variability in pre-clinical testing of primary stability of acetabular cups requires a software pipeline that can handle a large volume of analyses. To reduce the time cost associated with manually generating a new model for each analysis, a pipeline must be developed containing automated processes to generate an FE model of the implanted hemipelvis, run the FE analysis and post-process the output metrics. In the methodology presented, models of the geometry and bone material properties of 103 intact hemipelvises were manually generated from CT scan data. Once these models were generated, the pipeline could automatically size, position and implant an acetabular cup, apply loading and boundary conditions, and run the FE analysis. The output metrics describing the primary stability of the cup could then be calculated.

3.2 Computed Tomography Images

3.2.1 Subject Demographics

This work was based on CT scans collected as part of the Melbourne Femur Collection (MFC). The cohort in this study comprised of 103 cadavers with no obvious signs of hip disease. Of these subjects, 50 were male (average age, 74.1 years) and 53 were female (average age, 75.1 years) (Table 3.1). The average age of the cohort was 74.6 years (range, 60 - 95 years). The age range was similar to the age distribution in national joint registries which report an average age of 73.4 years for total hip arthroplasty recipients at the time of surgery (National Joint Registry for England and Wales, 2015) and a majority between 65 and 74 years (Australian Orthopaedic Association, National Joint Replacement Registry, 2016; Canadian Joint Replacement Registry, 2015). The average body mass index (BMI) in the cohort was 27.1 kg m^{-2} (range, 17.4 – 41.2 kg m^{-2}) and was similar to UK registry data, which reported the average BMI is 28.7 and most recipients are between 20 and 40 (National Joint Registry for England and Wales, 2015). Male subjects had larger intact acetabulum geometries than females, with diameters of 54.3 ± 2.1 mm and depths of 28.6 ± 2.7 mm compared to 47.9 ± 2.4 mm and 24.0 ± 2.6 mm.

Factor	Male (N = 50)	Female (N=53)	p
Age (yrs)	74.1 ± 10.2	75.1 ± 9.6	0.62
Bodyweight (kg)	74.8 ± 15.5	70.4 ± 15.8	0.16
BMI (kg m^{-2})	26.0 ± 2.1	28.1 ± 5.5	0.05
Intact Acetabular Diameter (mm)	54.3 ± 2.1	47.9 ± 2.4	< 0.0005*
Intact Acetabular Depth (mm)	28.6 ± 2.7	24.0 ± 2.6	< 0.0005*

* $p < 0.05$ in an independent-samples t-test

Table 3.1 Subject demographics for the 103 subjects in the cohort, divided into gender groups.

3.2.2 CT Scan Protocol

The CT scans were obtained with an Aquilion 16 MDCT scanner (Toshiba Medical Systems Corporation, Tokyo, Japan) through a helical scan protocol and typical settings for clinical examination (tube current: 180 mA, 120 kVp). The slice thickness was 2.0 mm and the spacing was 1.6 mm. The in-plane pixel dimensions were 0.976 x 0.976 mm.

The MFC was originally established with ethical oversight from the Victorian Institute of Forensic Medicine (ethics approval EC26/2000). The radiological studies took place with VIFM approvals EC9/2007 and EC10/2007. Later, sole ethical oversight for the collection was transferred to The University of Melbourne with ethics approval 115392.1. The use of the CT scans for this thesis was approved by the Southern Adelaide Clinical Human Research Ethics Committee.

3.3 Generation of Intact Hemipelvis Models

3.3.1 Image Segmentation and Model Generation

Segmented hemipelvis volumes for 47 CT scans in the cohort were available from a database generated by an automated segmentation (Zhang, 2013). In brief, an active shape model was combined with a statistical model with local image texture to iteratively segment a surface from a given CT image (Felson and Zhang, 1998). Manual refinement of the volume was carried out if the geometry was not sufficiently captured by the automatic method. For the remaining 56 subjects, hemipelvis volumes were manually segmented from the CT scans. A bone geometry was segmented using a threshold-based algorithm and manual refinement of the geometry boundaries (ScanIP, Simpleware Ltd., Exeter, UK). Segmentation of each hemipelvis took approximately 1 – 2 working days. The segmented volume was meshed to form a triangulated surface model of the hemipelvis geometry and a volumetric model with linear tetrahedral elements with an average element edge length of 0.75 mm and assigned cancellous bone material properties (ScanIP, Simpleware Ltd., Exeter, UK). The average edge length of the

elements was set below the pixel size (0.976 x 0.976 mm) and slice thickness (2 mm) of the CT scan to ensure convergence of the material property field. As shown in a previous study, convergence of the material property field is only achieved when the element size approaches the size of the pixel size (Perillo-Marcone et al., 2003).

3.3.2 Material Property Assignment

Inhomogeneous material properties for cancellous bone were extracted from the CT data (ScanIP, Simpleware Ltd., Exeter, UK). The density of the marrow in the medullary canal of the femur was considered to be the equivalent to the density of water and the lowest Hounsfield Unit (HU) in the canal was assigned an apparent density of 0 g/cm^3. The highest HU in the femur was considered to be cortical bone and assigned an apparent density of 1.73 g/cm^3 (Bryan et al., 2012). A linear relationship between the apparent bone density (ρ_{app}) and the HUs was assumed based on these two correspondences. The relationship between the apparent bone density and the cancellous bone elastic modulus (E_{bone}) was determined by an empirical power relation (Dalstra et al., 1993) (See 2.7.1).

$$E_{bone} = 2017.3\ \rho_{app}^{2.46} \qquad (1)$$

3.3.3 Establishing Landmarks and a Local Co-ordinate System

In order to fully automate pre-processing of the implanted hemipelvis, it was necessary to establish landmarks and measurements on the intact acetabulum by which the cup could be sized and aligned. A set of nodes were manually selected within the acetabulum in order to fit a best-fit sphere and a plane normal to the acetabular rim (Hypermesh®, Altair Engineering, Inc., Troy, MI) (Figure 3.1). The best-fit sphere determined the diameter and centre of the intact acetabulum, while the plane established the native orientation. A local co-ordinate system was established for the hemipelvis with the x-axis aligned along the normal vector of the acetabular rim plane (MATLAB 2015a, The Maths Work Inc., MA, USA) (Figure 3.2). The axes of the co-ordinate system were determined by computing the orthonormal basis of the best-fit plane.

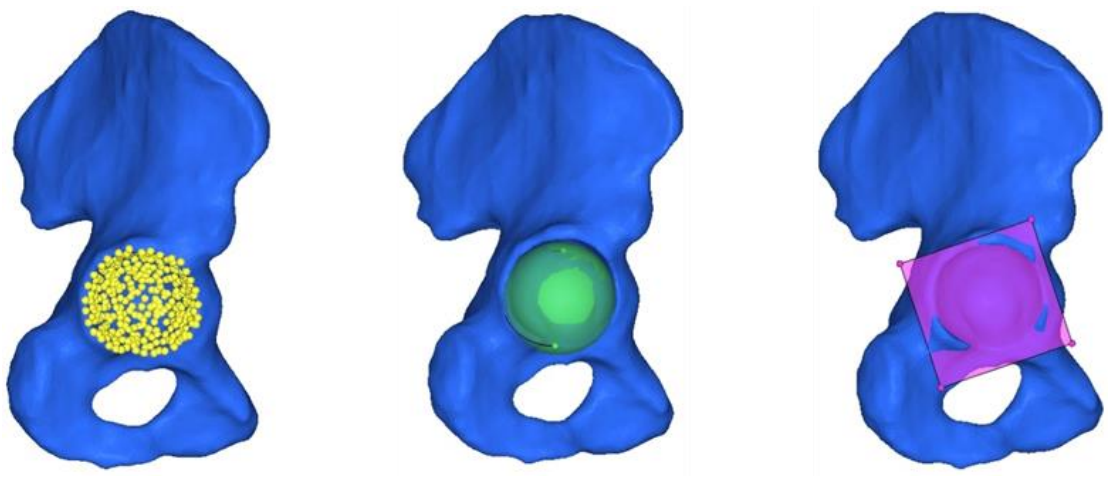

Figure 3.1 Landmarks manually placed in the acetabulum (left) from which a best-fit sphere (middle) and best-fit plane (right) were generated and used to determine the appropriate cup diameter and orientation.

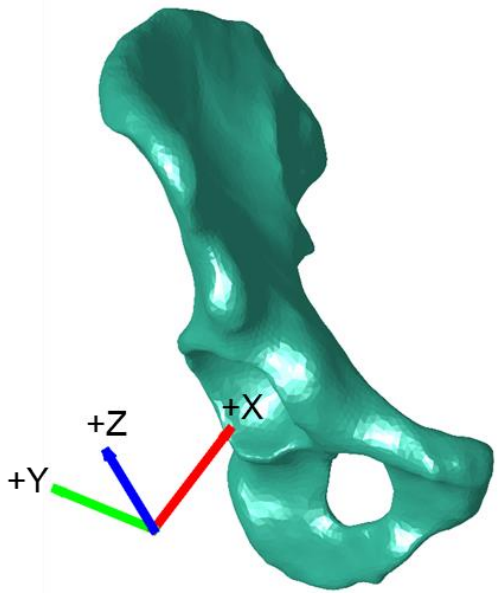

Figure 3.2 The local hemipelvis coordinate system.

3.4 Implanted FE Model Pre-Processing

3.4.1 Acetabular Cup FE Model

The geometries of the Pinnacle ® 100 Series acetabular shell, polyethylene liner and prosthetic femoral head were used to represent the cementless cup in this study (DePuy-Synthes) (Figure 3.3). Pinnacle ® is one of the most widely used cementless cup designs and has been associated with long-term clinical success. National joint registries reported 10-year survivorships of 92.8 – 97.9 % for non metal-on-metal hip prostheses with Pinnacle (Registry, 2016; National Joint Registry for England and Wales, 2015). In addition, clinical reports have demonstrated good clinical outcomes (Powers et al., 2010) and very low revision rates for aseptic loosening after 10 years (Bedard et al., 2014; Howard et al., 2011).

The titanium acetabular shell was assigned a Young's modulus of 115 GPa and a Poisson's ratio of 0.3. Surface-to-surface contact with Coulomb friction was modelled for the cup-bone interface and a coefficient of friction of 0.5 was assigned to represent the frictional properties of porous-coated surfaces (Rancourt et al., 1990; Shirazi et al., 1993). The polyethylene liner had a Young's modulus of 700 MPa and Poisson's ratio of 0.45. The Pinnacle 100 series cup has a 10° taper locking mechanism near the equator of the shell to prevent dissociation and a series of interlocking nubs and divots around the cup rim for rotational stability. The interface between the liner and the acetabular shell in the model was assumed to be fully bonded. The prosthetic femoral head was assumed to be cobalt-chrome alloy ($E = 200$ GPa, $v = 0.3$). Idealised frictionless contact was modelled between the polyethylene liner and prosthetic head. All cup materials were considered to be isotropic and linear-elastic.

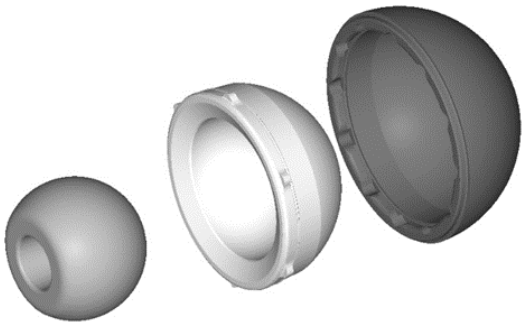

Figure 3.3 CAD geometries of the Pinnacle ® 100 Series acetabular shell, liner and prosthetic femoral head used in the FE models.

3.4.2 Cup Sizing and Alignment

The Pinnacle ® acetabular shells were available in 48 - 66 mm outer diameter sizes, increasing in 2 mm increments. The most suitable shell size was automatically determined for a subject using the intact acetabular best-fit sphere diameter. The best-fit sphere diameter was rounded to the nearest integer. The selected shell diameter was 4 mm greater for an even-numbered integer and 3 mm greater for an odd number to ensure reaming reached the floor of the acetabular fossa and widened the acetabulum by 2 – 3 mm in the anteroposterior direction (Callaghan et al., 1995). The cup was aligned parallel to the mouth of the acetabulum, along the x-axis of the local hemipelvis co-ordinate system, in order to match the native acetabular inclination and anteversion (Archbold et al., 2006).

3.4.3 Reaming

To prepare the acetabulum for cup insertion, it was virtually reamed by Boolean operation (Hypermesh®, Altair Engineering, Inc., Troy, MI) (Figure 3.4). The intact hemipelvis surface model was imported to Hypermesh ® and converted to a solid geometry. The Boolean operation was carried out with a CAD reamer aligned parallel to the mouth of the acetabulum, along the x-axis of the local hemipelvis co-ordinate system, to match the alignment of the cup. The subchondral bone plate was assumed to be removed during reaming and the cavity extended to the acetabular fossa, consistent with surgical practice (Callaghan et al., 1995; Schmalzried et

al., 1992a; Schwartz Jr et al., 1993). If a Boolean operation failed during the automated process, the reamer was translated by 0.01 mm into the acetabulum along the x-axis of the local co-ordinate system.

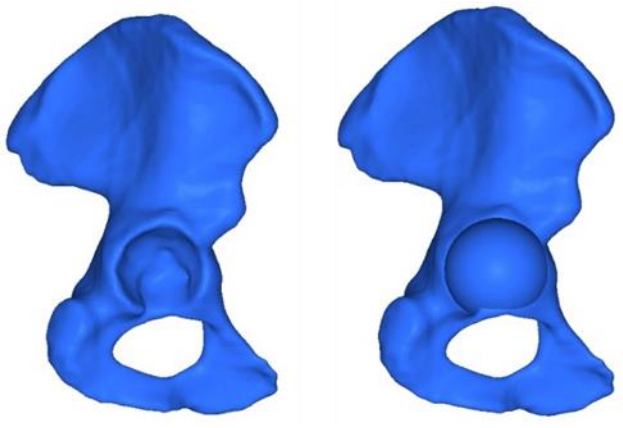

Figure 3.4 Intact acetabulum (left) and acetabulum reamed by Boolean operation (right).

3.4.4 Interference Fit

In vivo and *in vitro* studies have found the exact dimensions of the reamed acetabulum to be different from the dimensions of the last-reamer used (Macdonald et al., 1999; MacKenzie et al., 1994). Deviations from the nominal interference fit varies and depends on surgical technique and reamer type (Macdonald et al., 1999). In a preliminary investigation, cup insertion was performed with an interference of 1 mm on 7 subjects from the cohort. The volume of bone exceeding the cancellous yield criterion of 7000 μstrain (Morgan and Keaveny, 2001) was localised in the acetabulum and ranged from 55 – 83% for subjects with 1 mm interference fit. The median bone volume yielding was 66%. To choose the appropriate interference fit, a range of 0.1 – 1 mm interference fits were investigated on the subject with the median volume of bone exceeding the cancellous bone yield criterion of 7000 μstrain (Figure 3.5). An interference fit of 0.3 mm was chosen as it was consistent with previous *in vivo* and *in vitro* findings on the departure of cavity diameter from the last reamer-used and did not have an excessive percentage of the bone volume exceeding the yield criterion.

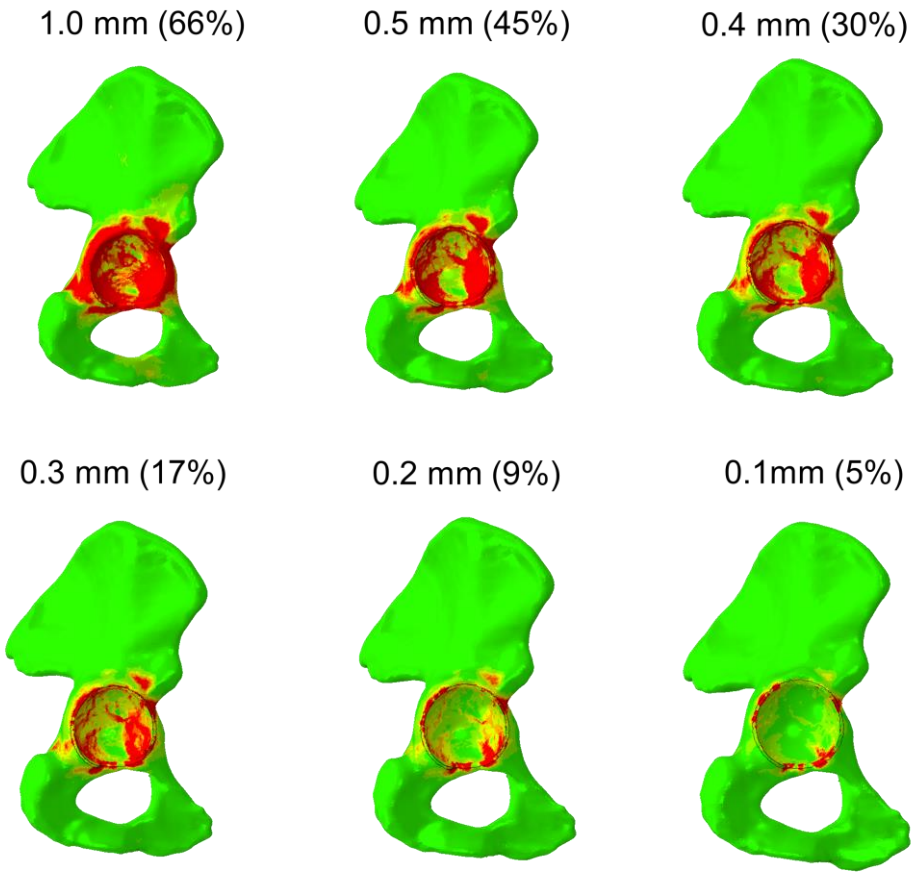

Figure 3.5 The strain fields and percentage volume of bone exceeding the yield criterion (in red) for the range of interference fits 1 - 0.1mm in the subject with the median bone yielding in 7 subjects with 1 mm interference fit.

3.4.5 Mesh Generation and Material Property Reassignment

The solid geometry of the reamed hemipelvis was meshed with linear tetrahedral elements with an average element edge length of 0.75 mm (Hypermesh®, Altair Engineering, Inc., Troy, MI). The cancellous bone properties were assigned to the implanted hemipelvis by interpolating the material properties at the nodes of the intact hemipelvis onto the closest implanted hemipelvis nodes. The elemental modulus was determined by averaging the four nodes of each element (MATLAB 2015a, The Maths Work Inc., MA, USA). The cancellous bone was assigned a Poisson's ratio of 0.2 (Dalstra and Huiskes, 1995). The hemipelvis was modelled as a sandwich structure (Dalstra and Huiskes, 1991) and the outer cortical layer was represented by shell elements of 1.5 mm thickness (Cilingir, 2010) (See 2.7.1). The cortical bone was assigned an elastic modulus of 17 GPa and Poisson's ratio of 0.3 (Reilly and Burstein, 1974). Bone was considered to be locally isotropic and linear-elastic.

3.4.6 Boundary Conditions

The hemipelvis was rigidly fixed at the pubic symphysis and sacroiliac joint (See 2.7.1). The boundary condition was set by constraining automatically selected surface nodes on the sacroiliac and pubic symphysis articulation sites in all degrees-of-freedom. The node set for the pubic symphysis included all nodes that were within 10 mm from the marker (magenta colour) on the pubic symphysis (MATLAB 2015a, The Maths Work Inc., MA, USA) (Figure 3.6). The set of nodes on the sacroiliac articulation lay on a plane that passed through three markers on the hemipelvis. The plane was determined by the posterior-most (green), superior-most (blue) and the pubic symphysis (magenta) markers on the hemipelvis (Figure 3.7).

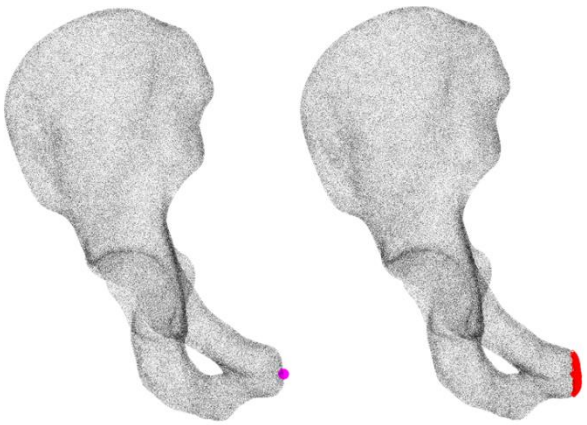

Figure 3.6 The automatic application of the boundary condition at the pubic symphysis. The nodes on the surface of the hemipelvis that were with 10 mm of the magenta-coloured marker on the pubic symphysis (left) were selected to be rigidly fixed.

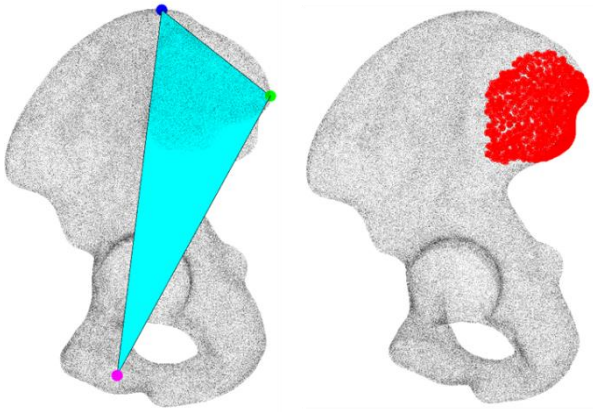

Figure 3.7 The automatic application of the boundary condition at the sacroiliac articulation site on the hemipelvis. The nodes on the surface of the hemipelvis that lay on the plane that passed through the posterior-most (green), superior-most (blue) and pubic symphysis (magenta) markers were selected to be rigidly fixed.

3.5 Subject-Specific Finite Element Analysis

Explicit, dynamic FE analyses were performed on each subject. The analysis simulated the insertion of a press-fit acetabular shell into the reamed acetabular cavity. Following insertion, a complete level gait cycle was simulated. All analyses were performed in ABAQUS/Explicit v6.13.

3.5.1 Cup Insertion

The acetabular cup was inserted into the reamed cavity by displacement control from a position outside the hemipelvis. The cup was advanced along the longitudinal axis of the cavity for 0.15s simulation time until it pressed against the acetabular floor and then held at this position for a further 0.05s (Figure 3.8). To allow energy to dissipate during elastic spring back of the cup, viscous damping with a coefficient of 0.2 was applied to the cup for 0.45s (Figure 3.9). The cup was allowed to settle to an equilibrium position as the damping was gradually released over the final 0.15s. This resulted in a gap being produced between the implant and bone at the polar region, as observed in previous studies (MacKenzie et al., 1994).

Cup insertion was simulated with a fixed time increment of 5×10^{-6} s. However, if a simulation failed part way through, the time increment was decreased by 1×10^{-6} s. Throughout the analysis, a fixed mass scaling factor was applied to elements with element stable increments below the set time increment. The fixed mass scaling was used to increase the stable time increment of the few critical elements in the model that controlled the stable time increment size, with a negligible effect on the overall behaviour of the model. Each simulation was processed with 28 CPUs (Intel ® Xeon ® 2.4 GHz processor, 32 GB RAM). The average simulation time for cup insertion among the cohort of 103 subjects was approximately 4.75 hrs.

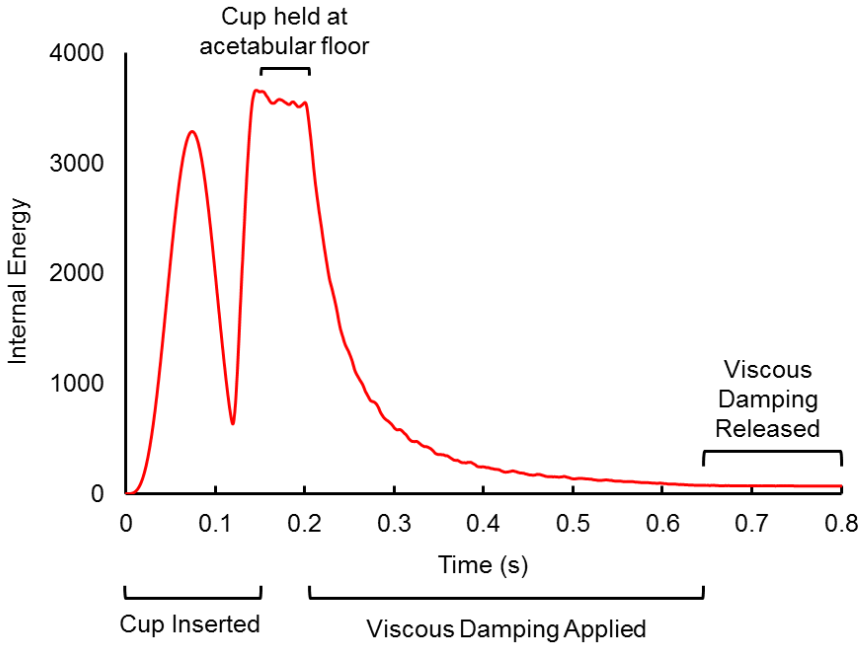

Figure 3.8 Internal energy plot of the cup insertion in the FE model. The cup was inserted to the floor of the acetabulum and held at the floor. Viscous damping was applied to the cup to dissipate energy during elastic spring back. The damping was gradually released to allow the cup to settle to an equilibrium position.

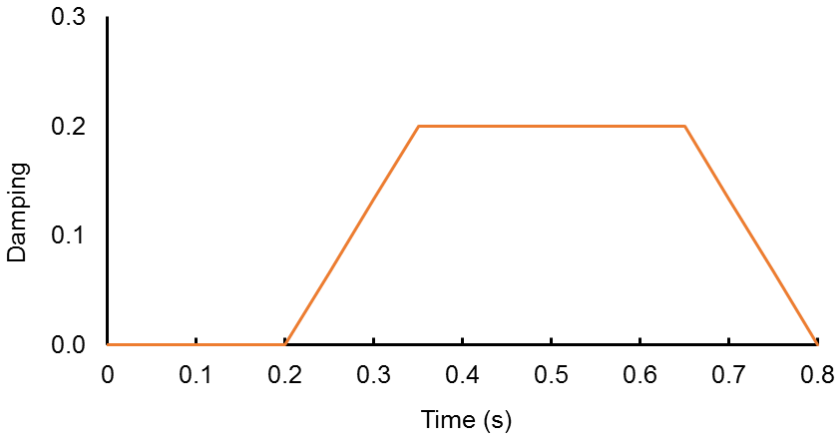

Figure 3.9 The profile of the viscous damping applied to the cup during insertion. At 0.2s, the viscous damping was gradually applied during elastic spring back of the cup. Damping was maintained at a coefficient of 0.2 between 0.35s and 0.65s to dissipate the energy of the cup. The damping was then gradually released at 0.65s as the cup settled to an equilibrium position.

3.5.2 Gait

Each subject underwent one complete gait cycle following cup insertion. The applied forces were adopted from a level walking trial of a male patient in the Orthoload dataset (H6R) who was closest in age to the mean age of the cohort (Bergmann, 2001) (Figure 3.10). For each hemipelvis, the forces from Orthoload were adopted to the local hemipelvis coordinate system, scaled to the bodyweight of the subject and applied in 50 discrete samples to the base of the prosthetic femoral head over 0.5s simulation time (Figure 3.11).

The gait cycle was simulated in a model with the same fixed time increment and mass scaling used for the cup insertion. However, if a simulation failed part way through, the time increment was decreased by 0.5×10^{-6} s. Each simulation was processed with 28 CPUs (Intel ® Xeon ® 2.4 GHz processor, 32 GB RAM). The average simulation time for gait among the cohort of 103 subjects was approximately 5 hrs.

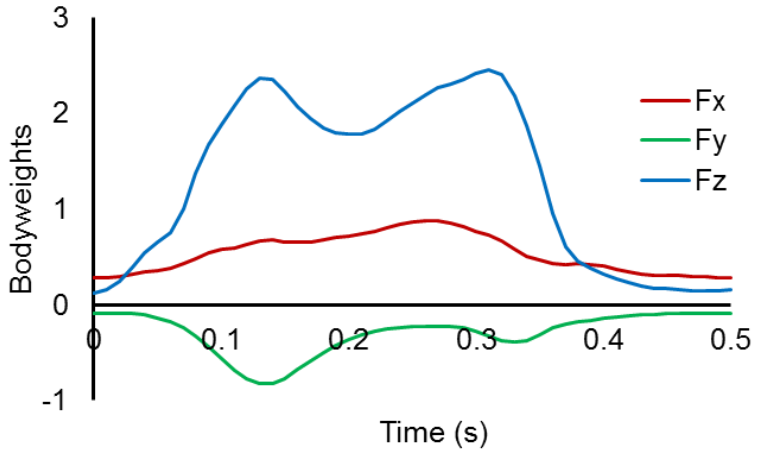

Figure 3.10 The force components of one gait cycle of a 68-year-old male level walking trial presented in the global coordinate system (Bergmann, 2001).

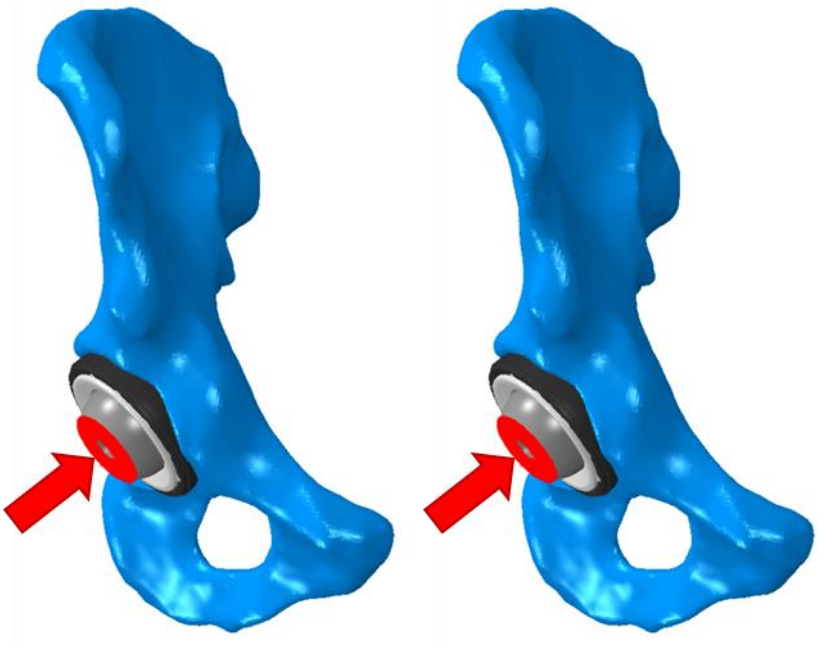

Figure 3.11 The gait cycle load applied to the base of the prosthetic femoral head (red).

3.6 Primary Stability Output Metrics

3.6.1 Polar Gap

The polar gap was measured between the pole of the cup and bone at its equilibrium position following insertion (Figure 3.12).

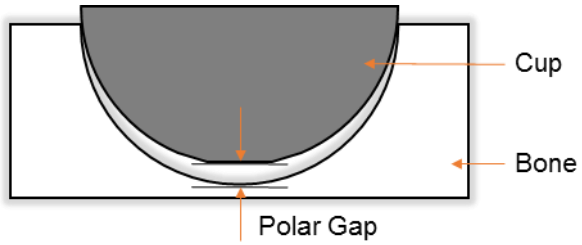

Figure 3.12 Illustration of a cup seated within the acetabular cavity at equilibrium with a gap between the cup and bone in the polar region.

3.6.2 Composite Peak Micromotion

Micromotion was measured by tracking the magnitude of the relative displacement of cup-bone node pairs relative to the zero-load condition throughout the complete gait cycle. Composite peak micromotion (CPM) was the peak micromotion of each node on the cup surface which occurred during the gait cycle (Figure 3.13) (Galloway et al., 2013). As primary stability is likely to depend on the combined effect of the tangential and radial components of micromotion (Spears et al., 2000), the resultant CPM was assessed in the statistical analysis.

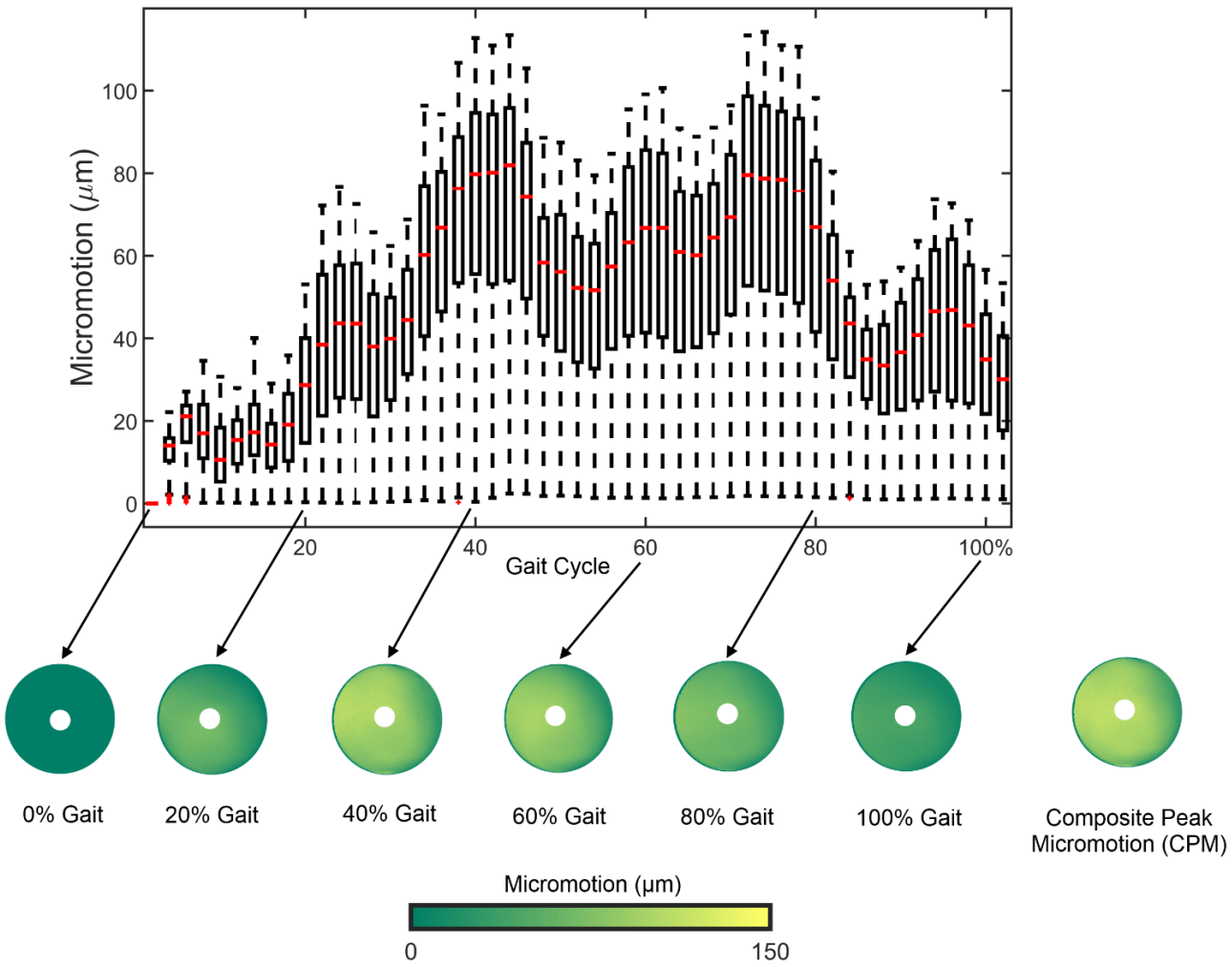

Figure 3.13 The graphic demonstrates how composite peak micromotion (CPM) was calculated. The graph shows the boxplot of micromotion at each discrete sample in the gait cycle. The images show the micromotion pattern on the cup surface at a given point in the gait cycle. CPM was the aggregate peak micromotion of each node on the cup surface.

3.6.3 Potential Ingrowth Area

The potential ingrowth area is a measure that indicates the amount of cup surface over which bone ingrowth may occur and corresponds to the clinical assessment of radiolucency of radiographs of hip prostheses (Ong et al., 2008). It is computed as the percentage cup surface area associated with each cup node that had a normal gap distance within 50 μm of the bone (Bloebaum et al., 1994) during gait and a composite peak tangential micromotion of the less than 150 μm (Pilliar et al., 1986)

3.6.4 Maximum Change in Polar Gap

The change in gap between the cup and bone may indicate access for particulate debris dispersed within joint fluid to the periprosthetic joint space during loading (Schmalzried et al., 1992a). The maximum change in polar gap was calculated as the difference between the smallest and largest polar gaps throughout gait (Figure 3.14).

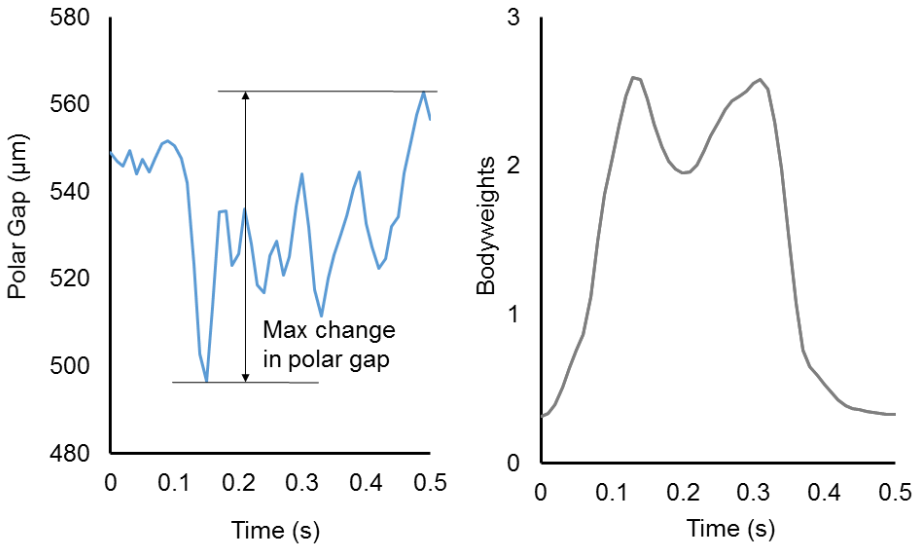

Figure 3.14 Change in polar gap throughout the gait cycle for a typical subject. The maximum change in polar gap was calculated as the difference in smallest and largest polar gap observed in the gait cycle.

Chapter 4

Patient Variability in the Primary Stability of a Cementless Acetabular Cup[2]

4.1 Introduction

To comprehensively assess the primary stability of prospective acetabular cup designs, pre-clinical FE testing regimes need to account for the variation in anatomy and material properties that exist between individuals. Most FE studies of the primary stability of cups are typically performed on a single hip joint which cannot fully consider variations in anatomy and material property distribution that exist between individuals. With 4 hemipelvis models, Clarke et al. demonstrated that bone anatomy was highly influential on the micromotion of metal-on-metal cementless cups (Clarke et al., 2012b). While this is indicative of the need for including multiple subjects in an FE study, this is a significantly smaller sample size than would be expected in equivalent clinical work to investigate patient variability and there are limits to how much the results can be extrapolated to the population (Radcliffe et al., 2007).

[2] Work in this chapter has been published in the following journal article:

O'Rourke, D., Al-Dirini, R., and Taylor, M., 2017, *Primary stability of a cementless acetabular cup in a cohort of patient-specific finite element models* Journal of Orthopaedic Research, In press.

With a larger number of subjects, the spread in primary stability of a cup can be predicted and allow for statistically meaningful analysis to be performed on the influence of patient-related factors (Taylor et al., 2013). Previously, studies comprising of large cohorts of FE models have investigated load transfer in a femoral resurfacing prosthesis (Bryan et al., 2012) and the primary stability of cementless tibial trays (Galloway et al., 2013) and short femoral stems (Bah et al., 2015). In addition, if the variation in primary stability of a cementless acetabular cup with a proven track record in a large cohort of subjects is known, it can provide a benchmark for prospective new designs in the pre-clinical stage. However, generating and analysing a large cohort of subject-specific FE models has a significant time cost. Assessment of primary stability in a large cohort for every new cup design may be unfeasible in future pre-clinical testing. Appropriate sampling of the large cohort could provide a representative subset of subjects to describe the variability in primary stability while reducing the number of FE models required.

Therefore, the aims of the present study were:

- Explore the primary stability of an established cementless cup in a large cohort of patient-specific FE models.
- Investigate the association between patient-related factors and the observed variability.
- Predict the variability in the acetabular cup primary stability output metrics in the cohort with a reduced subset of subjects.

4.2 Methods

The study was based on patient-specific implanted hemipelvis models of 103 subjects that were developed in accordance with the methodology described in Chapter 3.

4.2.1 Patient-Related Factors

To investigate whether patient-related factors contributed to the variation in primary stability, the parameters studied were 1) gender, 2) intact acetabular diameter, 3) acetabular depth, 4)

mean elastic modulus in the reamed cavity and 5) bodyweight. The acetabular diameter was taken to be the diameter of a best-fit sphere fitted to the intact acetabulum (See 3.3.3). The acetabular depth is important in restoring the hip joint mechanics (Murtha et al., 2008) and was measured as the distance from the mouth of the acetabulum to the acetabular fossa along the normal vector of the acetabular rim plane. Mean elastic modulus in the cavity gave an indication of bone quality in the reamed acetabulum. Bodyweight was only analysed for the output metrics relating to the gait cycle.

Factor	Male (N = 50)	Female (N=53)	p
Age (yrs)	74.1 ± 10.2	75.1 ± 9.6	0.62
Bodyweight (kg)	74.8 ± 15.5	70.4 ± 15.8	0.16
BMI (kg/m^2)	26.0 ± 2.1	28.1 ± 5.5	0.05
Intact Acetabular Diameter (mm)	54.3 ± 2.1	47.9 ± 2.4	< 0.0005*
Intact Acetabular Depth (mm)	28.6 ± 2.7	24.0 ± 2.6	< 0.0005*
Mean Bone Elastic Modulus (MPa) †	155 (61 – 1198)	146 (52 – 654)	0.36

* $p < 0.05$ in an independent-samples t-test

† Mean bone elastic modulus was not normally distributed. As such, the median and range are displayed. A Mann-Whitney U test was performed to compare male and female groups for this factor.

Table 4.1 Patient characteristic data for male and female subjects in the cohort

4.2.2 Data Analysis

Separate simple linear regressions were performed (IBM SPSS Statistics v23.0) between the primary stability output metrics as dependent variables and the patient-related factors as independent variables. In addition, the factors were categorised into quartiles and differences in the groups of the output metrics were evaluated with a Kruskal-Wallis test followed by pairwise comparisons with the Dunn-Bonferroni adjustment for multiple comparisons.

4.2.3 Sampling Methods

Anatomic Sampling

Subsets of subjects were chosen based on spread of patient-related factors in the cohort. A subset of 12 subjects were made up with the minimum, median and maximum of the cohort age, bodyweight, mean elastic modulus, and intact acetabulum diameter. Moreover, there was another set based on the anatomical parameters but stratified by male and female to ensure equal representation of both genders.

Random Sampling

Subsets of 12 and 24 subjects were randomly selected from the cohort. The set of 12 subjects were sampled from the cohort and each subject in the cohort had equal probability of being selected. For the set of 24 subjects, the cohort was stratified by gender and the set was made up from 12 random male subjects and 12 random female subjects. There were 100 randomly sampled sets of each sample size for the primary stability output metrics.

Convex Hull Sampling

The convex hull of a given a set of points P in space is the smallest collection of points that encloses P (Chan, 1996). In two dimensions, a convex hull resembles an elastic rubber band snapped around a set of nails sticking out of the plane (Figure 4.1). In this study, the subjects in the cohort were represented in a 4-dimensional parameter space by a point with co-ordinates of their age, bodyweight, mean elastic modulus, and intact acetabulum diameter. The subset of subjects produced by this sampling were the convex hull of these points.

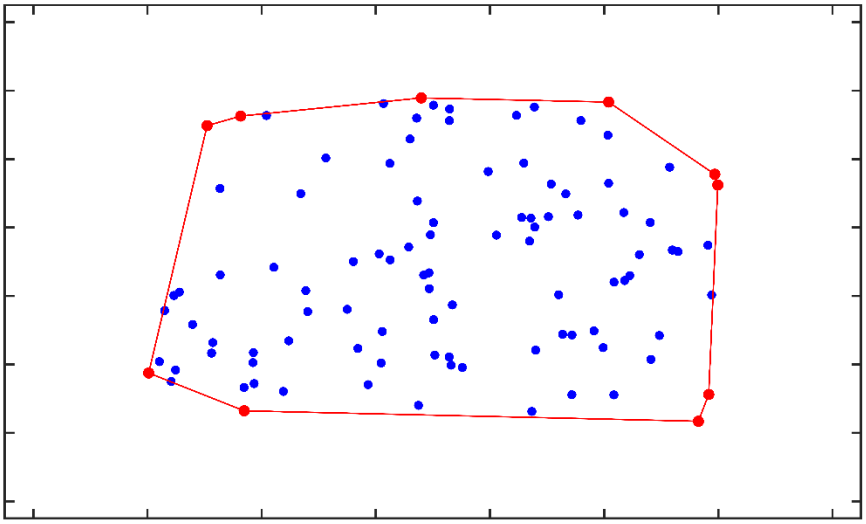

Figure 4.1 A convex hull in two-dimensional space. The convex hull (red) is made up of the smallest collection of points to enclose all points in the plane.

4.3 Results

4.3.1 Primary Stability in the Cohort

Gaps between the cup and bone were observed at cup pole in all subjects following insertion. Polar gaps showed a non-normal distribution (Figure 4.2) with a median value of 467 μm and a range between 284 and 1112 μm. The distribution of the 95th percentile CPM was non-normal, with a median value of 136 μm and a range of 18 to 624 μm (Figure 4.3). The 95th percentile CPM mostly occurred during stance phase of gait, between 40 and 60% of the loading cycle (Figure 4.4). The 95th percentile CPM between these phases of gait had a range between 26 and 591 μm. The potential ingrowth area ranged over the cohort from 0.2 – 51% (Figure 4.5). The distribution was non-normal, with a median value of 14% and 24 subjects with a potential ingrowth area of less than 5%. The distribution of the maximum change in polar gap throughout gait was non-normal, with median value of 59 μm and a range of 9 – 184 μm. Most values occurred between 20 and 80 μm (Figure 4.2).

Two distinct equivalent strain patterns were observed in the acetabular cavities following insertion (Figure 4.6). Areas of high strain indicated the location of bone compression on the cup and subjects were subjectively categorised based on having a "rim-dominant" strain pattern (N = 53) or "uniform" strain pattern (N = 50). The equivalent strain in all acetabular cavities exceeded the cancellous bone yield strain of 7000 μstrain (Morgan and Keaveny, 2001) in some areas. The median equivalent strain in the cavities had a range of 2194 - 20000 μstrain. There were statistically significant differences in polar gap ($p = 0.002$), potential ingrowth area ($p < 0.0005$) and maximum change in polar gap ($p = 0.001$) between the two strain pattern groups (Figure 4.7).

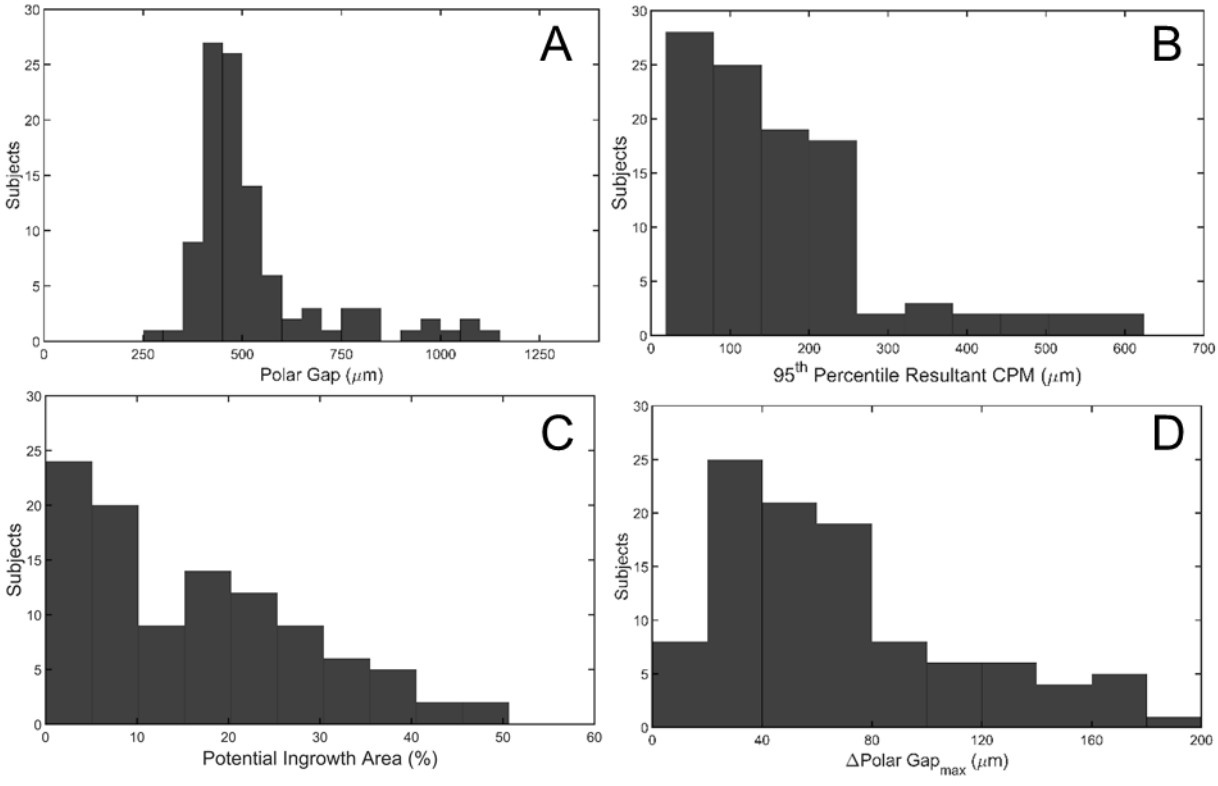

Figure 4.2 Frequency distribution of the (A) polar gap, (B) 95th percentile Composite Peak Micromotion, (C) potential ingrowth area, and (D) maximum change in polar gap in the cohort of 103 subjects simulated in the present study.

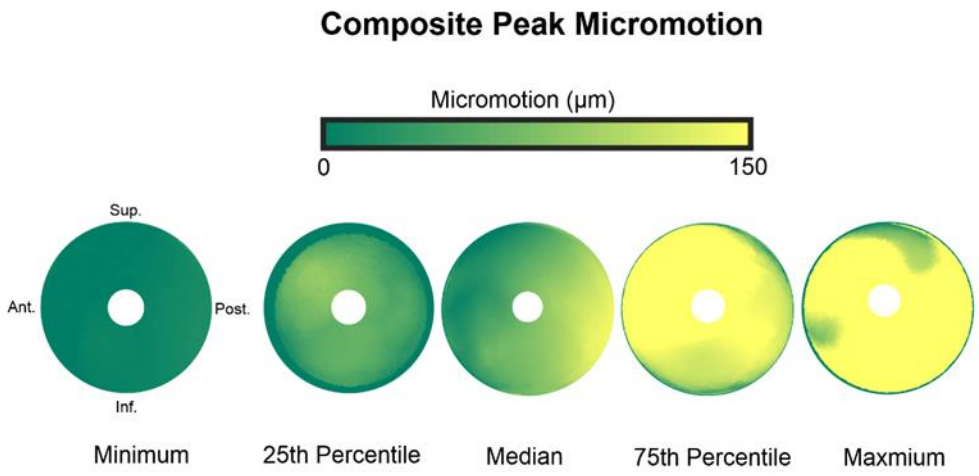

Figure 4.3 An illustration of the variation in micromotion in the cohort. From left to right, the models with the minimum, 25th percentile, median, 75th percentile and maximum of the 95th percentile Composite Peak Micromotion are shown.

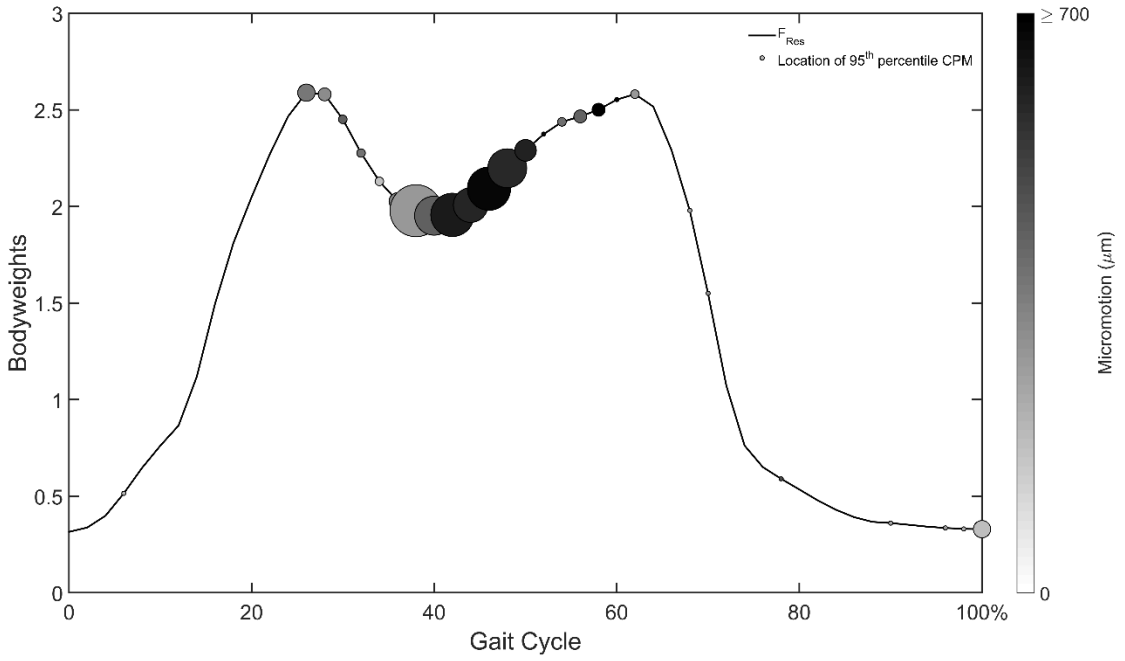

Figure 4.4 Location of the 95th percentile Composite Peak Micromotion in the gait cycle. The size of the circle indicates the proportion of subjects with 95th CPMs at the given location and the shade of the circle indicates the mean 95th CPM in that group.

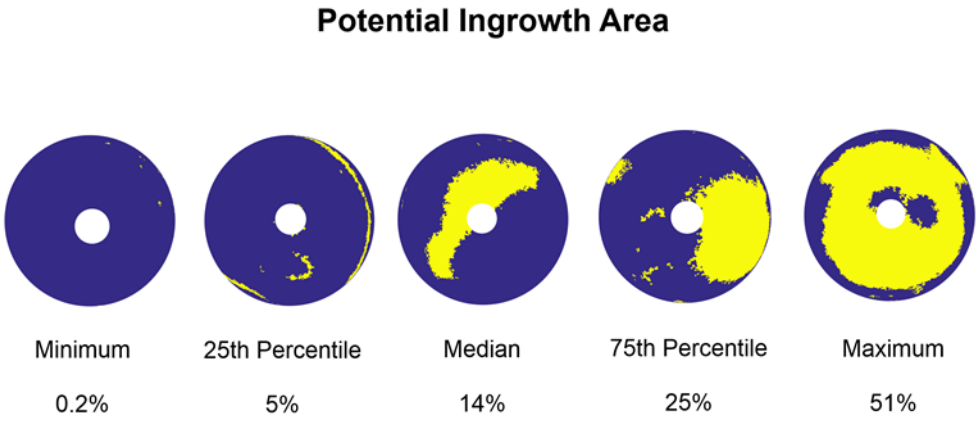

Figure 4.5 An illustration of the variation in potential ingrowth area in the cohort. From left to right, the models with the minimum, 25th percentile, median, 75th percentile and maximum of the 95th percentile potential ingrowth area are shown.

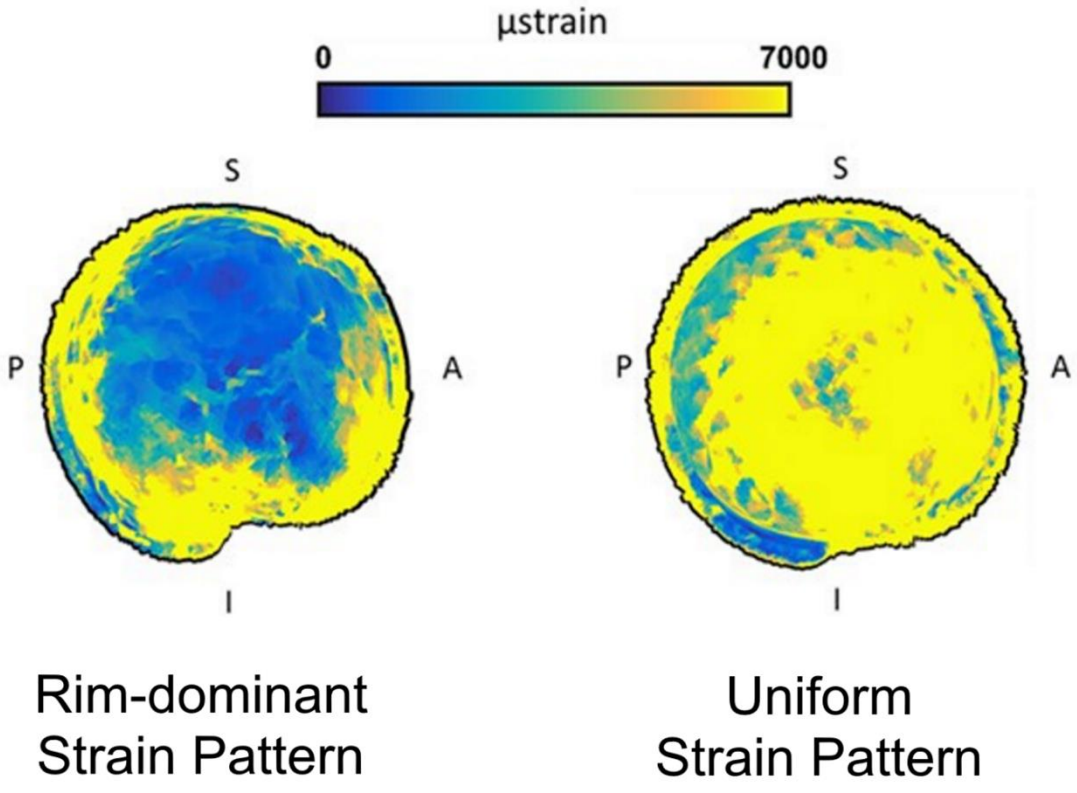

Figure 4.6 Typical representations of the equivalent strain patterns observed in the acetabular cavities following insertion.

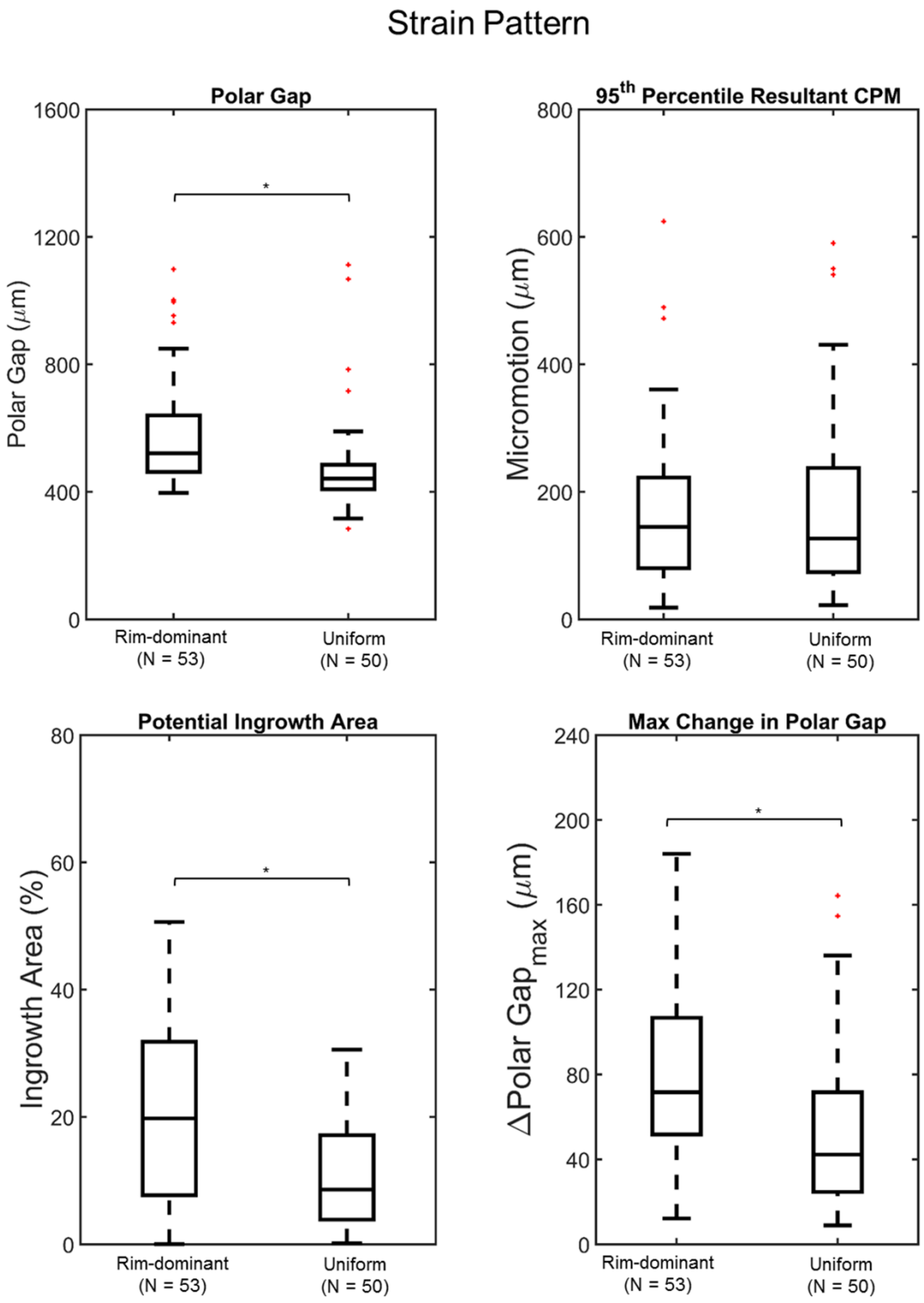

Figure 4.7 Comparisons between strain pattern groups for the output metrics.

* statistically significant difference ($p < 0.05$).

4.3.2 Associations with Patient-Related Factors

Linear regression did not indicate strong relationships between primary stability output metrics and the patient-related factors of the cohort studied (Table 4.2). The highest-ranking relationship occurred between the polar gap and the intact acetabular depth. As normal distribution was not observed for the polar gap, a reciprocal transformation was applied for linear regression. While some trend could be observed between polar gap and intact acetabular depth, a strong linear relationship could not be demonstrated ($R^2 = 0.4$). A similar trend was suggested with polar gap and acetabular diameter but a strong association could not be demonstrated ($R^2 = 0.2$). All other relationships between output metrics and patient-related factors were not evident with regression ($R^2 < 0.2$).

There was a decreasing trend in polar gap from when the intact acetabular depth was categorized into quartiles (Figure 4.8). Post hoc analysis revealed the polar gap in < 24 cm group was significantly larger than in the 26 – 29 and > 29 mm groups (median difference = 136 μm, 95% CI [123, 149], $p < 0.0005$ and median difference = 164 μm, 95% CI [154, 182], $p < 0.0005$). The polar gap in 24 – 25 cm group was also statistically significantly higher than the 26 – 29 and > 29 mm group (median difference = 63, 95% CI [55, 69], $p = 0.015$ and median difference = 86, 95% CI [79, 94], $p < 0.0005$). A similar trend in polar gap and groups differences were observed for the intact acetabular diameter groups (Figure 4.9). Females had significantly larger polar gaps than males ($p < 0.0005$) (Figure 4.10).

There was a deceasing trend in 95th percentile CPM was observed from the first quartile to the fourth quartile of the mean elastic modulus (Figure 4.11). Post hoc analysis revealed a significantly higher micromotion in the < 124 MPa group than the 124 – 148 MPa and > 198 MPa groups (median difference = 94, 95% CI [74, 108], $p = 0.02$, and median difference = 125, 95% CI [112, 140], $p < 0.0005$). The 149 – 198 MPa group was statistically significantly higher than the > 198 MPa group (median difference = 72, 95% CI [60, 80], $p = 0.02$). Micromotion was also statistically significantly different between bodyweight groups. Post hoc analysis revealed

significant differences between the < 61kg group and 71 – 83 kg group (median difference = 81, 95% CI [71, 94], p = 0.01) and the 61 – 70 kg and 71 – 83 kg groups (median difference = 73, 95% CI [58, 88], p = 0.04) (Figure 4.12).

A trend of decreasing maximum polar gap change was observed in quartile groups of elastic modulus and statistically significant differences were present between groups (p = 0.007). Post hoc analysis revealed the < 124 MPa group was statistically different to the > 198 MPa group (median difference = 40, 95% CI [38, 46], p = 0.005) (Figure 9). No trends within quartile groups could be demonstrated between potential ingrowth area and the patient-related factors of the cohort studied.

	Linear Regression			
	Polar Gap	95th Percentile CPM	Potential Ingrowth Area	Max Change in Polar Gap
Intact Acetabular Diameter	0.23	0.01	0.01	0.0001
	(p < 0.0005)	(p =0.38)	(p = 0.47)	(p = 0.92)
Intact Acetabular Depth	0.4	0.01	0.04	0.02
	(p < 0.0005)	(p = 0.37)	(p = 0.04)	(p = 0.18)
Mean Elastic Modulus	0.002	0.15	0.01	0.12
	(p = 0.62)	(p < 0.0005)	(p = 0.24)	(p < 0.0005)
Bodyweight	-	0.08	0.03	0.02
	-	(p =0.004)	(p = 0.06)	(p = 0.20)

Table 4.2 Coefficient of determination (R^2) values and p-values for linear regression performed between the primary stability output metrics and the patient-related factors. Due to the non-normal distributions of the output metrics and mean elastic modulus, a reciprocal transformation was applied to the data for the regression analysis.

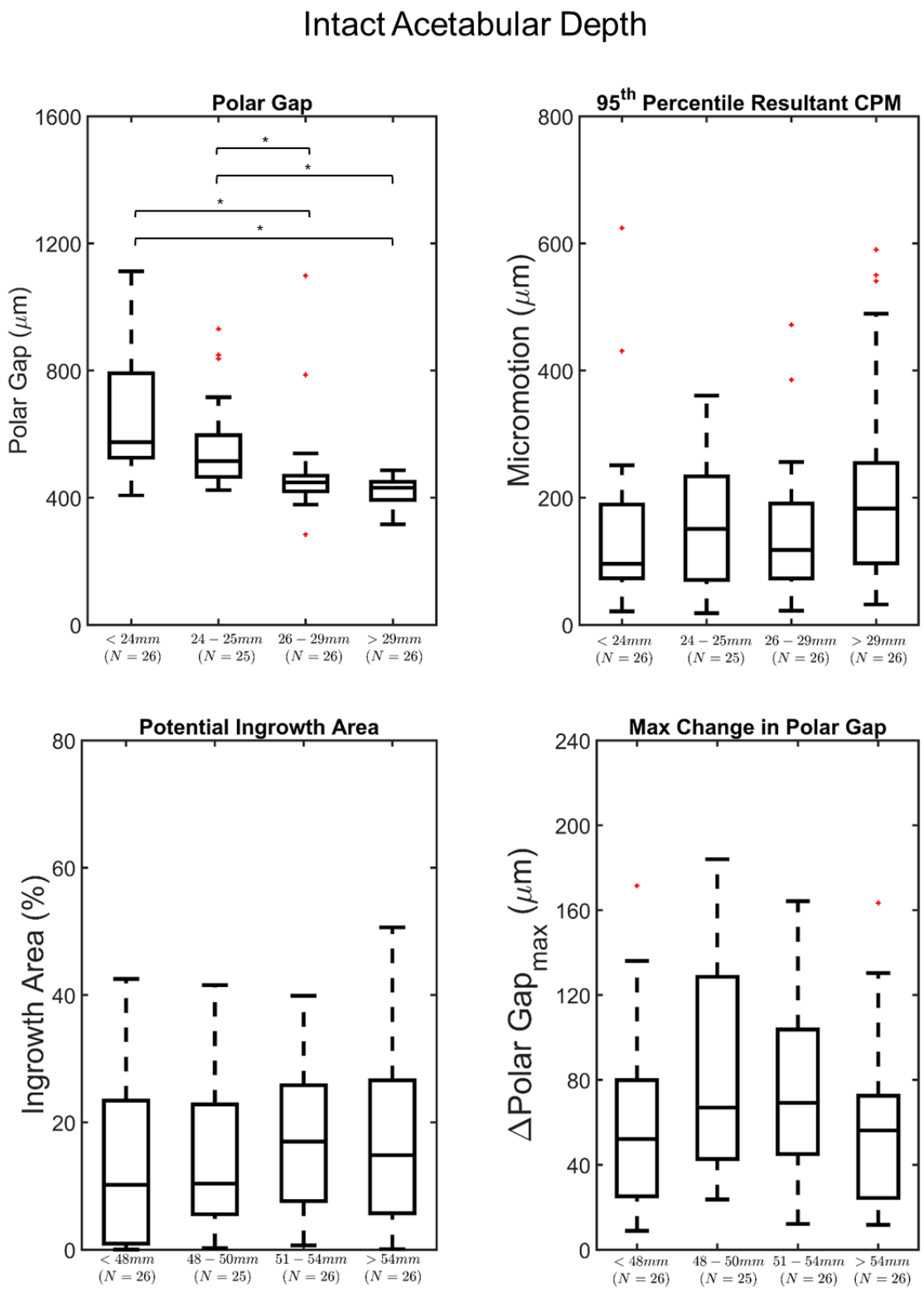

Figure 4.8 Comparisons between intact acetabular depth quartile groups for the output metrics.
* statistically significant difference ($p < 0.05$).

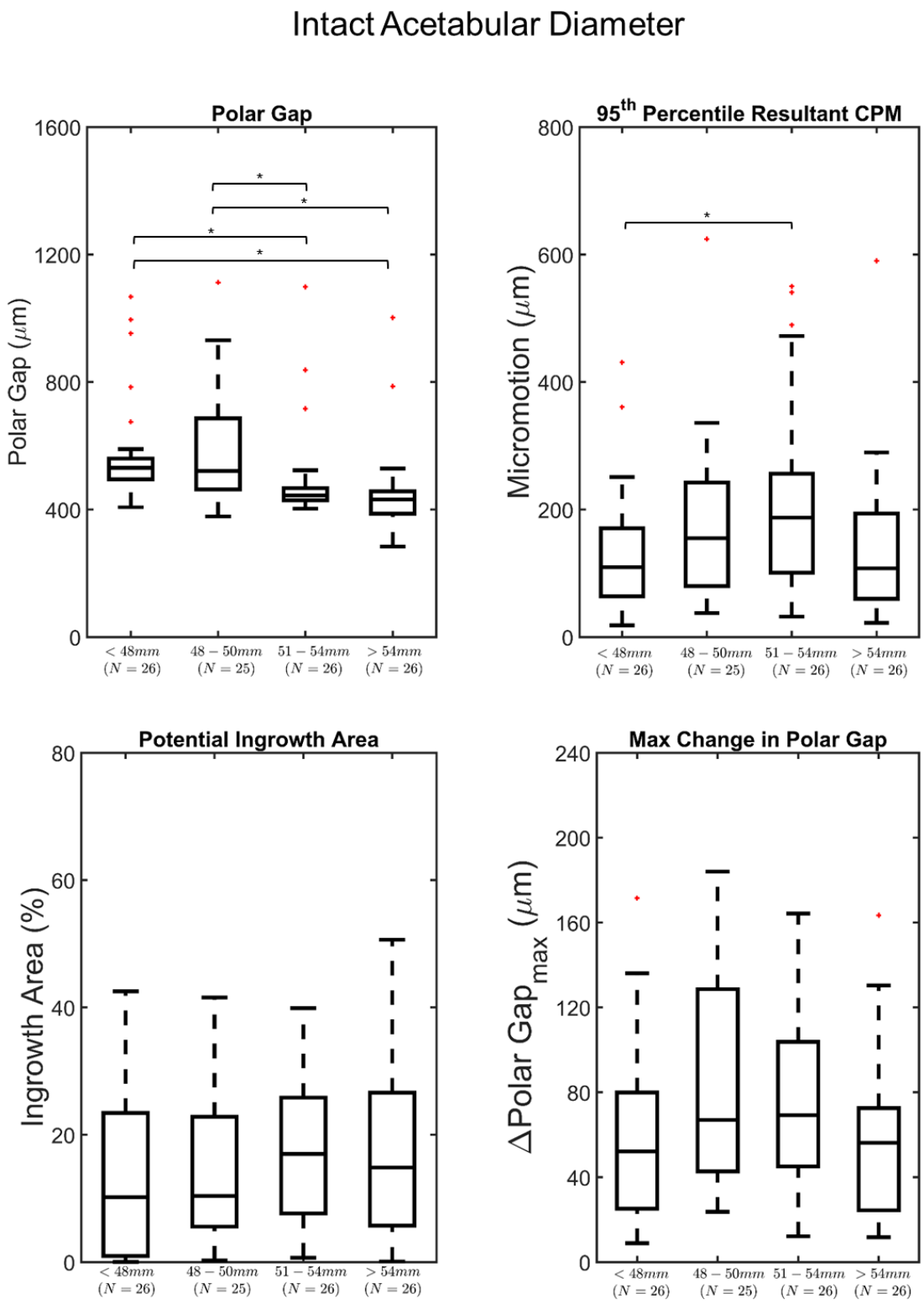

Figure 4.9 Comparisons between intact acetabular diameter quartile groups for the output metrics. * statistically significant difference ($p < 0.05$).

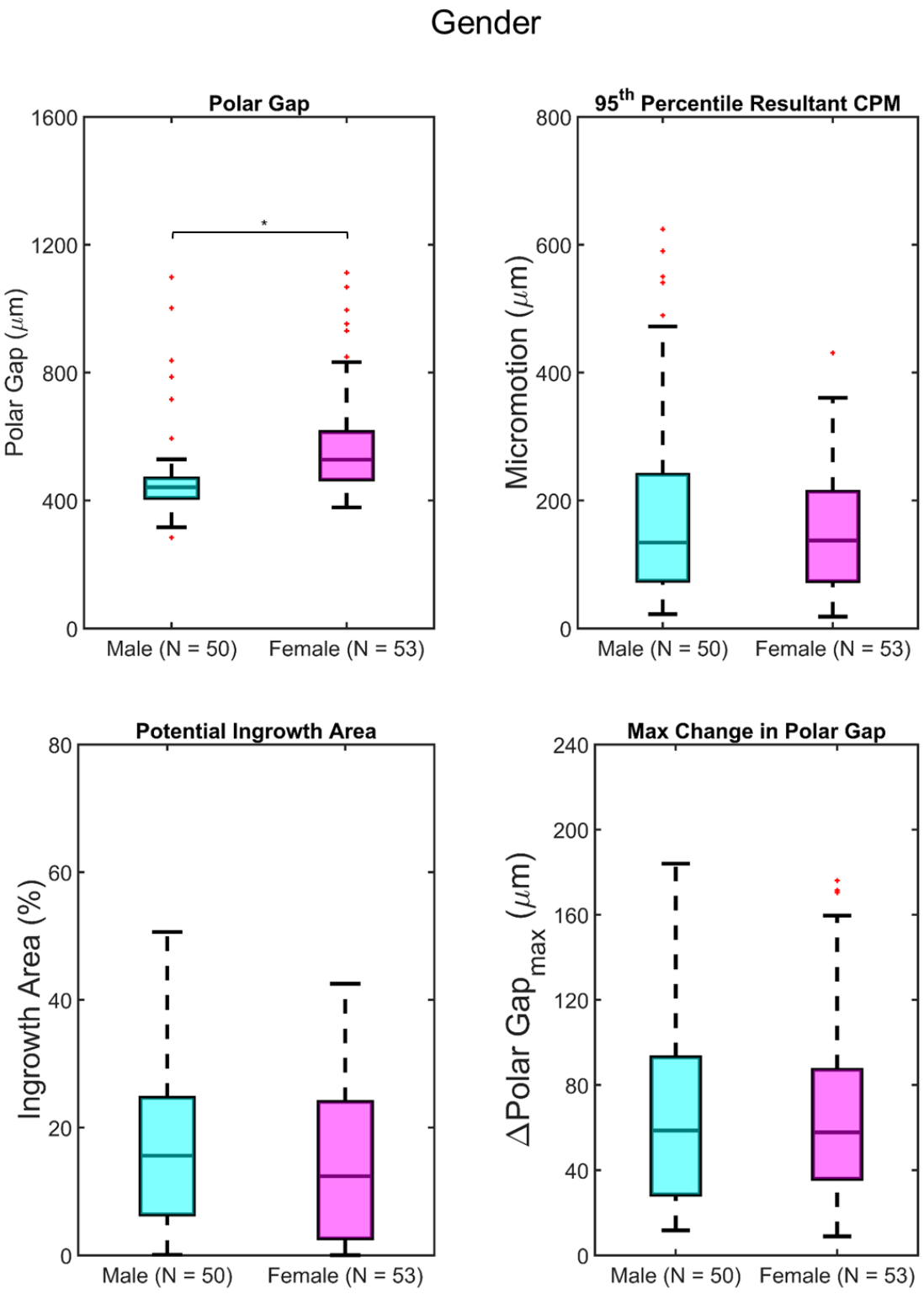

Figure 4.10 Comparisons between genders for the output metrics.

* statistically significant difference ($p < 0.05$).

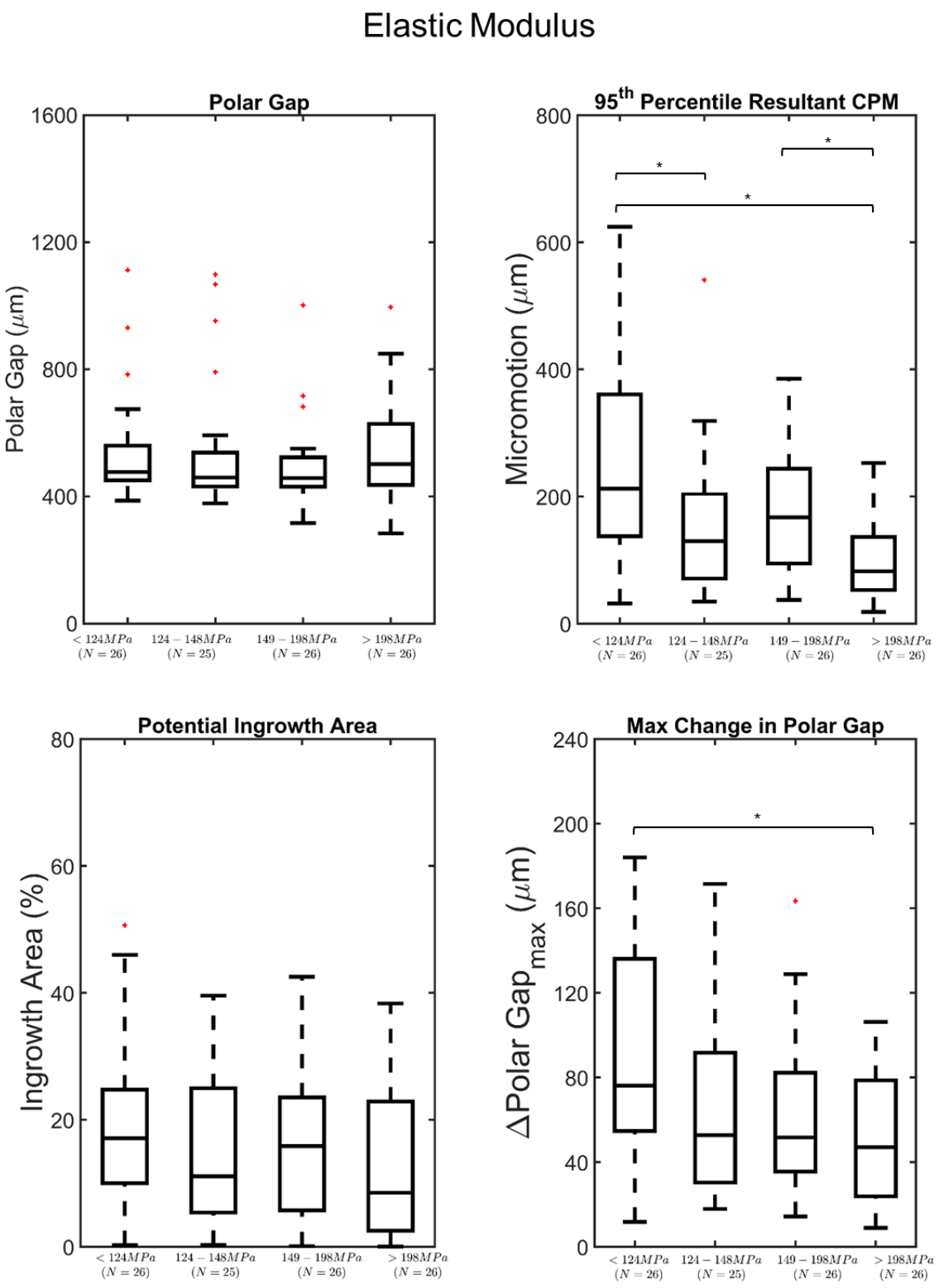

Figure 4.11 Comparisons between mean elastic modulus quartile groups for the output metrics.
* statistically significant difference ($p < 0.05$).

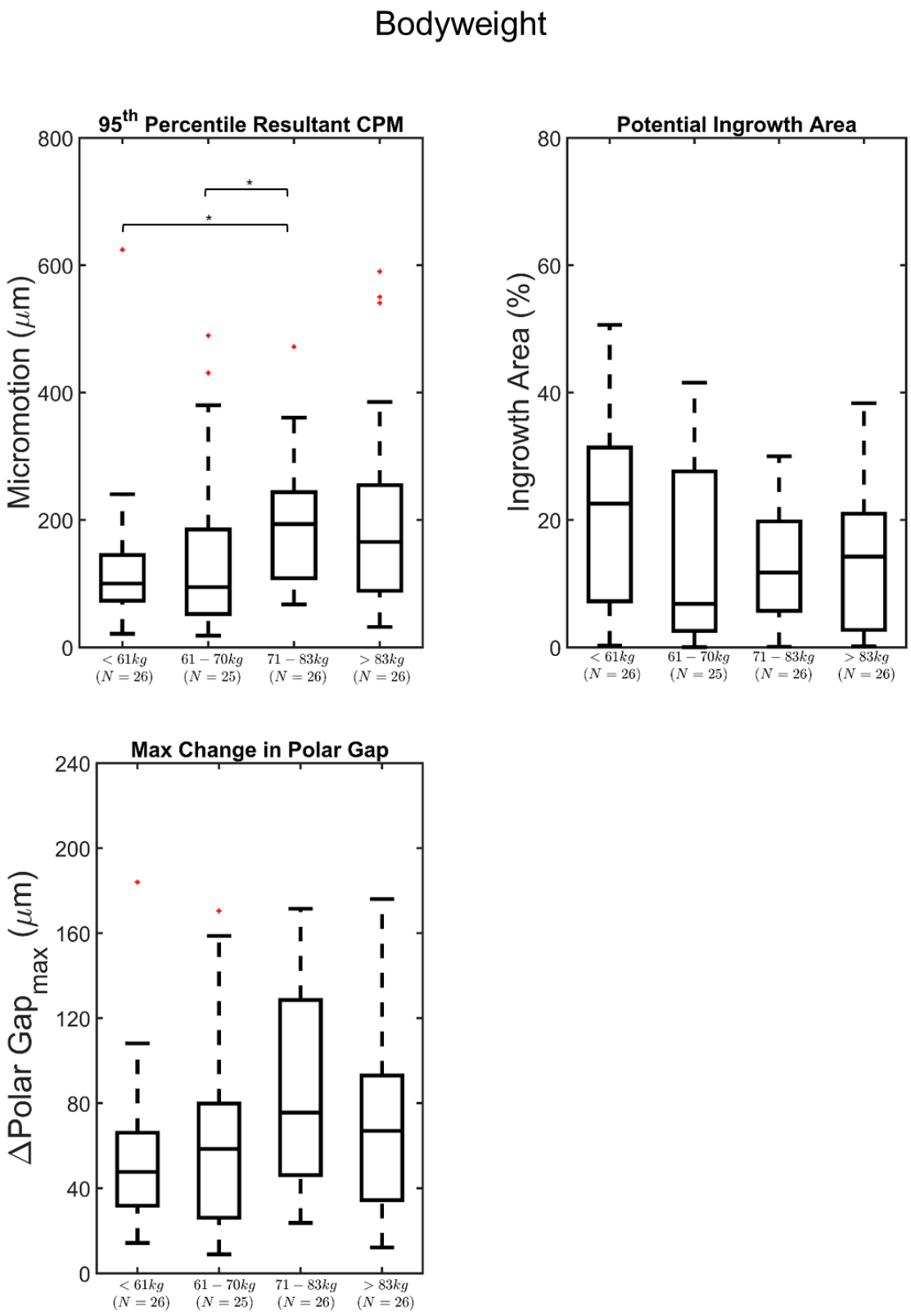

Figure 4.12 Comparisons between bodyweight quartile groups for the output metrics relating to gait. * statistically significant difference ($p < 0.05$).

4.3.3 Population Sampling

The distribution of the 95th percentile CPM in the cohort was non-normal, with a median value of 136 µm, an interquartile range of 74 - 230 µm and a range of 18 - 624 µm. Random sampling produced highly variable subsets for all output metrics. In the 100 random sets of 12 subjects, the sets with the lowest and highest interquartile ranges of the 95th percentile CPM had medians of 127 µm and 244 µm while the interquartile ranges were 84 – 138 µm and 161 – 437 µm respectively. For the 100 random sets of 24 subjects, the lowest and highest interquartile range sets had medians of 108 µm and 201 µm while the interquartile ranges were 78 – 161 µm and 71 – 358 µm (Figure 4.13). A similar trend of variability among the random sets were observed for the other output metrics (Figure 4.14 to Figure 4.16).

Anatomic sampling approximated the variation of all output metrics in the cohort and stratifying by gender slightly improved the approximations. For the 95th percentile CPM, the cohort median was 136 µm and the interquartile range was 74 – 230 µm. The subset of 12 subjects based on the patient-related factors had a median of 158 µm and an interquartile range of was 78 – 236 µm. Meanwhile, the subset of 24 subjects based on anatomic sampling that was stratified by gender had a median of 136 µm and interquartile range of 73 – 228 µm (Figure 4.13). A similar trend of approximating the variability in the cohort was observed for the other output metrics (Figure 4.14 to Figure 4.16).

Convex Hull sampling produced a subset of 41 subjects that closely matched the variation in all output metrics in the cohort. For the 95th percentile CPM, the convex hull subset performed worse than the subsets based on anatomic sampling, a median of 99 µm and an interquartile range of 70 – 191 µm (Figure 4.13). However, the convex hull subset was closer to approximating the variation in the remaining output metrics (Figure 4.14 to Figure 4.16). Moreover, the convex hull subset contained the subjects with the minimum and maximum values of each output metric.

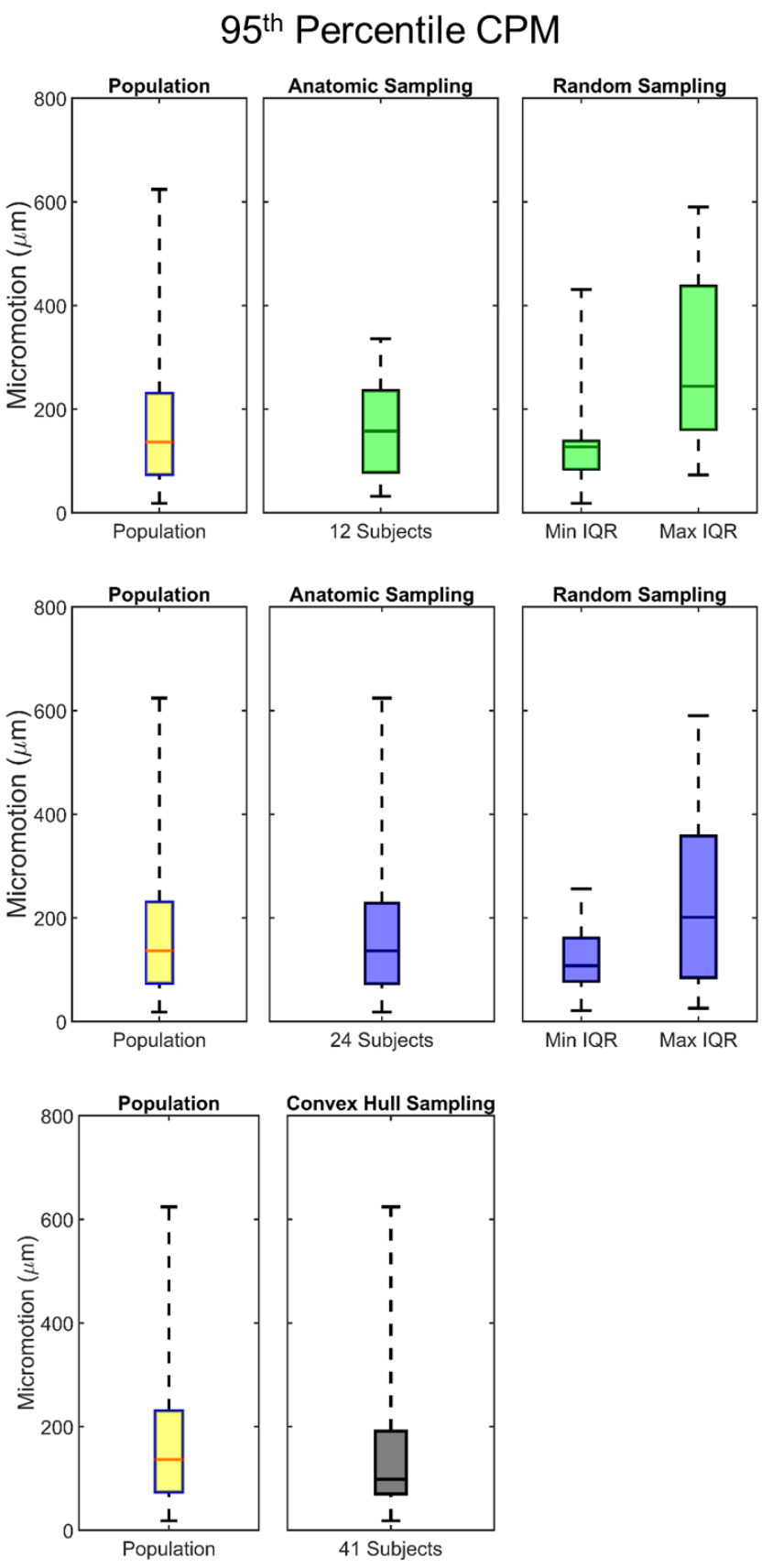

Figure 4.13 Distribution of the 95th percentile Composite Peak Micromotion in the cohort compared with subsets based on 12 subjects (first row), subsets based on 24 subjects (second row), and a subset based on convex hull sampling.

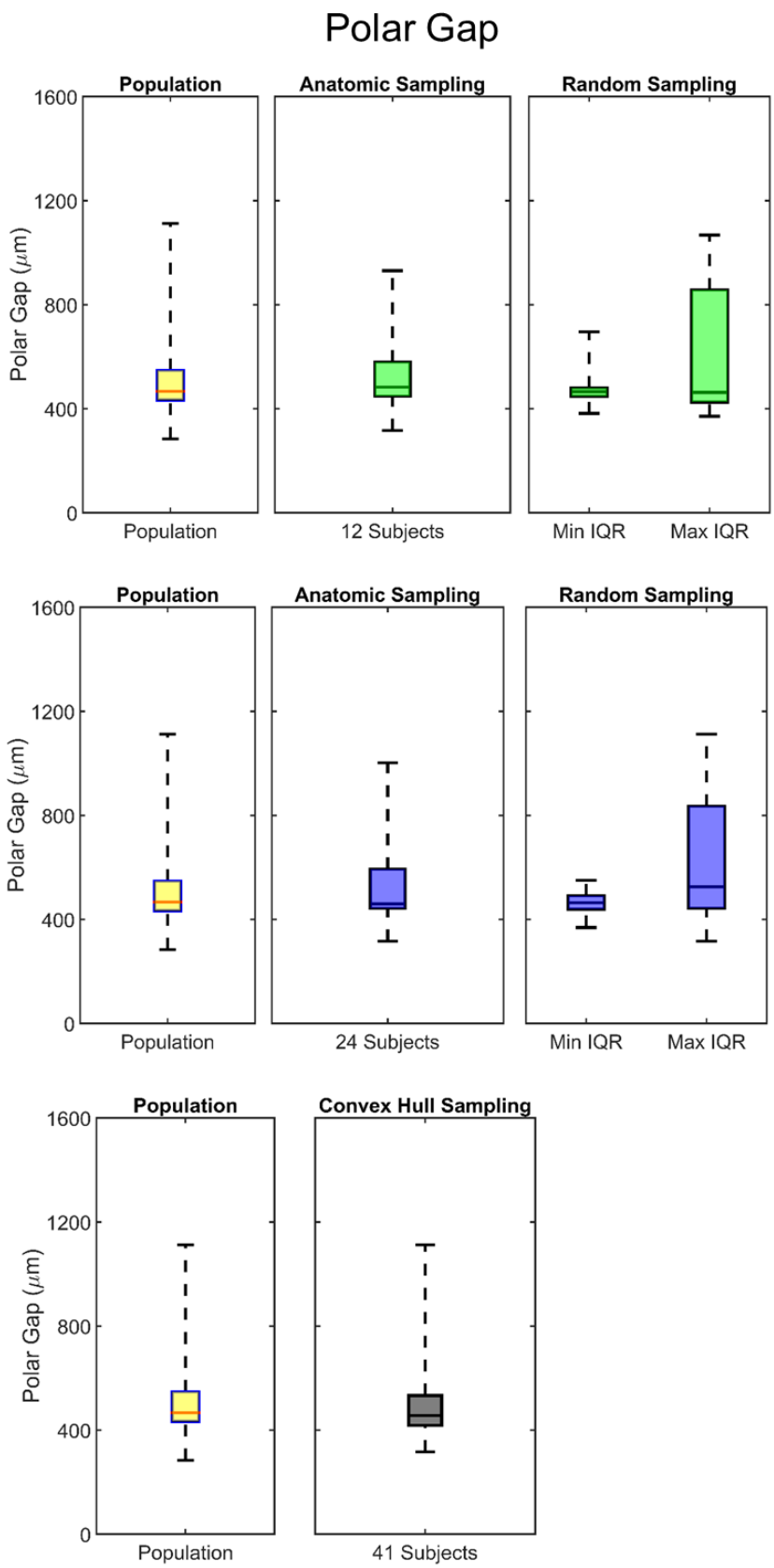

Figure 4.14 Distribution of the polar gap in the cohort compared with subsets based on 12 subjects (first row), subsets based on 24 subjects (second row), and a subset based on convex hull sampling.

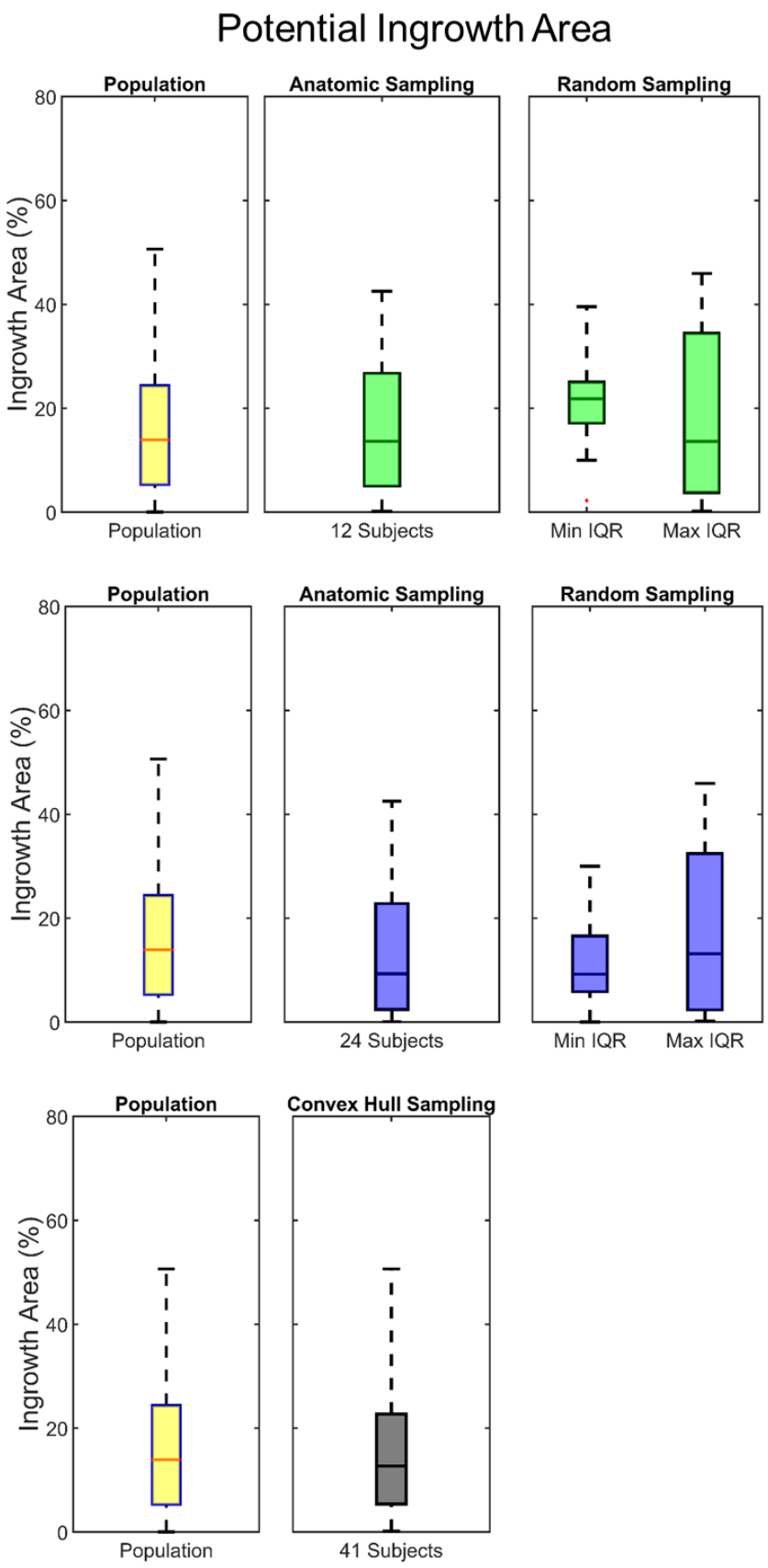

Figure 4.15 Distribution of the potential ingrowth area in the cohort compared with subsets based on 12 subjects (first row), subsets based on 24 subjects (second row), and a subset based on convex hull sampling.

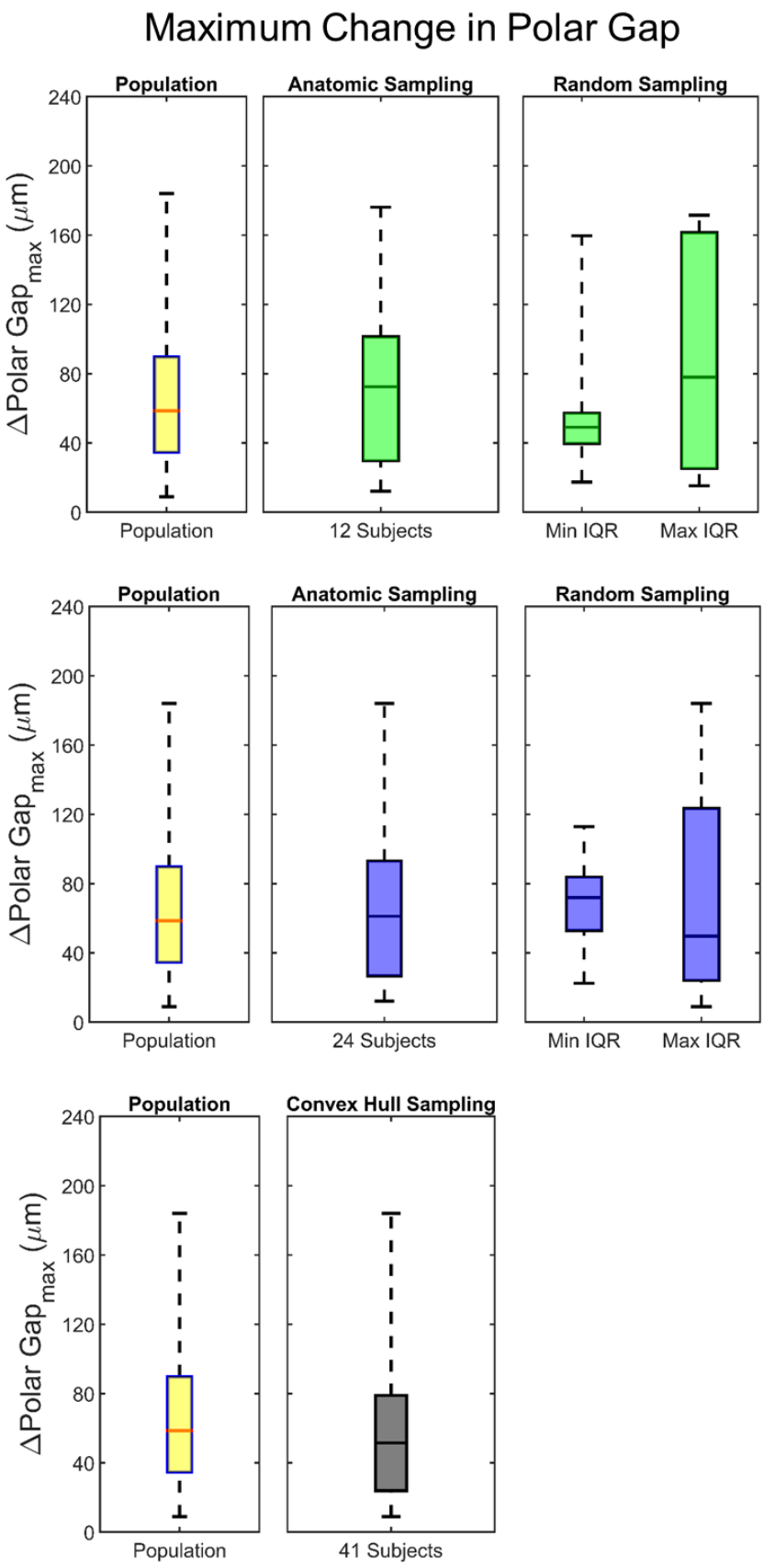

Figure 4.16 Distribution of the maximum change in polar gap in the cohort compared with subsets based on 12 subjects (first row), subsets based on 24 subjects (second row), and a subset based on convex hull sampling.

4.4 Discussion

The aims of the present study were to explore the variation in primary stability of a cementless acetabular cup in a cohort of patient-specific finite element models, investigate the association between patient-related factors and primary stability, and produce a subset of subjects that could represent the variability in output metrics in the cohort.

The models predicted a wide variation in interfacial gaps and micromotion in the cohort for a cementless cup design with excellent clinical survivorship after 10 years (See 3.4.1). The cohort in this study were representative of the age, BMI and bone quality of the patient population who most commonly undergo total hip arthroplasty (See 3.2.1). Therefore, the variation in interfacial gaps and micromotion in the study can provide a suitable benchmark for future comparisons with new acetabular cup designs in the same set of models. Sampling the cohort based on the patient-related factors produced subsets of subjects that could describe the variability in the primary stability output metrics in the cohort. Results indicated no clear linear relationship between any patient-related factor and the primary stability output metrics. However, when the factors were categorized into quartiles, trends suggested larger polar gaps were present in subjects with small acetabular diameters and depth. Meanwhile, there was evidence of a decreasing trend in micromotion and change in polar gap during gait in bodyweight and elastic modulus quartile groups.

While the extent of the polar gaps was variable within the cohort, 64 of the 103 subjects had polar gaps below 500 μm and 99 subjects had below 1000 μm. This distribution of polar gaps was comparable to Schmalzried et al. and Udomkiat et al. who reported gaps to measure mostly below 500 μm and never greater than 1000 μm on series of initial postoperative radiographs (Schmalzried et al., 1992b; Udomkiat et al., 2002). An *in vitro* study found gaps near the polar region had a range of <1000 to 1370 μm for various interference fits (MacKenzie et al., 1994).

The significant difference in polar gap between genders and the trends in the acetabular diameter and depth groups suggested larger polar gaps occurred in smaller acetabula. This

trend was similar to Adler et al. who found that small or shallow cavities in foam blocks prevented complete seating of the cup (Adler et al., 1992). Based on findings of larger polar gaps in cadaveric specimens with higher interference fits, MacKenzie et al. postulated that larger gaps occur with the insertion of smaller components into a smaller acetabulum when the same interference fit is performed (MacKenzie et al., 1994). A possible explanation for the trend in this study may be that that there is proportionally higher change in acetabular volume in a small acetabulum when expanding during insertion (Ries et al., 1997), resulting in a higher relative cup-bone stiffness and thus allowing for larger polar gaps following insertion.

The 95th percentile CPM most commonly occurred between 40% and 60% of the gait cycle, when the hip joint is in extension (Kadaba et al., 1990). This is in agreement with Spears et al. and Hsu et al. who reported peak micromotion occurred at 40% of gait when loads were not at peak value (Hsu et al., 2007; Spears et al., 2001). Pakvis et al. found the largest micromotions at the beginning of the swing phase (63%) of gait (Pakvis et al., 2014), which occurred in a smaller proportion of the subjects in this study. However, the 95th percentile CPM was higher in magnitude than micromotion predicted in previous FE models (Hsu et al., 2007; Spears et al., 2000). The magnitudes were in closer agreement to Pakvis et al. who reported micromotions were much greater than 150 μm in three different press fit cups with interference fits of 1.5 – 2mm (Pakvis et al., 2014). Higher micromotion may have been observed in this study because of the lower interference fit and elastic modulus within the acetabular cavity than previously applied in FE studies which have both been shown to affect micromotion in models (Hsu et al., 2007; Janssen et al., 2010).

Subjects with rim-dominant strain patterns had higher potential ingrowth area than uniform strain pattern which suggests that compression at the rim may resist tangential micromotion more than at the floor of the acetabulum. However, subjects with rim-dominant strain patterns had greater polar gaps which allowed for higher changes in the polar gap during gait than uniform strain patterns. The larger interfacial gaps and greater gap changes may

provide more access for joint fluid and particulate debris to penetrate the periprosthetic joint space (Schmalzried et al., 1992a). The median equivalent strain values in the cavities were in accordance with maximum principal strain in previous FE models also using a linear elastic assumption (Ries and Harbaugh, 1997; Ries et al., 1997). However, equivalent strains predominantly exceeded the yield criterion of 7000 μstrain for cancellous bone (Morgan and Keaveny, 2001) in all subjects and the values may not have represented values *in vivo*.

Trends in micromotion and maximum polar gap changes suggested more motion of the cup occurred in higher bodyweight and in lower elastic modulus groups. Previous clinical studies have not found increased bodyweight to influence the failure of cementless cups (Röder et al., 2010) or increased risk of loosening in obese (BMI > 30) versus non-obese groups (Cherian et al., 2015). However, there is some evidence to suggest higher aseptic loosening and increased risk of mechanical failure of the cup occurs in obese patients within 5 years (Electricwala et al., 2016; Röder et al., 2010). Previous FE studies on cementless cup stability found poorer bone quality resulted in higher micromotion at the bone-implant interface (Hsu et al., 2007; Janssen et al., 2010; Ong et al., 2008). Ong et al. found lower elastic moduli increased the change in gap volume after loading and unloading of the peak gait force (Ong et al., 2008).

The cups demonstrated limited potential ingrowth areas and variable ingrowth patterns in the cohort. In a previous FE study, Ong et al. found higher potential ingrowth areas (15 – 30%) in a single subject than in this study using the same measurement criteria (Ong et al., 2008). Compared with porous-coated acetabular cups retrieved post mortem, the potential ingrowth areas found in this study were similar to the bone ingrowth areas found by Bloebaum et al. in 7 cups (mean 12%, range 4 – 21%) (Bloebaum et al., 1997), higher than found by Sumner et al. in 25 cups (median 3.6%, range 0 – 85%) (Sumner et al., 1993) but lower than reported by Engh et al. in 9 cups (mean 32%, range 3 – 84%) (Engh et al., 1993). The potential ingrowth areas compared well with the distribution of bone ingrowth area in 23 Pinnacle® shells retrieved

by Swarts et al. and there was agreement in the proportion of cups with an ingrowth area below 5% (23% vs 26% in Swarts et al.) (Swarts et al., 2015).

By including the extremes of variability in the patient-related factors, the subset of 12 subjects based on anatomic sampling could reasonably approximate the variation in the output metrics in the cohort. In contrast, the subsets produced by random sampling were highly variable and not suitable for describing the primary stability in a population. While stratifying by gender did improve the approximation, the improvement of 24 subjects was not significant. In the pursuit of an assessment of patient and surgical variability in pre-clinical testing with as reduced a time and computational cost as possible, this may double the computation time required. Similarly, the convex hull produced a subset that approximated the variation in output metrics and could capture the full range of variation with the inclusion of the minimum and maximum of each output metric. However, the subset consisted of 41 subjects that would require a significantly higher time cost. The subset of 12 subjects can be representative of the cohort and, in turn, the target total hip arthroplasty population in providing a gross indication of the level of variability in primary stability in pre-clinical testing of prospective cementless acetabular cups.

There are limitations with this study. Pelvic muscle forces were not included in the models. Inclusion of muscle forces may have altered the biomechanics of the hemipelvis. Bone was assumed to be linear-elastic and the permanent deformation of the hemipelvis during insertion was not considered. The residual strain in the acetabulum acting on the acetabular shell is responsible for primary stability and higher post-insertion strain observed may have underestimated micromotion. Taking the gait cycle from one level walking trial and scaling to the bodyweight of each subject meant the loading on each hemipelvis was not truly patient-specific. In order to provide a more realistic creation of polar gaps during insertion, viscous damping was applied to the cup. While the method has not been experimentally validated, the polar gaps measured in the study were consistent with previous *in vivo* and *in vitro* studies.

In conclusion, this study presented the variation in primary stability of a Pinnacle ® cup in a large cohort of FE models and investigated the association with patient-related factors. Moreover, it investigated subset of subjects that could represent the variability in output metrics in the cohort. The study cannot be wholly conclusive on the relationship between patient-related factors and primary stability of the cup. However, observed trends suggest the polar gap was influenced by acetabular geometry and cup motion during a gait cycle was affected most by elastic modulus and bodyweight. By considering patient variability in the primary stability of an established cementless acetabular cup, this work can play a role in the comprehensive pre-clinical assessment of prospective cementless acetabular cup designs.

Chapter 5

A Computational Efficient Method to Assess the Sensitivity of Finite Element Models: An Illustration with the Intact Hemipelvis[3]

5.1 Introduction

Surrogate modelling speeds up solutions of large statistical problems and may facilitate the assessment of model sensitivity. The technique involves generating a response surface by interpolating a subset of solutions so that output metrics can be predicted without expensive simulation code. The approach is based on the assumption that the surrogate model, once built, will be faster than the original simulation while still being accurate when predicting outside the known data points (Forrester et al., 2008). Previous computational studies that adopted a surrogate modelling approach used linear functions (Fitzpatrick et al., 2014; Halloran et al., 2008), Bayesian Gaussian process models (Bah et al., 2011), Random Forests (Donaldson et al., 2015), artificial neural networks (Eskinazi and Fregly, 2015) or Kriging models (Lin et al., 2010;

[3] Work in this chapter has been published in the following journal article:

O'Rourke, D., Martelli, S., Bottema, M., and Taylor, M., 2016, *A Computational Efficient Method to Assess the Sensitivity of Finite-Element Models: An Illustration with the Hemipelvis* Journal of Biomechanical Engineering, 138(12).

Pant et al., 2011) built from a set of training data. Surrogate models can predict the output of a high volume of FE models in a short period of time and have the potential to be a computationally cheap alternative to running a full factorial design analysis.

The aim of this study was to use a surrogate modelling approach to develop a time-efficient method for quantifying FE model sensitivity to input parameters and their interactions. As an illustration, the method was applied to an FE model of the intact hemipelvis. The hemipelvis is an important weight-bearing structure in the human body (Anderson et al., 2005) and is one of the most complex models in biomechanics. This study focused on the sensitivity of strain outputs in the model to typical uncertainties in geometrical parameters and material properties. The accuracy of the surrogate modelling approach and computational time required to test model sensitivity was assessed by comparing it to a full factorial design analysis of the same FE model.

5.2 Methods

5.2.1 Finite Element Model of the Intact Hemipelvis

The study was based on a CT scan of healthy intact hemipelvis from a male donor (65 yrs, 68 kg). The CT scan was obtained with an Aquilion 16 MDCT scanner (Toshiba Medical Systems Corporation, Tokyo, Japan) through a helical scan protocol and typical settings for clinical examination (tube current: 180 mA, 120 kVp). The slice thickness was 2.0 mm and the spacing was 1.6 mm. The pixel spacing was 0.976 x 0.976 mm.

The geometry of the hemipelvis, femoral head and an intermediate soft tissue layer were segmented using a threshold-based algorithm and a manual refinement of the geometry boundaries (ScanIP, Simpleware Ltd., Exeter, UK). The segmented volumes were meshed with linear tetrahedral elements with an average element edge length of 0.75 mm. The sacroiliac joint and pubic symphysis were fully constrained. The soft tissue layer was fully bonded to the surface of the acetabulum and assigned a Young's Modulus of 15 MPa and Poisson's ratio of 0.3.

It was included to mimic a realistic hemipelvis-femur pressure distribution (Daniel et al., 2005). The femoral head and the hemipelvis interface was a frictionless surface-to-surface contact.

Inhomogeneous material properties for the cancellous bone were extracted from the CT data. The density of the marrow in the medullary canal of the femur was considered to be equivalent to the density of water and the Hounsfield Unit (HU) was assigned an apparent density of 0 gcm^{-3}. The highest HU in the femur was considered to be cortical bone and assigned an apparent density of 1.73 gcm^{-3} (Bryan et al., 2010; Ghosh et al., 2015). A linear relationship between the apparent bone density (ρ_{app}) and the HUs on the CT image was assumed based on these two HU and apparent density correspondences and was given by:

$$\rho_{app} = 0.00102HU + 0.0864 \qquad (1)$$

The relationship between the apparent density and the cancellous bone elastic modulus (E_{bone}) was determined by an empirical power relation (Dalstra et al., 1993).

$$E_{bone} = 2017.3\rho_{app}^{2.46} \qquad (2)$$

The hemipelvis was modelled as a sandwich structure and an outer cortical bone shell was represented by constant thickness shell elements (Dalstra and Huiskes, 1991). All materials in the model were assumed to be locally isotropic and linear-elastic.

A load of 1730 N (F_x = 445 N, F_y = -550 N, F_z = 1578 N) was applied to the base of the femoral head in each simulation. This represented the peak load of a level walking trial of a male patient (H6R) in the Orthoload dataset (Bergmann, 2001) who was closest in age to the male donor in this study and scaled to the bodyweight of the donor (68 kg). The median, 95th

percentile and maximum equivalent strains in the cancellous bone were calculated from the acetabular region of interest (Figure 5.1). The single strain values were taken as aggregate information about the strain distribution in the region of interest and these output metrics are often the object of the analysis in implant stability studies (Dopico-González et al., 2010). Characterising the response of cancellous bone to physiologic alterations is an important topic in musculoskeletal research (Goldstein, 1987; Keaveny et al., 2001). Strain measurements in bone may be more statistically powerful for cancellous bone and yield strain can be considered uniform within an anatomic site (Morgan and Keaveny, 2001). Thus, the equivalent strain of the cancellous bone was chosen as the output metric to be assessed (Ghosh et al., 2015) as it contains contributions from compressive and tensile strain to give an indication of the overall strain level in the bone. The cancellous bone behind the acetabulum contact surface was chosen as the region of interest because it is a critical region for the load transfer between the hemipelvis and the femur load (Dalstra and Huiskes, 1995).

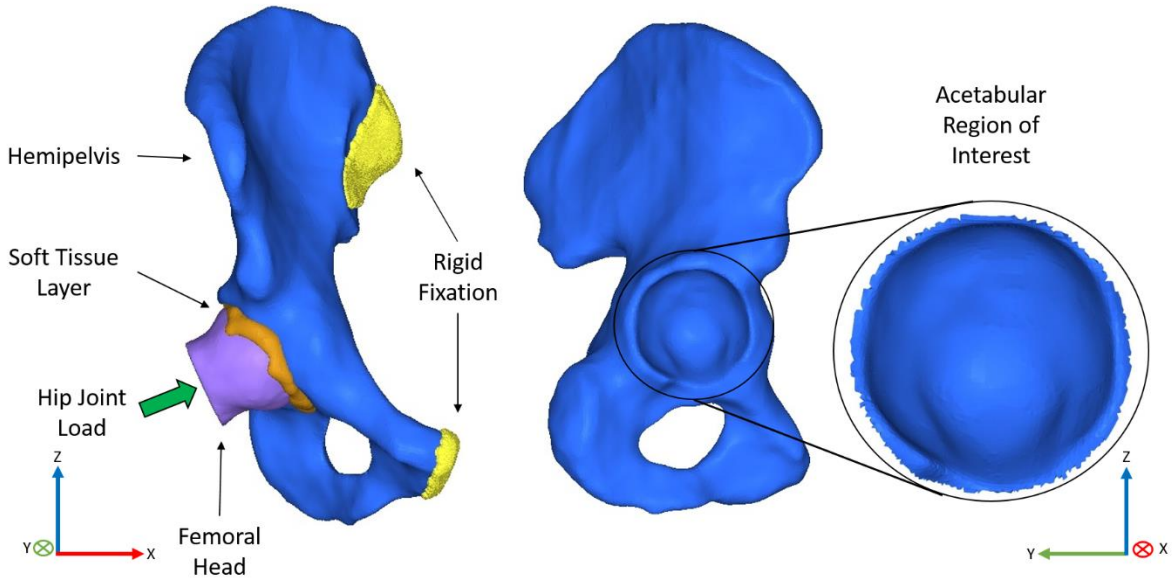

Figure 5.1 The Finite Element model of the intact hemipelvis, soft tissue layer and femoral head with the boundary conditions and the acetabular region of interest. A load, representing the peak load experienced during gait, was applied to the base of the femoral head.

5.2.2 Sensitivity Analysis

The model input parameters investigated as part of the sensitivity study were 1) bone geometry, 2) cortical bone elastic modulus, 3) cancellous bone elastic modulus, 4) cortical bone shell thickness, 5) cortical bone Poisson's ratio and 6) cancellous bone Poisson's ratio. Three levels were chosen for each input parameter and represented the range of values typically reported in the literature. The input parameters and their levels are summarised in Table 5.1.

A scale factor represented variation in acetabular geometry due to uncertainty in boundary definition during segmentation. In this study, segmentation was carried out with a threshold-based algorithm, the results of which can depend on the threshold value chosen (Taddei et al., 2006). The ranges of cancellous bone elastic moduli were determined by varying the upper bound of the apparent density of bone to offset the empirical power relation. The upper bounds were varied to match the variation in apparent density measured on CT scans of six pelvic bones (Dalstra et al., 1993). The cancellous Poisson's ratio was varied based on measurement

uncertainty of unconstrained compressive mechanical testing on specimens from pelvic bone (Dalstra et al., 1993). The levels for the cortical bone shell thickness (Anderson et al., 2005; Dalstra and Huiskes, 1991; Manley et al., 2006; Phillips et al., 2007) and cortical bone elastic modulus (Anderson et al., 2005; Dalstra et al., 1995; Majumder et al., 2007; Reilly and Burstein, 1974; Zhang et al., 2010) were chosen to encompass the range of assumed values in FE models of the intact hemipelvis. Values of cortical bone Poisson's ratio were assigned ± 0.05 of the most common value reported in the literature (Anderson et al., 2005; Dalstra et al., 1995).

Input Parameter	Level 1	Level 2	Level 3	References
Uniform Scale Factor	0.95	1	1.05	(Taddei et al., 2006)
Cortical Bone Elastic Modulus (MPa)	12000	17000	22000	(Anderson et al., 2005; Dalstra and Huiskes, 1991; Manley et al., 2006; Phillips et al., 2007)
Cancellous Bone Elastic Modulus (MPa)	16-3706	22-5227	69-7228	(Dalstra et al., 1993)
Cortical Bone Thickness (mm)	1	1.5	2	(Anderson et al., 2005; Dalstra and Huiskes, 1991; Dalstra et al., 1995; Majumder et al., 2007; Reilly and Burstein, 1974)
Cortical Bone Poisson's Ratio	0.25	0.3	0.35	-
Cancellous Bone Poisson's Ratio	0.08	0.2	0.32	(Dalstra et al., 1993)

Table 5.1 The model input parameters investigated in the sensitivity analysis with their values.

5.2.3 Full Factorial Design

In the full factorial design, all possible combinations of the input parameters and their levels were simulated in static analyses (ABAQUS/Standard v6.13). For the six input parameters, at three levels, there were a total of $3^6 = 729$ simulations. Each simulation was processed with 8 CPUs (Intel ® Xeon ® 2.4 GHz processor, 32 GB RAM).

5.2.4 Surrogate Models

Linear and Kriging models were used to develop the surrogate models. The linear model is based on a multilinear regression model that expresses a predictor of an unknown output variable as a linear combination of the input parameters. Kriging is an optimal interpolation used to predict unknown output variables based on the regression of surrounding data. Kriging makes a prediction for a 'new', unknown output variable as a weighted sum of all the known output metrics. Weightings are derived from the covariances between the known output metrics and the covariances between the known and the unknown output metrics. These optimal weightings vary with the unknown output variable to be predicted according to the relative proximity of the known output metric (Forrester et al., 2008). The SUrrogate MOdeling (SUMO) toolbox (Gorissen et al., 2010), developed for MATLAB, was used to build the Kriging and linear surrogate models.

5.2.5 Data Analysis

Surrogate models were built from training sets consisting of size 10, 20, 30, 40, 50, 100 and 200 training simulations for each of the equivalent strain output metrics. Training sets were random samples of analyses from the full factorial design. The surrogate models were then used to predict the output metrics of the remaining analyses in the full factorial design that were not included in the training set. In order to study the influence of the sampling method, the surrogate models were built 100 times per training set size. The surrogate model predictions

were plotted against the corresponding FE predictions and the slope, coefficient of determination (R^2) and root mean square error (RMSE) were computed.

The influence of the input parameters and possible interactions on the output metrics were determined by ANOVA (Dar et al., 2002; Isaksson et al., 2008). For the full factorial design and surrogate model, the ANOVA calculated the sum of squares for each input parameter and up to the 3-way interaction terms. The influence of a term was determined by expressing its sum of squares as a percentage of the total sum of squares (%TSS). ANOVA of the surrogate model predictions was conducted on the model that produced the best R^2 value.

5.3 Results

The median, 95th percentile and maximum equivalent strains were recorded from the acetabular region of interest for all simulations in the full factorial design. The median strain had a range of 19 – 934 μstrain. The 95th percentile strain had a range of 71 – 5298 μstrain. The maximum strain had a range 738 – 37489 μstrain (Figure 5.2).

Increasing the training set size from 30 to 200 saw little improvement in the accuracy of the linear surrogate model. Between these training sets the mean slope for the median equivalent strain was 0.79, the 95th percentile had a range 0.73 – 0.76 and the maximum had a range 0.86 – 0.88. Meanwhile, the R^2 values had a range of 0.75 – 0.78 for the median, 0.68 – 0.73 for the 95th percentile and 0.85 – 0.87 for the maximum equivalent strains. The best-case R^2 did not change for training sets greater than 40 analyses for all strain output metrics. Best-case R^2 values reached a saturation point of 0.79 for the median strain, 0.74 for the 95th percentile and 0.87 for the maximum strain. There were small differences between the mean and the best-case scenarios for the slope and R^2 values for training sets of 40 analyses or greater (Table 5.2).

The Kriging model surrogate model reached a high accuracy with a training set of 30 analyses with no further improvement seen with the further addition of training simulations.

The mean slope range for training sets greater than 30 analyses was 0.95 – 1.00 for the median, 0.91 – 1.00 for the 95th percentile and 0.94 – 1.00 for the maximum strains. The mean R^2 was approximately 0.99 for all output metrics in training sets greater than 30 analyses. Similar to the linear model, there was little difference between the mean and best-case slopes and R^2 values after saturation (Table 5.3).

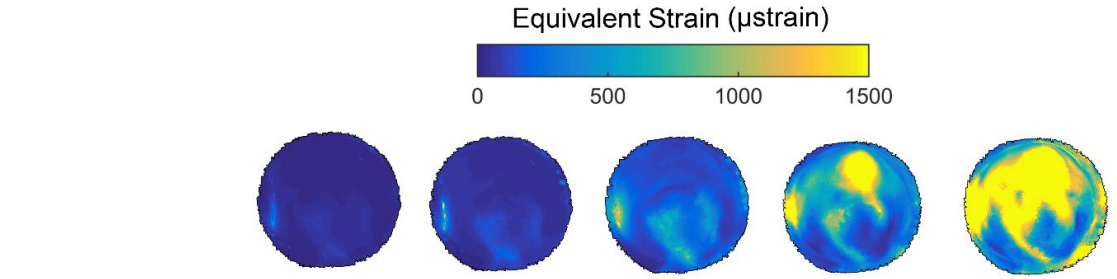

Median	20	47	147	379	912
95th Percentile	71	149	567	1760	4881
Max	738	1737	7944	14320	37489

Figure 5.2 An illustration of the variation in equivalent strain in the acetabular region of interest. From left to right, the models with the minimum, 25th percentile, median, 75th percentile and maximum of the maximum equivalent strain are shown. The median, 95th percentile and maximum equivalent strains (μstrain) are given for each of the regions of interests displayed.

Increasing the training set size resulted in an RMSE improvement for the Kriging surrogate model but not for the linear model. In the Kriging model, improvements in the RMSE continued to be observed as the training set size increased. The RMSE had a range of 178.9 – 2.7 for the median, 938.4 – 15.7 for the 95th percentile, and 5383.2 – 134.5 for the maximum strains (Table 5.3). In contrast, the linear model had only marginal improvements in the RMSE in training sets greater than 40 analyses. In training sets from 40 to 200 analyses the RMSE had a range of 113.8 – 104 for the median, 651.1 – 595 for the 95th percentile and 3291.2 – 3038.7 for the maximum equivalent strains (Table 5.2).

Linear Surrogate Model									
	Slope			R^2			RMSE		
Training Dataset	Median	95th Percentile	Max	Median	95th Percentile	Max	Median	95th Percentile	Max
10	0.77 (0.99)	0.77 (1.01)	0.85 (1.01)	0.56 (0.78)	0.50 (0.73)	0.73 (0.86)	195.7 (116.64)	1108.3 (665.37)	5156.4 (3188.97)
20	0.81 (1.00)	0.73 (0.99)	0.88 (1.01)	0.72 (0.78)	0.66 (0.73)	0.83 (0.87)	130.6 (108.7)	736.7 (609.9)	3806.8 (3141.4)
30	0.79 (1.01)	0.74 (1.00)	0.88 (1.00)	0.75 (0.78)	0.68 (0.74)	0.85 (0.87)	119.0 (105.1)	682.5 (594.4)	3372.8 (3032.0)
40	0.79 (0.99)	0.76 (0.99)	0.88 (1.00)	0.76 (0.79)	0.70 (0.74)	0.86 (0.87)	113.8 (103.6)	651.1 (596.7)	3291.2 (2982.8)
50	0.79 (1.00)	0.75 (1.04)	0.86 (1.01)	0.77 (0.79)	0.71 (0.74)	0.86 (0.87)	111.1 (103.2)	635.0 (591.5)	3245.9 (2945.9)
100	0.79 (0.97)	0.73 (0.94)	0.88 (1.01)	0.78 (0.79)	0.72 (0.74)	0.87 (0.88)	106.9 (103.1)	609.0 (581.8)	3079.3 (2953.3)
200	0.79 (0.88)	0.73 (0.85)	0.87 (0.99)	0.78 (0.80)	0.73 (0.74)	0.87 (0.88)	104.0 (100.3)	595.0 (565.2)	3038.7 (2884.1)

Table 5.2 Mean and best (in parentheses) slope, R^2 and RMSE values for the 100 repeats of the Linear surrogate model at each training set size.

Kriging Surrogate Model									
	Slope			R^2			RMSE		
Training Dataset	Median	95th Percentile	Max	Median	95th Percentile	Max	Median	95th Percentile	Max
10	0.45 (1.03)	0.49 (1.01)	0.63 (1.01)	0.44 (0.94)	0.47 (0.92)	0.64 (0.95)	178.9 (64.9)	938.4 (354.1)	5383.2 (2132.3)
20	0.84 (1.00)	0.81 (1.00)	0.88 (1.00)	0.89 (0.98)	0.85 (0.98)	0.91 (0.98)	71.5 (29.4)	444.2 (147.5)	2527.5 (1156.2)
30	0.95 (1.00)	0.91 (1.00)	0.94 (1.00)	0.97 (1.00)	0.95 (0.99)	0.96 (0.99)	34.6 (16.0)	263.6 (89.8)	1618.2 (859.0)
40	0.96 (1.00)	0.96 (1.00)	0.97 (1.00)	0.99 (1.00)	0.98 (1.00)	0.98 (0.99)	24.7 (12.4)	166.7 (68.0)	1257.7 (609.6)
50	0.98 (1.00)	0.97 (1.00)	0.98 (1.00)	0.99 (1.00)	0.99 (1.00)	0.99 (1.00)	18.2 (9.3)	123.3 (56.3)	931.4 (471.0)
100	0.99 (1.00)	0.99 (1.00)	0.99 (1.00)	1.00 (1.00)	1.00 (1.00)	1.00 (1.00)	6.5 (4.3)	46.6 (25.3)	338.8 (199.1)
200	1.00 (1.00)	1.00 (1.00)	1.00 (1.00)	1.00 (1.00)	1.00 (1.00)	1.00 (1.00)	2.7 (1.9)	15.7 (9.0)	134.5 (85.6)

Table 5.3 Mean and best (in parentheses) slope, R^2 and RMSE values for the 100 repeats of the Kriging surrogate model at each training set size

The ANOVA revealed that changes to the bone geometry induced the greatest change in bone strain but that interaction terms also had a strong influence (Table 5.4). For the median and 95th percentile equivalent strain, geometry had %TSS of 60% and 52% and the cancellous bone modulus was next most influential with 22% and 26% respectively (Table 5.4 and Table 5.5). The geometry was more dominant on the maximum equivalent strain at 76.6% and the second most influential input was the cortical bone thickness (7.84%). The interaction between the scale and cancellous bone modulus was ranked as the third most influential factor on the median and 95th percentile equivalent strains (median 12.8%, 95th percentile 13.1%). For the maximum equivalent strain, the interaction between the scale factor and the cortical bone thickness, 7.23%, was ranked third most influential term (Table 5.6).

There was <1% difference between %TSS of the full factorial design and Kriging for all input parameters and interaction terms in training sets greater than 20 analyses. The linear model matched the rank of the individual input parameters in the full factorial design but there was more variability in the %TSS values. For example, for the median strain the geometry had a %TSS of 60%. On the other hand, the ANOVA based on the linear model predictions had a range of 63.64 – 70.90% (Table 5.4). Similar variability was seen for the remaining individual input parameters on all output metrics. The linear model could not describe the influence of any of the interaction terms (%TSS values were approximately zero for all interaction terms in all output metrics).

There was a significant time and computational saving associated with the surrogate modelling approach. Running the 729 FE models in the full factorial design took approximately 20.25 days (486 h) simulation time. A Kriging surrogate model with an R^2 of at least 0.95 for the median, 95th percentile and maximum equivalent strains required a training set of 30 analyses. Assuming an average simulation time per analysis, this would take approximately 20 h simulation time to evaluate the strain outputs for all combinations of input parameters.

ANOVA (%TSS)															
Median Equivalent Strain	Full Factorial Design	Linear							Kriging						
Training Dataset:	729	10	20	30	40	50	100	200	10	20	30	40	50	100	200
Uniform Scale Factor	59.93	63.64	69.30	64.53	70.90	69.89	67.84	66.58	66.67	61.46	59.58	60.15	60.41	59.93	59.96
Cancellous Bone Modulus	22.01	32.99	26.98	31.35	25.32	26.51	25.89	24.89	18.99	22.52	22.70	21.94	21.99	22.09	22.00
Cortical Bone Thickness	0.85	2.15	1.52	1.67	0.40	0.45	0.65	0.89	0.24	0.86	0.99	0.87	0.85	0.86	0.84
Cortical Bone Modulus	0.79	0.73	0.91	1.46	1.80	0.66	1.33	0.78	0.0065	0.66	0.53	0.75	0.67	0.77	0.79
Cancellous Bone Poisson's Ratio	0.061	0.40	0.0066	0.0041	0.19	0.44	0.24	0.042	0.0094	0.16	0.042	0.069	0.049	0.064	0.066
Cortical Bone Poisson's Ratio	0.0066	0.08	0.99	0.12	0.22	0.40	0.32	0.071	0.13	0.014	0.0055	0.0053	0.025	0.0080	0.0058
Scale*Cancellous Bone Modulus	12.79	0.000066	0.0062	0.024	0.037	0.059	0.25	0.98	13.38	12.75	12.65	12.25	12.43	12.73	12.78
Scale*Cortical Bone Thickness	2.60	0.000046	0.0027	0.016	0.0069	0.045	0.093	0.27	0.32	1.04	2.42	2.95	2.59	2.60	2.60
Cortical Bone Thickness*Cancellous Bone Modulus	0.24	0.000088	0.0016	0.006	0.0041	0.025	0.056	0.054	0.042	0.043	0.35	0.37	0.22	0.26	0.23
Scale*Cortical Bone Modulus	0.17	0.000036	0.00096	0.0024	0.0023	0.0043	0.035	0.051	0.030	0.071	0.046	0.062	0.14	0.17	0.17
Scale*Cortical Bone Thickness*Cancellous Bone Modulus	0.44	0.000042	0.0046	0.0059	0.0069	0.043	0.043	0.069	0.031	0.12	0.61	0.50	0.50	0.43	0.44

Table 5.4 The percentage of the total sum of squares (%TSS) of the individual input parameter factors and the most important interactions accounting for 99% of the relative influence on the median equivalent strain. For the surrogate models, the %TSS are displayed for the training sets with the best R^2 value

ANOVA (%TSS)															
95th Percentile Equivalent Strain	Full Factorial Design	Linear							Kriging						
Training Dataset:	729	10	20	30	40	50	100	200	10	20	30	40	50	100	200
Uniform Scale Factor	52.53	68.57	67.75	69.46	59.77	60.32	63.49	58.53	44.19	54.45	53.64	52.21	52.57	52.41	52.39
Cancellous Bone Modulus	26.43	26.72	28.07	28.51	36.89	36.38	31.84	30.25	35.10	26.41	24.87	26.00	26.18	26.59	26.53
Cortical Bone Thickness	0.99	4.10	2.61	0.66	1.19	0.87	0.21	1.34	0.29	0.47	1.36	1.21	0.99	1.01	0.98
Cortical Bone Modulus	0.63	0.45	0.65	0.59	0.87	1.10	0.97	0.97	0.0009	0.25	0.38	0.59	0.49	0.60	0.62
Cancellous Bone Poisson's Ratio	0.057	0.00071	0.016	0.0065	0.080	0.05	0.13	0.084	0.0068	0.088	0.14	0.11	0.060	0.053	0.054
Cortical Bone Poisson's Ratio	0.0066	0.14	0.12	0.020	0.062	0.006	0.012	0.066	0.0081	0.00044	0.028	0.020	0.015	0.0054	0.0074
Scale*Cancellous Bone Modulus	13.10	0.00023	0.011	0.013	0.035	0.038	0.12	1.30	17.99	14.35	13.98	13.00	13.60	13.16	13.16
Scale*Cortical Bone Thickness	3.04	0.000039	0.0069	0.020	0.0074	0.013	0.059	0.28	1.56	1.82	2.39	3.00	3.00	2.99	3.02
Cortical Bone Thickness*Cancellous Bone Modulus	0.84	0.00023	0.0034	0.0050	0.00063	0.0039	0.015	0.12	0.48	0.51	1.15	1.10	0.86	0.89	0.84
Scale*Cortical Bone Modulus	0.27	0.000052	0.0015	0.0065	0.014	0.010	0.015	0.05	0.012	0.061	0.32	0.20	0.24	0.23	0.26
Scale*Cortical Bone Thickness*Cancellous Bone Modulus	1.45	0.00047	0.010	0.012	0.025	0.028	0.059	0.22	0.32	1.30	1.13	1.64	1.47	1.42	1.45

Table 5.5 The percentage of the total sum of squares (%TSS) of the individual input parameter factors and the most important interactions accounting for 99% of the relative influence on the 95th percentile equivalent strain.

ANOVA (%TSS)															
Max Equivalent Strain	Full Factorial Design	Linear							Kriging						
Training Dataset:	729	10	20	30	40	50	100	200	10	20	30	40	50	100	200
Uniform Scale Factor	76.57	88.68	87.30	85.87	85.23	83.33	86.70	82.60	79.27	74.69	75.87	76.18	76.42	76.58	76.62
Cancellous Bone Modulus	1.16	2.15	0.32	1.62	2.27	0.96	0.95	1.30	0.19	0.54	1.11	1.03	1.20	1.21	1.15
Cortical Bone Thickness	7.84	4.76	8.15	8.45	7.71	9.46	7.35	7.88	7.03	10.37	7.69	7.96	7.53	7.82	7.86
Cortical Bone Modulus	3.30	4.16	4.10	3.69	3.92	4.66	2.48	3.68	2.67	2.56	2.51	3.59	2.99	3.33	3.26
Cancellous Bone Poisson's Ratio	0.042	0.026	0.020	0.0093	0.015	0.14	0.073	0.061	0.073	0.0044	0.011	0.042	0.058	0.034	0.042
Cortical Bone Poisson's Ratio	0.015	0.18	0.029	0.070	0.0025	0.086	0.024	0.0051	0.074	0.016	0.0026	0.0053	0.029	0.014	0.015
Scale*Cancellous Bone Modulus	0.83	0.00022	0.00032	0.0013	0.0026	0.019	0.056	0.19	0.052	1.38	0.97	0.50	0.98	0.86	0.82
Scale*Cortical Bone Thickness	7.23	0.00058	0.0012	0.0063	0.021	0.046	0.24	0.74	6.82	7.50	8.81	6.82	7.57	7.17	7.27
Cortical Bone Thickness*Cancellous Bone Modulus	0.53	0.00020	0.00047	0.00072	0.0047	0.021	0.031	0.073	0.013	0.47	0.30	0.82	0.59	0.52	0.53
Scale*Cortical Bone Modulus	1.55	0.00035	0.00076	0.0019	0.016	0.030	0.058	0.26	3.17	1.07	1.50	1.68	1.56	1.61	1.54
Scale*Cortical Bone Thickness*Cancellous Bone Modulus	0.64	0.00082	0.00051	0.0030	0.029	0.017	0.051	0.092	0.0018	1.18	0.54	0.99	0.72	0.57	0.62

Table 5.6 The percentage of the total sum of squares (%TSS) of the individual input parameter factors and the most important interactions accounting for 99% of the relative influence on the maximum equivalent strain.

5.4 Discussion

The aim of this study was to combine biomechanical FE models and surrogate modelling to efficiently quantify the sensitivity of an FE model's equivalent strain output to bone geometry and material property input parameters and their possible interactions. An FE model of the intact hemipelvis was chosen to illustrate the method because it represented a complex model in biomechanics and is an important weight-bearing structure in the human body (Anderson et al., 2005). A full factorial analysis was performed on six geometric and material property input parameters to predict the equivalent strain in the cancellous bone in the acetabulum of the intact hemipelvis. Linear and Kriging surrogate models were built from training sets and used to also predict the strain output metrics of the FE model. ANOVA was conducted on the predictions from the full factorial analysis and surrogate models to quantify the influence of the input parameters and their possible interactions.

The current study found that conducting 729 simulations of an intact hemipelvis model in a full factorial design took 486 h on 8 CPUS (Intel ® Xeon ® 2.4 GHz processor, 32 GB RAM) h with a mean simulation time of 40 ± 7 minutes. Surrogate models reduced the computational cost to 30 simulations and estimated 20 h by predicting the strain output of a full factorial analysis with and RMSE of 34.6 for the median, 263.6 for the 95th percentile and 1618.2 for the maximum equivalent strains. The ANOVA conducted on the full factorial design found that equivalent strain in the cancellous bone of the acetabulum was most sensitive to variation in bone geometry, the cancellous bone modulus and the interaction between bone geometry and cancellous bone modulus. There was less than 1% difference between the ANOVA of the full factorial design and the Kriging model predictions based on a training set of 30 simulations for all input parameters and their interactions.

The strain values in this study have not been validated against experimental data. However, the geometry, material properties and loads represented a physiological variation and

the median and 95th percentile equivalent strains in the model were consistent with the equivalent strains (0.1-0.7%) seen in an acetabulum loaded with an anatomical femur with a soft tissue layer in a previous study (Ghosh et al., 2015). Thus, the performance of the model could be appreciated in a realistic case and support the conclusions about the surrogate models in the study. The maximum equivalent strains were higher than the range reported by (Ghosh et al., 2015). This was likely due to a single or a small group of elements with a low modulus experiencing high strains which are not physiological and not representative of the overall strain field. The hemipelvis bone geometry was the dominant input parameter for the strain which is in agreement with an earlier study into the sensitivity of finite-element models of the human femur (Taddei et al., 2006). The modulus of the cancellous bone was ranked as second most influential input parameter in the median and 95th percentile strain which is similar to (Anderson et al., 2005) who found changes to the elastic modulus had a large effect on the bone strain.

The linear surrogate model reduced the computational cost of running a full factorial analysis but was less accurate in predicting the output metrics than the Kriging. Previous studies that have used linear surrogate models also found a reduction in the number of simulations required to make predictions (Fitzpatrick et al., 2014; Halloran et al., 2008). In this study, the linear model adequately predicted the strain output metrics but there was very little difference in the accuracy between training sets 30 and 200 simulations. Similarly, (Fitzpatrick et al., 2014) found that, with a linear surrogate model, a small number of simulations in the training set appropriately captured the overall dataset but there was no additional improvement in accuracy in training sets greater than 50. Linear response surface methods, provide a reasonable estimation if the data locations are distributed uniformly over the parameter space but lose accuracy if the data are distributed in clusters and there is a large distance between clusters (Forrester et al., 2008).

The Kriging model accurately predicted all strain output metrics and drastically reduced the computational time required. This is consistent with (Pant et al., 2011) who found the Kriging model reduced the number of FE models of coronary stents requiring 120h on 8 CPUS (2.8 GHz processor, 16 GB RAM) for a single design to 30 to build the surrogate model. Similarly, (Lin et al., 2010) reported that a Kriging surrogate approach to running a high volume of elastic contact analyses of a total knee replacement required a total CPU time of 7.4 h for one Monte Carlo analysis compared to an estimated 284 h with the contact models.

The ANOVA conducted on the full factorial design indicated that the interaction between input parameters had an important influence on the strain output. Varying one input parameter at a time and fractional factorial designs may not help to fully explain the observed variation in the output if interaction effects are confounded with the main effects of input parameters (Yao et al., 2005). The approach demonstrated in this study may help overcome this limitation.

There are several limitations with the FE model in this study. Linear tetrahedral elements were used in the model. These elements predict stiffer behaviour of the bone and may not accurately predict strains in regions with large strain gradients. The cortical shell was assumed to have a constant thickness. However, this idealised representation of the cortical bone has been adopted in previous studies (Anderson et al., 2005; Dalstra and Huiskes, 1991; Manley et al., 2006; Phillips et al., 2007). Materials in the model were assumed to be locally isotropic, similar to previous studies (Anderson et al., 2005; Dalstra and Huiskes, 1991; Ghosh et al., 2015), and the pelvic cancellous bone has been shown to not be highly anisotropic (Dalstra et al., 1993). The contact conditions between the femoral head and the intermediate soft tissue layer were a simplification of the hip joint contact mechanics. However, the adopted simplifications have been used in previous studies that have examined stress and strain in the hemipelvis (Leung et al., 2009; Phillips et al., 2007). Overall, these limitations of the intact hemipelvis model do not affect the applicability of the presented surrogate modelling approach to comprehensively testing the sensitivity of a model to its input parameters.

There are several limitations with the surrogate modelling approach in this study. The surrogate modelling approach has been applied in one representative case. The intact hemipelvis provided a good illustration of the method as it is one of the most complex models in biomechanics and involves contact. Simpler models may require less than this for a sufficient training set to reproduce an accurate ranking of the most influential terms. Discontinuities may alter the accuracy of the surrogate models and the results in this study may not apply in all cases. If a model discontinuity exists in the surrogate model, conducting a full factorial analysis or calculating the standardised cross-validated residuals (Bah et al., 2011; Fitzpatrick et al., 2014) may be done to indicate that the surrogate model can be used to replace the FE simulations with a high level of confidence.

The sensitivity analysis approach described in this study is dependent on the chosen input parameters and their levels and is only valid within the chosen parameter space. This means that if an input parameter is studied over too narrow a range the effect may go undetected but, in general, increasing the range will increase the contribution to %TSS (Dar et al., 2002). Large variations in the cancellous bone modulus were seen by varying the upper bound of the apparent density and offsetting the density-modulus power relation, which may have affected calculated sensitivities. The levels for the input parameters in this study were based on the range of credible values available and so produced a true assessment of the relative influence of the input parameters and their interactions (Dar et al., 2002). While %TSS for each input parameter may have diluted the influence of possible outlier strain results, it is a recommended method to investigate the influence of each input parameter (Dar et al., 2002) that has been adopted in previous computational studies (Isaksson et al., 2008; Isaksson et al., 2009).

In conclusion, this study describes a method with a low computational cost to quantify the influence of model input parameters and their possible interactions on an FE model's output metrics. Using the Kriging surrogate model approach, a comprehensive test of an FE model's

sensitivity can be conducted in a fraction of time taken for a full factorial analysis. This approach can help researchers include sensitivity analyses into FE studies

.

Chapter 6

Surgical Variability in the Primary Stability of a Cementless Acetabular Cup

6.1 Introduction

The goal in replacing the acetabulum with a cementless cup is to provide the intimate bone-prosthesis contact and primary stability that allows weight-bearing until bone ingrowth into the porous surface occurs (Ochsner and Schweizer, 2003). During surgery, a reamer removes native acetabular bone so that the cup will be oversized with respect to the newly formed cavity. Bone expands and then recoils to grip the cup firmly as it is firmly impacted into position. Compressive forces act on the cup periphery to provide stability upon implantation (Mathieu et al., 2013). However, uncertainty affects each stage of the procedure which makes obtaining an optimal fit between cup and bone challenging. Imprecise reaming can affect the level of desired interference fit and cause the acetabulum to deviate from an ideally hemispherical shape (Kim et al., 1995). Malalignment of the cup may occur during insertion due to poor visualisation of the acetabulum or inaccuracies of external mechanical guides (DiGioia III et al., 2002), while assessment of cup seating can be difficult to infer solely by surgeon proprioception (Kroeber et al., 2002). A poor fit between the cup and the reamed cavity at the time of surgery results in an

unstable cup, leading to inconsistent bone ingrowth. Thus, it is necessary to assess variation in the primary stability that can be achieved by a surgeon for each new cup design.

The effect of surgical uncertainties on the primary stability of cementless cups has been investigated with *in vitro* and computational studies during pre-clinical testing. However, even the most extensive *in vitro* study can only explore a small subset of all possible surgical scenarios (Viceconti et al., 2006) and most FE studies are performed under a set of ideal conditions. Thus, only the average performance of a prosthesis is explored and results cannot be extrapolated to all clinical cases (Taylor et al., 2013). Probabilistic analysis techniques allow uncertainty to be incorporated into FE models investigating primary stability of acetabular cups so as to build up a distribution of the output metrics (Dar et al., 2002) (See 2.7.4). However, by including multiple surgical parameters, large numbers of simulations are required to sample the parameter space and can result in significant computational cost. By focusing on the surgical parameters that are critical to the primary stability and discarding those with negligible effect, the computational cost of examining surgical variability can be minimised.

The aim of this study was to identify the most influential surgical parameters on the primary stability of a cementless acetabular cup. A Latin Hypercube Design was used to sample the surgical parameter space for FE models which were used as training data for Kriging surrogate models which were subsequently applied to conduct regression analyses on primary stability output metrics.

6.2 Methods

The study was based on CT scans of two female cadavers with no obvious signs of hip disease (65 years, 79 kg and 78 years, 62 kg). The 95th percentile CPMs of 228 μm and 140 μm previously calculated for these subjects in Chapter 4 represented mean and maximum cases for females in the cohort examined. The hemipelvis models of the subjects in this study were generated using the automated methodology described in Chapter 3. However, modifications were made during

acetabular preparation and cup insertion stages of the model development process to represent different surgical scenarios.

6.2.1 Surgical Parameters

The surgical parameters investigated as part of the study were 1) interference fit, 2) acetabular cavity eccentricity, 3) cavity axis orientation, 4) cup inclination, 5) cup anteversion, 6) acetabular cavity depth and 7) cup insertion depth. The parameters and their investigated ranges are summarised in Table 6.1

Surgical Parameters	Range	References
Interference Fit (mm)	0.15 – 0.55	(MacKenzie et al., 1994)
Acetabular Cavity Eccentricity (mm)	-0.1 – 0.1	(Kim et al., 1995; MacKenzie et al., 1994)
Cavity Axis Orientation (°)	0 – 360	-
Cup Inclination (°)	30 – 50	(Lewinnek et al., 1978)
Cup Anteversion (°)	5 – 25	(Lewinnek et al., 1978)
Acetabular Cavity Depth (mm)	0 – 4	(Bonnin et al., 2012)
Cup Insertion Depth (mm)	-0.5 – 0.25	(Ong et al., 2006)

Table 6.1 The range of values for the surgical input parameters investigated in the study.

Interference fit represented the amount by which the diameter of the acetabulum was undersized compared to the cup. Typically, interference fit is quoted as the nominal oversizing of the cup with respect to the last-reamer used. However, dimensions of the reamed acetabulum have been found to be different from the dimensions of the last-reamer used (Kim et al., 1995; Macdonald et al., 1999; MacKenzie et al., 1994). Therefore, interference fit values in this study represented the range of values for the 'effective' interference fit between the cup and acetabular cavity. The range of 0.15 to 0.55 mm investigated in this study was within the deviations from the last-reamer used measured on 10 cadaveric pelvis bone (MacKenzie et al., 1994). Acetabular cavity eccentricity represented principal transverse axis departures of -0.1 to 0.1 mm from the spherical diameter of the acetabulum (Figure 6.1). (Kim et al., 1995; MacKenzie et al., 1994).

The orientation of the principal transverse axis was set between 0 and 360°, where an angle of 0° signified the axis was aligned in the superior-inferior direction.

Acetabular cavity depths of 0 to 4 mm represented the relative distance to which the acetabulum was reamed medially. A depth of 0 mm corresponded to the reamer being level with the acetabular floor. The anteversion and inclination angles of the cup were within the "safe zone" that is used as a standardised range of cup positions (Lewinnek et al., 1978). The cup insertion depth was the amount the cup was displaced into the acetabulum during insertion. Zero insertion depth corresponded to the cup being level with the acetabular floor, while values less than zero corresponded to further displacement into the acetabulum and values greater than zero represented incomplete seating. Preliminary analysis indicated cups bottomed out when the acetabular dome was displaced by 0.25 mm.

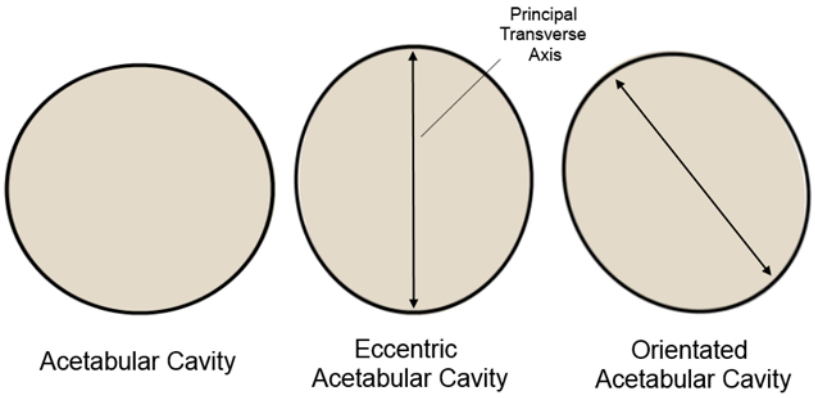

Figure 6.1 Alterations to the acetabular geometry investigated in the study. The principal transverse axis was varied from -0.1 to 0.1 mm from an ideal hemisphere geometry and orientated between 0 and 360°.

6.2.2 Surrogate Models

Similar to the methodology in Chapter 5, Kriging surrogate models were built from training sets for each of the primary stability output metrics with the SUrrogate MOdeling (SUMO) toolbox (Gorissen et al., 2010). An initial training set of 30 simulations was generated with a pre-optimised maximin Latin Hypercube Design for each subject (Grosso et al., 2009). The Latin Hypercube Design of 30 simulations and 7 parameters was divided into a 30 x 7 matrix where each simulation, or design point, was a random permutation of parameter values such that only one design point was present in each row and column in the matrix. The design points were evenly spaced in the matrix using the maximin-distance criterion which sought to maximise the minimum distance between points with Iterated Local Search heuristics (Grosso et al., 2009). The size of the initial training set was selected based on the saturation point of the Kriging model demonstrated in Chapter 5.

To obtain sufficiently accurate surrogate models for the output metrics, the performance of the Kriging model for the 95th percentile CPM was estimated using a five-fold cross-validation root-mean-square error (RMSE). To use this measure, the training set was divided into 5 smaller sets, or folds, and a surrogate model was trained using 4 folds as training data. The resulting model was used to predict the outputs of the remaining fold of training set. A target RMSE was set to $\leq$ 25 μm for 95th percentile CPM and simulations were added to the training set until the target was reached. Surrogate models for the remaining primary stability output metrics were then built from the same training set. In addition, surrogate model and FE predictions of a randomly generated test case that was not included at any time in the training of the surrogate models were compared.

6.2.3 Data Analysis

A 1000-trial Latin Hypercube Design dataset of surgical scenarios was evaluated by the surrogate models for data analysis. Simple linear regression analysis was performed separately for each subject (IBM SPSS Statistics v23.0) to determine the relationships between individual surgical parameters and the primary stability output metrics. In addition, stepwise reduction for linear regression was applied separately for each subject (MATLAB 2015a, The Maths Work Inc., Massachusetts, USA) with the surgical parameters and two-way interactions terms to identify the parameters that made an important contribution to the variability in primary stability. A term was retained in the regression model if the increase in the proportion of variation accounted for by the model (R^2) was above 10%.

6.3 Results

The Kriging surrogate models reached the target RMSE for the 95th percentile CPM with training set sizes of 29 and 37 simulations. For Hemipelvis 1, a simulation failed due to mesh distortion during cup insertion but the remaining training set of 29 simulations built a surrogate model with an RMSE of 24.9 μm. For Hemipelvis 2, an additional 7 analyses were required and the training set of 37 built a surrogate with an RMSE of 24 μm. The RMSEs of the remaining output metrics based on these training sets were 10 μm and 20 μm for the polar gap, 2% and 5% for the potential ingrowth area, and 11μm and 18 μm for the maximum change in polar gap for Hemipelvis 1 and Hemipelvis 2 respectively. All surrogate models provided a good approximation of the output metrics for the 'unseen' surgical scenarios (Table 6.2).

There was higher variability in the output metrics for Hemipelvis 2 compared to Hemipelvis 1 in the training sets used to build the Kriging surrogate models (Table 6.3). The subjects had similar median values for polar gaps but Hemipelvis 2 had a range of 520 - 720 μm compared to 526 - 612 μm in Hemipelvis 1. Similarly, the potential ingrowth area in Hemipelvis 1 had a median of 33% and a range of 21 to 39% (Figure 6.2), while Hemipelvis 2 had a median of 33% and a range of 17 - 52 % (Figure 6.3). The 95th percentile CPM was generally higher in

Hemipelvis 1 than Hemipelvis 2, with a median value of 282 μm and a range of 133 - 464 μm in Hemipelvis 1 (Figure 6.4) compared to 130 μm and 68 - 399 μm in Hemipelvis 2 (Figure 6.5). The range of maximum changes in polar gaps were 71 - 127 μm and 28 - 143 μm in Hemipelvis 1 and Hemipelvis 2 respectively.

	Hemipelvis 1		Hemipelvis 2	
	FE	Surrogate Model	FE	Surrogate Model
Polar Gap (μm)	531	533	538	524
95th Resultant CPM (μm)	399	426	412	419
Potential Ingrowth Area (%)	32	23	21	27
Max Change in Polar Gap (μm)	108	111	154	116

Table 6.2 FE and surrogate model predictions for the primary stability output metrics on a random test case for each subject.

	Hemipelvis 1 (N = 29)	Hemipelvis 2 (N = 37)
Polar Gap (μm)	544 (525 – 612)	536 (520 – 720)
95th Resultant CPM (μm)	282 (133 – 464)	130 (68 – 399)
Potential Ingrowth Area (%)	30 (21 – 39)	33 (17 - 52)
Max Change in Polar Gap (μm)	94 (71 – 127)	76 (28 - 143)

Table 6.3 The median (range) of the primary stability output metrics in the training sets used to build the Kriging surrogate models.

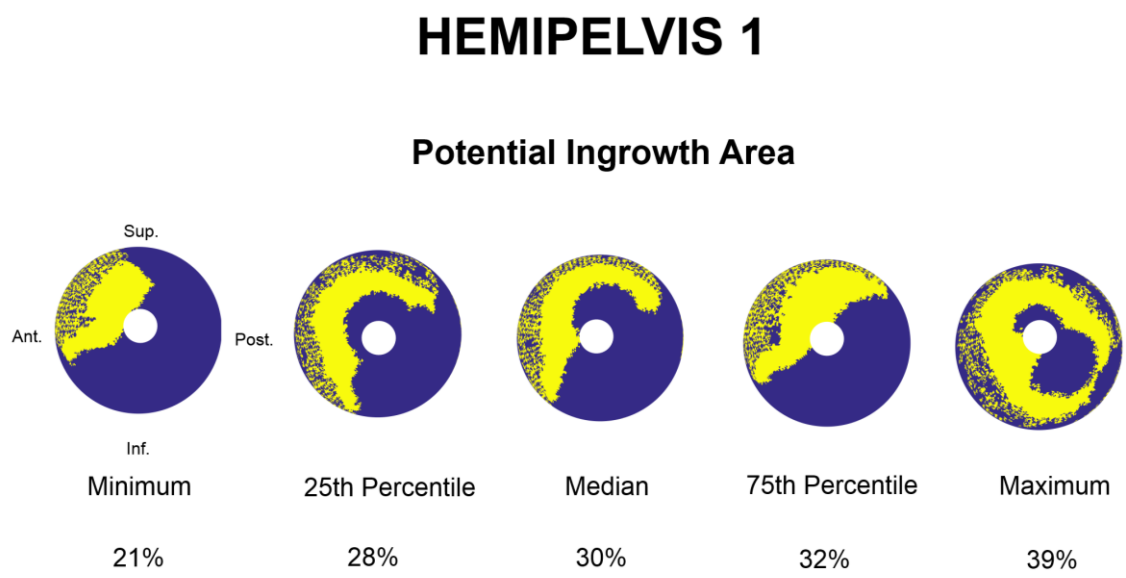

Figure 6.2 An illustration of the variation in potential ingrowth area in Hemipelvis 1. From left to right, the models with the minimum, 25th percentile, median, 75th percentile and maximum of the potential ingrowth area are shown.

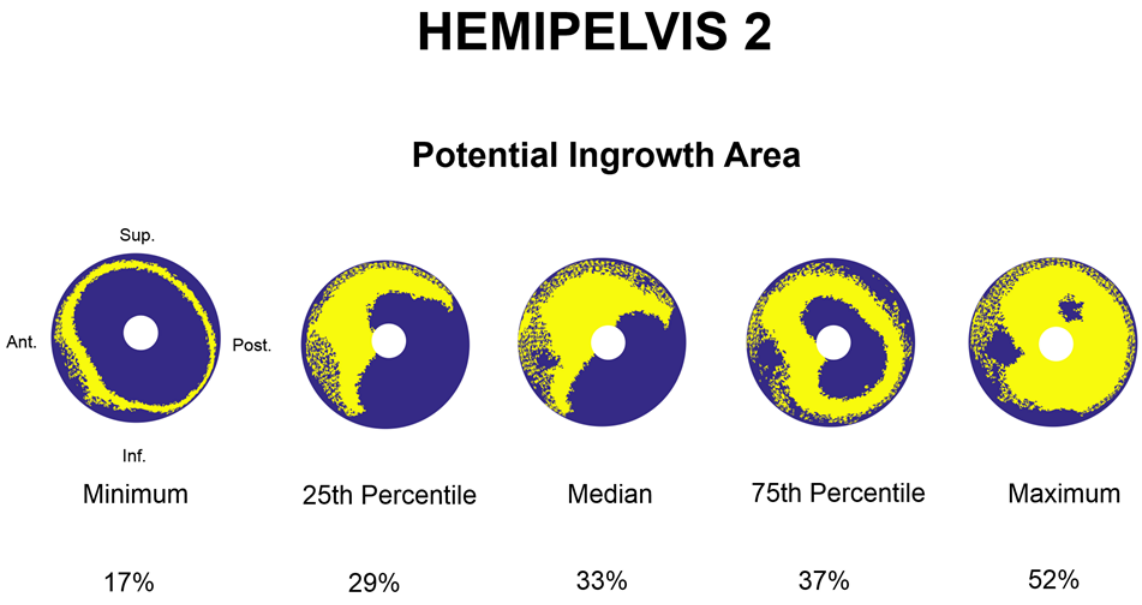

Figure 6.3 An illustration of the variation in potential ingrowth area in Hemipelvis 2. From left to right, the models with the minimum, 25th percentile, median, 75th percentile and maximum of the potential ingrowth area are shown.

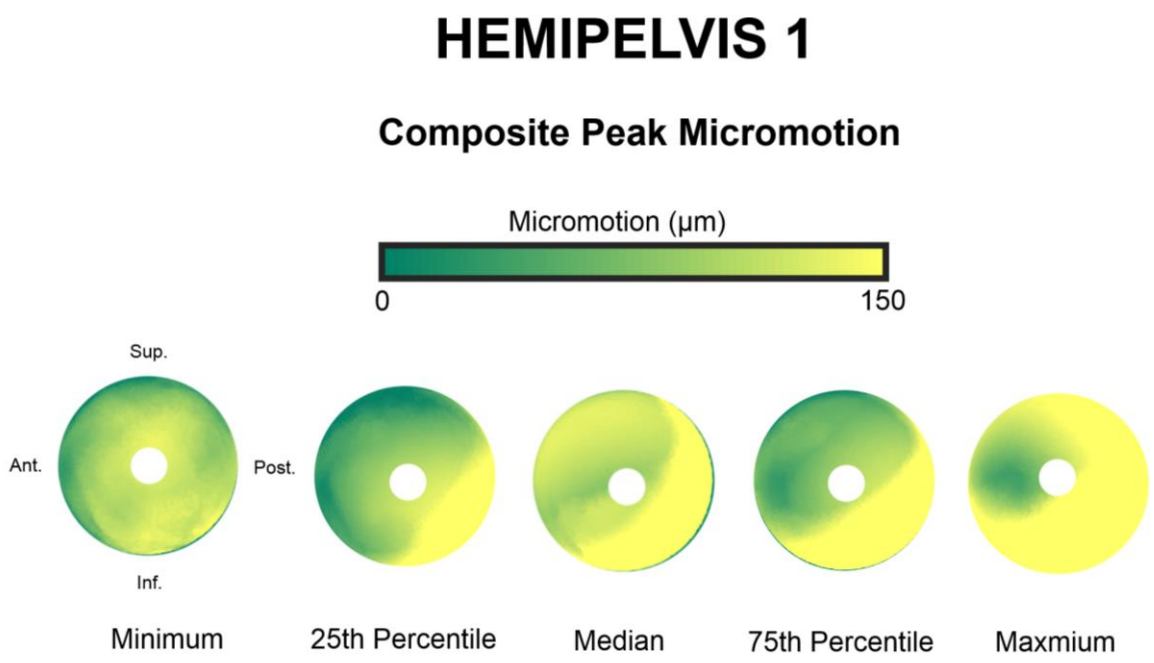

Figure 6.4 An illustration of the variation in micromotion in Hemipelvis 1. From left to right, the models with the minimum, 25th percentile, median, 75th percentile and maximum of the 95th percentile Composite Peak Micromotion are shown.

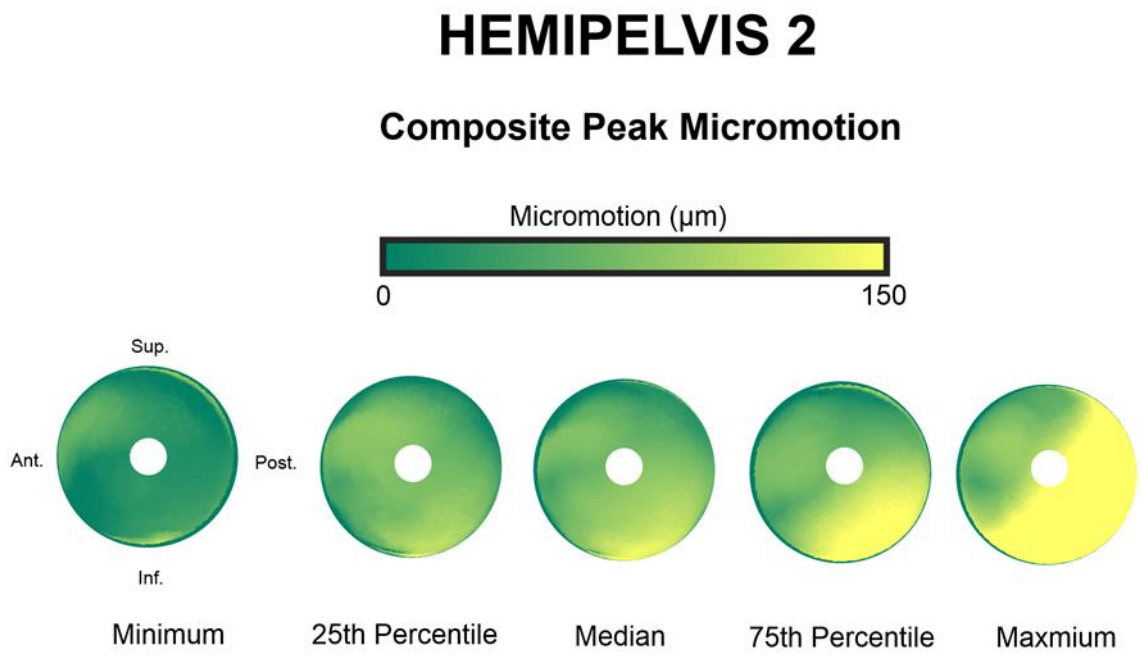

Figure 6.5 An illustration of the variation in micromotion in Hemipelvis 2. From left to right, the models with the minimum, 25th percentile, median, 75th percentile and maximum of the 95th percentile Composite Peak Micromotion are shown.

Simple linear regression conducted on the 1000-trial dataset indicated interference fit was linearly correlated with micromotion but the remaining surgical parameters did not strongly affect primary stability. There was a strong relationship between interference fit and the 95th percentile CPM in Hemipelvis 1 ($R^2 = 0.78$) (Figure 6.6) and in Hemipelvis 2 ($R^2 = 0.55$) (Figure 6.7). While there was no strong relationship between seating depth and polar gap in Hemipelvis 1 ($R^2 = 0.22$), a trend of increasing polar gap was evident for values greater than zero (incomplete seating) (Figure 6.8). The trend between incomplete seating and the polar gap was not present in Hemipelvis 2 (Figure 6.9). Linear relationships between remaining output metrics and surgical parameters could not be demonstrated ($R^2 < 0.3$) (Table 6.4 and Table 6.5).

	Simple Linear Regression			
Hemipelvis 1	Polar Gap	95th Percentile CPM	Potential Ingrowth Area	Max Change in Polar Gap
Interference fit	0.04 (p < 0.0005)	**0.78** (p < 0.0005)	0.002 (p = 0.16)	0.04 (p < 0.0005)
Acetabular Cavity Eccentricity	0.0003 (p = 0.58)	0.1 (p < 0.0005)	0.001 (p = 0.24)	0.03 (p < 0.0005)
Cavity Axis Orientation	0.0004 (p = 0.54)	0.0002 (p = 0.68)	0.0003 (p = 0.61)	0.001 (p = 0.46)
Cup Inclination	0.05 (p < 0.0005)	0.03 (p < 0.0005)	0.002 (p = 0.21)	0.01 (p = 0.004)
Cup Anteversion	0.03 (p < 0.0005)	0.01 (p < 0.0005)	0.12 (p < 0.0005)	0.16 (p < 0.0005)
Acetabular Cavity Depth	0.001 (p = 0.25)	0.01 (p = 0.006)	0.3 (p < 0.0005)	0.001 (p = 0.25)
Cup Insertion Depth	0.21 (p < 0.0005)	0.003 (p = 0.097)	0.19 (p < 0.0005)	0.17 (p < 0.0005)

Table 6.4 Coefficient of determination (R^2) values and p-values for simple linear regression performed for Hemipelvis 1 between the primary stability output metrics and surgical parameters.

	Simple Linear Regression			
Hemipelvis 2	Polar Gap	95th Percentile CPM	Potential Ingrowth Area	Max Change in Polar Gap
Interference fit	0.18	**0.55**	0.1	0.001
	(p < 0.0005)	(p < 0.0005)	(p < 0.0005)	(p = 0.25)
Acetabular Cavity Eccentricity	0.17	0.04	0.0001	0.0004
	(p < 0.0005)	(p < 0.0005)	(p = 0.82)	(p = 0.52)
Cavity Axis Orientation	0.06	0.004	0	0.006
	(p < 0.0005)	(p = 0.05)	(p = 1.0)	(p = 0.02)
Cup Inclination	0.01	0.21	0.11	0.22
	(p < 0.0005)	(p < 0.0005)	(p < 0.0005)	(p < 0.0005)
Cup Anteversion	0.001	0.03	0.006	0.28
	(p = 0.39)	(p < 0.0005)	(p = 0.02)	(p < 0.0005)
Acetabular Cavity Depth	0.06	0.005	0.0009	0.05
	(p < 0.0005)	(p = 0.02)	(p = 0.35)	(p < 0.0005)
Cup Insertion Depth	0.11	0.002	0.006	0.13
	(p < 0.0005)	(p = 0.19)	(p = 0.01)	(p < 0.0005)

Table 6.5 Coefficient of determination (R^2) values and p-values for simple linear regression performed for Hemipelvis 2 between the primary stability output metrics and surgical parameters.

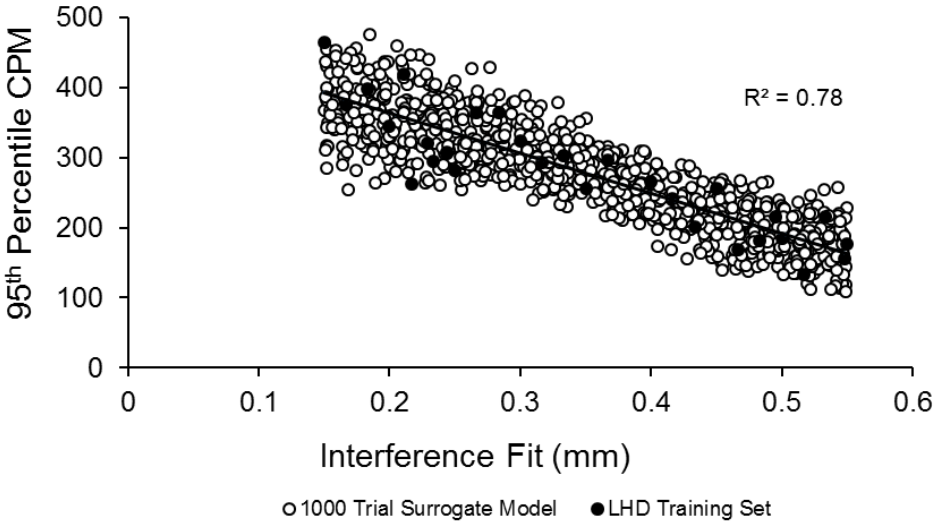

Figure 6.6 Plot between the interference fit and 95th Percentile Composite Peak Micromotion in Hemipelvis 1 with the Latin Hypercube Design (LHD) training set (black) and the 1000 trials predicted by the Kriging model (white).

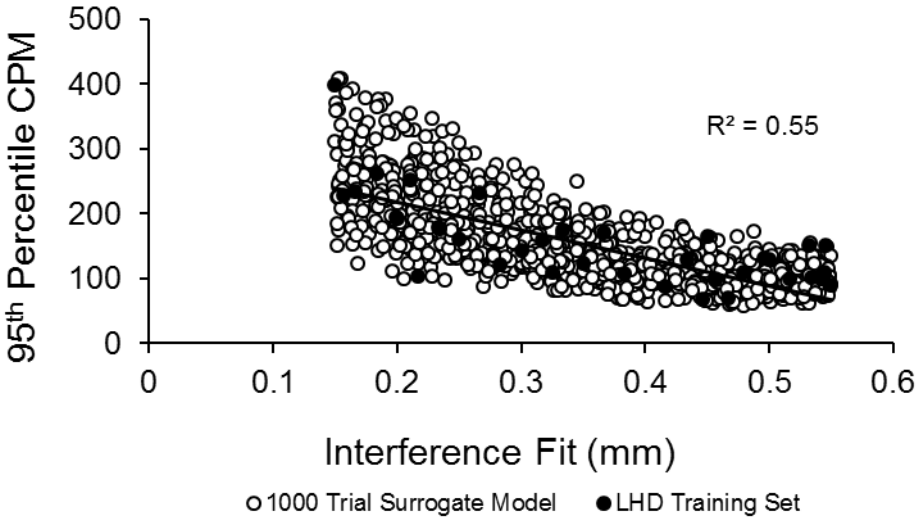

Figure 6.7 Plot between the interference fit and 95th Percentile Composite Peak Micromotion in Hemipelvis 2 with the Latin Hypercube Design (LHD) training set (black) and the 1000 trials predicted by the Kriging model (white).

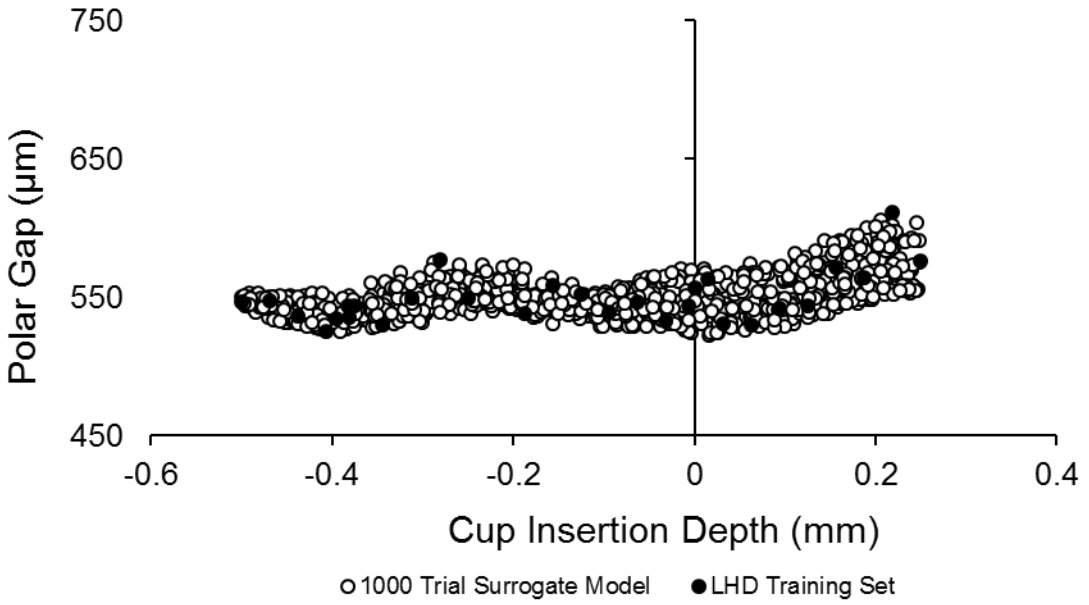

Figure 6.8 The plot between the cup insertion depth and the polar gap in Hemipelvis 1 with the Latin Hypercube Design training set (black) and the 1000 trials predicted by the Kriging models (white). The plot indicates a trend of increasing polar gap with incomplete seating of the cup (cup insertion depth values > 0)

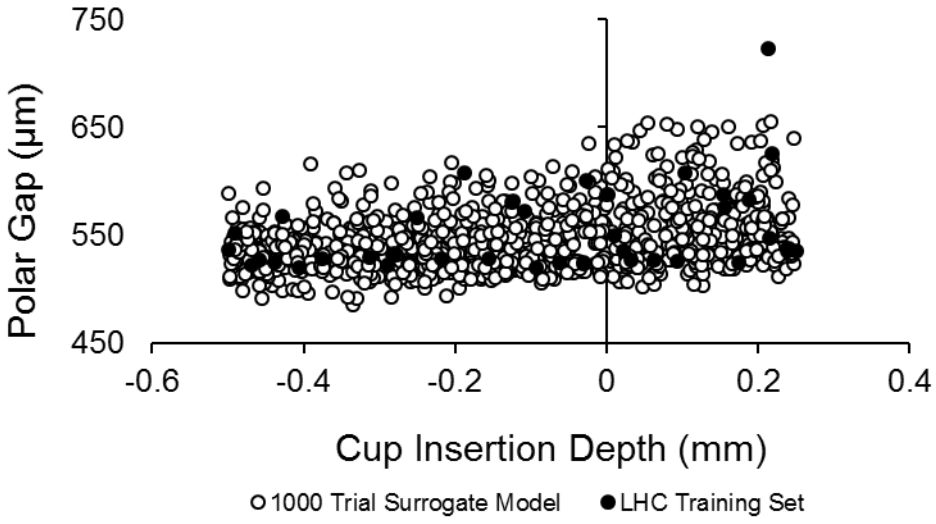

Figure 6.9 The plot between the cup insertion depth and the polar gap in Hemipelvis 2 with the Latin Hypercube Design training set (black) and the 1000 trials predicted by the Kriging models (white). The plot indicates no trend between polar gap and seating of the cup.

For the polar gap, interference fit and cup insertion depth were selected by stepwise regression analysis as significant contributors in both subjects (R^2 = 0.5 and R^2 = 0.59) (Table 6.6). Interference fit was identified as a significant predictor of the 95th percentile CPM in both subjects and was the only parameter selected in the regression model in Hemipelvis 1. Stepwise regression identified different parameters as significant contributors to potential ingrowth area in each subject. Anteversion, cavity depth, and cup insertion depth were selected as predictors in Hemipelvis 1 (R^2 = 0.57), while interference fit and cup inclination were selected in Hemipelvis 2 (R^2 = 0.21). Similarly, for the maximum change in polar gap, stepwise regression showed different significant parameters in the maximum change in polar gap. Interference fit, cavity eccentricity, cup anteversion, and cup insertion depth were selected in the regression model in Hemipelvis 1 (R^2 = 0.52). Meanwhile, cup inclination, anteversion and cavity depth were selected for the maximum change in polar gap regression model in Hemipelvis 2 (R^2 = 0.62).

Surgical Parameters	Polar Gap		95th Percentile CPM		Potential Ingrowth Area		Max Change in Polar Gap	
	β (95% CI)		β (95% CI)		β (95% CI)		β (95% CI)	
	Hemipelvis 1	Hemipelvis 2	Hemipelvis 1	Hemipelvis 2	Hemipelvis 1	Hemipelvis 2	Hemipelvis 1	Hemipelvis 2
Interference Fit	0.22 (0.18 to 0.26)	0.43 (0.39 to 0.47)	-0.88 (-0.91 to -0.85)	-0.73 (-0.77 to -0.71)		-0.32 (-0.37 to -0.26)	-0.18 (-0.22 to -0.13)	
Acetabular Cavity Eccentricity		-0.39 (-0.43 to -0.35)					-0.18 (-0.22 to -0.14)	
Cavity Axis Orientation								
Cup Inclination				0.45 (0.42 to 0.48)		-0.33 (-0.39 to -0.28)		0.48 (0.45 to 0.52)
Cup Anteversion					0.32 (0.28 to 0.36)		-0.39 (-0.43 to -0.35)	-0.51 (-0.55 to -0.48)
Acetabular Cavity Depth					0.53 (0.49 to 0.57)			0.35 (0.31 to 0.39)
Cup Insertion Depth	0.48 (0.43 to 0.52)	0.33 (0.30 to 0.38)			-0.39 (-0.43 to -0.35)		0.38 (0.34 to 0.42)	
Interference Fit*Acetabular Cavity Eccentricity							-0.38 (-0.42 to -0.33)	
Interference Fit*Cup Insertion Depth	0.50 (0.46 to 0.54)	0.37 (0.33 to 0.41)						
Coefficient of Determination (R^2)	0.5	0.59	0.78	0.76	0.57	0.21	0.52	0.62

Table 6.6 Stepwise regression models for the primary stability output metrics. Standardised coefficients and 95% confidence intervals for the individual input parameters and interactions that contributed above 0.1 to the coefficient of determination in the model. Interactions not included in any of the regression models are not displayed. $p < 0.05$ for all terms in the models.

6.4 Discussion

The aim of this study was to determine influential surgical parameters on the primary stability of a cementless acetabular cup in order to reduce the parameter space for computationally efficient pre-clinical testing. To achieve this, Kriging surrogate models were built for output metrics from training sets of 29 and 37 simulations sampled with Latin Hypercube Design in two subjects respectively. Simple linear regression and stepwise regression were conducted on predictions evaluated with the surrogate models to determine the effect of surgical parameters on primary stability. The results indicated that interference fit was the most dominant surgical parameter, having the strongest relationship with micromotion in both subjects and being present, along with interaction terms, in stepwise models for all output metrics. Deviation of the reamed acetabulum from a hemisphere shape or the level of cup seating were not found to be influential within the range examined in the present study. In addition, the primary stability of the cup was robust to variation in acetabular cavity depth and cup orientation.

The effect of interference fit on primary stability was consistent with other studies on the press-fit acetabular cup. Previous FE studies showed models with exact-fit cups (0 mm interference fit) had greater micromotion compared to 0.5 or 1 mm interference fits (Janssen et al., 2010; Spears et al., 2001; Udofia et al., 2007). Furthermore, Ong et al. found interference fit contributed to the variation in potential ingrowth area (Ong et al., 2008). Increased resistance to micromotion with higher interference fits was largely due increased compressive forces in the acetabulum. At higher interferences of 2 mm, studies have found little difference or greater micromotion of the cup compared to exact-fit or 1 mm interference fits (Kwong et al., 1994; Spears et al., 2001; Udofia et al., 2007). Large polar gaps present at these higher interference fits due to the difficulty in full seating of the cup compromise stability (Kwong et al., 1994). A relationship between polar gap and micromotion was not detected in the small interference fit range examined in the present study but micromotion has been previously found to be affected by more extensive gaps at the pole (Adler et al., 1992; Clarke et al., 2012b). The high influence

of interference on primary stability means pre-clinical testing protocols should include this parameter into assessment.

The large variation in micromotion found within the range of 0.15 to 0.5 mm interference fit suggests precise reaming is critical for achieving primary stability in a clinical situation. Accurate removal of bone is challenging with handheld reamers due to instrument tolerance, bone quality, and surgical technique which impacts on the level of interference fit actually obtained at the time of surgery (Kwong et al., 1994). Further, discontinuous and asymmetric cutting points leave an irregular cavity shape (Macdonald et al., 1999). Data in the simple linear regression indicated that a cavity eccentricity of -0.1 to 0.1 mm was not influential on primary stability but reaming a dense region of bone in the acetabulum could cause it to wobble or slip and give an elliptical cavity shape outside the range examined in the present study (Kim et al., 1995). Accurate control of the reamer during surgery helps ensure stability for long-term success of press-fit cups.

Interference fit was selected for stepwise regression models for polar gap but was not found to have strong associations with simple linear regression in either subject, possibly due to the method of insertion. Spears et al. found an increase in polar gap of 240 μm to 700 μm between 0.25 and 0.5 mm interference fit in an FE model with a load-pulse insertion of the cup (Spears et al., 2001). While negative insertion depths in Hemipelvis 1 suggested increased polar gaps with incomplete seating, displacement-controlled insertion results in considerably higher insertion loads (Yew et al., 2006) that forces the cup into position without considering that surgeon blows may not fully seat the cup. *In vitro* studies have found more extensive polar gaps in all cases with high interference fits due to inadequate seating of cups (Adler et al., 1992; Kwong et al., 1994; MacKenzie et al., 1994). Examining a broader range of incomplete seating may help overcome the limitations of the cup insertion method in the present study.

Cup inclination and anteversion entered stepwise regression models for potential ingrowth area and maximum change in polar gap but simple regression did not demonstrate associations

between the cup orientation parameters and any of the output metrics. Previously, Clarke et al. found cup orientation did not have an influence on micromotion in metal-on-metal cups (Clarke et al., 2012a). Changing the orientation of the cup within the safe zone does not substantially alter the area of contact between cup and bone, thus not strongly affecting primary stability. Cup orientation may be more influential on the risk of dislocation, impingement, and polyethylene wear in total hip arthroplasty (Kennedy et al., 1998).

There were limitations with the present study. Analysis has been conducted on two representative subjects and the results from the simulations were not validated with any experimental data. Displacement-controlled insertion of the cup would have resulted in higher insertion loads than applied (Michel et al., 2016) in order to force the cup into position without considering mallet blows by the surgeon may not advance the cup at higher interference fits. The spread of results in the output metrics depended on the range chosen to investigate for each surgical parameter. The effect of a surgical parameter on primary stability may have been undetected if the parameter had a narrower range than that occurring during surgery. Deciding which parameters were included in the final regression model was conducted through parameter inference in stepwise regression. This can lead to the presence of parameters with no or weak relation to the output into the model and inflation of the coefficient of determination.

In conclusion, this study investigated the influence of surgical parameters on the primary stability of a cementless acetabular cup in two subjects. Interference fit was found to be highly influential on primary stability output metrics in both subjects. Focusing on this parameter in pre-clinical testing can reduce the computational cost of examining surgical variability

Chapter 7

Discussion, Conclusion, and Future Work

7.1 Discussion

The challenge in pre-clinical testing is to develop testing regimes capable of screening out poor designs in order to minimise the risk of failure for patients. By allowing input parameters to be easily adjusted, FE studies, unlike *in vitro* studies, can assess the effect of multiple surgical scenarios on the primary stability of different press-fit acetabular cups in the same set of subjects. However, the majority of FE studies use a single subject and are performed under a limited range of conditions. These studies do not consider the full spectrum of anatomical and material variation found in the population or large uncertainty in the surgical preparation and positioning of cups and it limits the extent to which their results can be extrapolated to the population. Therefore, pre-clinical FE studies must be capable of accounting for patient and surgical variability in order to comprehensively assess prospective prosthesis designs.

The aim of this thesis was to examine the patient and surgical variability in the primary stability of cementless acetabular cups with a view to incorporating the variability into pre-clinical testing.

Primary stability of cementless cups is achieved by a press-fit mechanism when an oversized cup into an undersized acetabular cavity. Therefore, assessing the primary stability

of press-fit cups required replicating the post-implantation environment. In this work, the effective interference fits chosen were consistent with previous *in vivo* and *in vitro* findings on the deviation of cavity diameter from the last reamer-used (Macdonald et al., 1999; MacKenzie et al., 1994). A displacement-controlled insertion process was developed to generate periacetabular strains which resulted in the compressive forces that act on the cup to restrict micromotion upon implantation (Curtis et al., 1992; Kroeber et al., 2002). While there were high local strain values, the inclusion of effective interference fits meant the models did not have an excessive amount of the acetabular bone volume exceeding the yield criterion. Cups in the models underwent elastic spring back due to the elastic recoil of the acetabulum which created a polar gap between the bone and cup as observed on initial postoperative radiographs (Udomkiat et al., 2002). The width of the polar gaps was consistent with previous *in vitro* and *in vivo* studies (Schmalzried et al., 1992b; Udomkiat et al., 2002). By simulating the cup insertion process, clinically relevant representations of the implanted hemipelvis were produced in the models.

To date, a barrier to investigating patient and surgical variability in FE is the manual generation of unique models (Taylor et al., 2013). The time cost associated with manual generation has limited previous FE studies to investigating primary stability of cementless cups in single, average subjects and a small number of subjects or surgical scenarios. An automated methodology was developed in this thesis that allowed a large number of models to be generated without intervention. There was an initial time cost associated with manual segmentation of hemipelvis geometries and placement of landmark points within each acetabulum but, once the cohort of hemipelvis volumes were established, models were generated and the methodology was flexible enough to allow automatic adjustments to be made to surgical parameters. Having the automated methodology helps reduce the overall time cost of investigating a high volume of subjects and surgical scenarios in pre-clinical testing.

Exploring the patient variability in primary stability in the cohort of 103 subjects demonstrated a wide variation of interfacial gaps and micromotion but at a high computational cost. The average time to simulate cup insertion and gait cycle loading was 9.75 hrs per subject. Therefore, when incrementally developing and refining a cup design early in the design process, testing it in the entire cohort may not be practical. Using the representative subset of subjects based on the extremes of variability may provide an approximation of the spread in primary stability in the cohort with a more manageable computational cost. However, further work is required on the subset to demonstrate that it would be able to detect differences between cup designs. The entire cohort may be then used for detailed performance assessment once a design is finalised.

The combination of a Latin Hypercube design and Kriging surrogate model provided an accurate and computationally efficient method to explore the input parameter space. In the illustrative example of the intact hemipelvis model, the Kriging model reached a high accuracy with a training set of 30 analyses with no further improvement seen with the further addition of training simulations. Similarly, accurate surrogate models were generated with sets of training simulations close to the initial training set size of 30 simulations when exploring the surgical parameter space. Interference fit was identified as the dominant surgical input parameter on primary stability, particularly micromotion, which can reduce the dimensionality of the parameter space to be explored and thus further reduce the computational cost of exploring surgical variability.

The performance of a cup in pre-clinical testing is typically defined by the comparison of predicted output metrics to a failure criterion associated with a given failure scenario. Studies suggest that up to 50 μm may be a threshold for micromotion to allow the bone ingrowth, while at micromotion above 150 μm complete fibrous differentiation occurs at the cup-bone interface (Pilliar et al., 1986). However, retrieval studies have previously reported mean bone ingrowth areas of 30% and as lows as 3% in well-functioning porous-coated acetabular cups (Engh et al.,

1993). Results in this work demonstrate that much of the cup experiences micromotions above 50 μm and potential ingrowth areas vary from 0.2 to 51% in the cohort. Simply using threshold values as a system to either pass or fail cup designs may not be the most suitable method for evaluating during pre-clinical testing.

Data on acetabular cup designs with proven clinical track records according to joint registries can provide a benchmark to estimate the performance of prospective cup designs. The Pinnacle ® cup modelled in this work is one of the most widely used cementless cup designs with 10-year survivorships of 92.8 – 97.9 % (Australian Orthopaedic Association, National Joint Replacement Registry, 2016; National Joint Registry for England and Wales, 2015) and very low revision rates for aseptic loosening after 10 years (Bedard et al., 2014; Howard et al., 2011). Comparisons can be made with the data on micromotion and interfacial gaps collected for the Pinnacle ® cup in this work in order to discard inferior designs or investigate the effect of minor design changes. Moreover, difference in the ranking of subjects based on their primary stability output metrics between designs may be investigated. Evaluating cup performance based on comparisons with successful designs rather than set failure criteria may help develop cups that improve on currently available designs.

Integrating the elements of the work in this thesis can create a computational tool to account for the patient and surgical variability during pre-clinical testing in the early stages of the design process. Evaluating a prospective cup design with such a tool consists of examining the effect of the interference fit on primary stability in each of the subjects from the representative subset. Results can be directly compared to the data on benchmark acetabular cups which have been simulated in the same set of models. Based on the work in this thesis, the most computationally efficient version of the computational tool would use a Kriging surrogate model generated from 30 training simulations in the representative subset of 12 subjects from the cohort. Given an average simulation time of 9.75 hours with 28 CPUS for each FE model (4.75 h for cup insertion + 5 h for gait), testing a prospective acetabular cup design with the

software tool would take a minimum of 9.75 h × 30 surgical scenarios × 12 subjects = 146 days (3500 h) simulation time. This estimate does not include additional simulations that may be required to generate a sufficiently accurate Kriging model or Boolean operation and meshing errors during model generation. This is a significant time and computational saving from analysis in the entire cohort and may be processed with a modest computer cluster in a short time. Future work can consider reducing simulation time by investigating the minimum volume of the hemipelvis bone required in the model.

7.2 Limitations

There were limitations with the FE models in this work. Bone was assumed to be a linear-elastic material. The effect of permanent deformation or viscoelastic behaviour of bone were not taken into consideration in the hemipelvis models. Higher periacetabular strains are expected with the assigned linear-elastic behaviour which may overestimate the level of compression of the bone on the press-fit cup and thus underestimate micromotion. A constant cortical bone thickness of 1.5 mm was assumed for all subjects. The cortical bone layer varies thickness in the hemipelvis and between individuals (Anderson et al., 2005; Dalstra et al., 1995; Ghosh et al., 2015). An over- or under-estimation of the cortical bone thickness at the acetabular rim may affect the contribution of the cortical bone to the compression on the cup and thus the primary stability.

The forces applied to the hip joint were adopted from one walking trial of a subject in the Orthoload dataset. Walking is the most common dynamic activity undertaken by total hip arthroplasty recipients (Morlock et al., 2001) but the primary stability of the cup may be more sensitive to the hip joint loading of other activities such as stair climb (Spears et al., 2000). Scaling the forces from one walking trial to the bodyweight of each subject did not consider the inter-patient variability in gait pattern. However, subject-specific loading was unavailable and Orthoload provides load data for a limited number of patients. Instead, the level walking trial of a patient (H6R) who was closest in age to the mean age in the cohort was selected. The

contribution of pelvic muscle forces to the loading conditions were not considered in the models. The forces acting on the hip prosthesis depend on the joint reaction forces as well as the muscle forces. While having muscle forces in the model gives a more accurate representation of loading conditions of the hemipelvis, excluding them may only introduce a systematic error when comparing acetabular cup designs with the pre-clinical computational tool.

Frictional torque generated in the implanted hip joint during activities was not considered in this work. Frictional torques arise due to shear transfer over the bearing interface and the highest magnitudes occurring in prostheses with large diameter metal-on-metal bearings (Bishop et al., 2008). The higher prevalence of loosening in hip prostheses with larger-diameter femoral heads has been previously considered to be due to the increased frictional torque (Morrey and Ilstrup, 1989). However, the prosthesis simulated in this thesis had metal-on-polyethylene bearings with small-diameter femoral heads (28 mm and 36 mm) which have sufficiently low frictional torques that are unlikely to overload the bone-cup interface (Bishop et al., 2008).

The cohort of 103 subjects examined in this work were assumed to be representative of a population of total hip arthroplasty recipients. The CT scans used comprised of cadavers with no obvious signs of hip disease and not patients with hip OA awaiting total hip arthroplasty. However, the age and BMI ranges of the cohort were similar to those of the total hip arthroplasty patients recorded in national joint registries (See 3.2.1) (Australian Orthopaedic Association National Joint Replacement, 2015; Canadian Joint Replacement Registry, 2015; National Joint Registry for England and Wales, 2015). In addition, mean apparent densities and elastic moduli in the acetabulum were similar to bone density measurements adjacent to cementless cups made on initial post-operative CT scans of 26 patients with a mean age of 67.6 years at the time of surgery (Wright et al., 2001).

The primary stability results examined in this work only provided a snapshot of the post-operative state of the cup. The initial bone ingrowth into the porous surface strengthens the

bond between the cup and bone, reducing micromotion and further enabling localised ingrowth (Spears et al., 2000). In addition, interfacial gaps present immediately after surgery can be gradually reduced or eliminated in the months and years following surgery (Udomkiat et al., 2002). However, the primary stability immediately post-operative, before any biological process take place, is a prime indicator for determining the risk of aseptic loosening (Pilliar et al., 1986).

The results for primary stability output metrics in this work have not been validated against experimental data. Experimental validation of large sample sizes of subjects and multiple surgical scenarios for acetabular cups is challenging. In this study, effort was made to ensure the bone geometry, material properties and surgical preparation represented realistic patient and surgical variation and the polar gaps and micromotion in the models were consistent with the previous computational and *in vitro* results (Janssen et al., 2010; MacKenzie et al., 1994), while the potential ingrowth areas were consistent with clinical data (Bloebaum et al., 1997; Engh et al., 1993; Swarts et al., 2015). In the future, comparisons to cups demonstrated to have long-term clinical success with the computational tool in the same set of models may still be relevant in pre-clinical assessment of a prospective cup design.

7.3 Future Work

The work in this thesis can be viewed as providing the elements for an initial version of a computational tool to account for patient and surgical variability in the primary stability of cementless acetabular cups in pre-clinical testing. A developed computational tool has tremendous potential to improve prosthesis assessment in the pre-clinical phase. Thus, with the foundations in place, there is scope for further development in pursuit of incorporating such a tool into pre-clinical testing protocols in the future.

Starting with the data collected in this study, we can begin building a database on acetabular cups and patients. Along with the Pinnacle ® cup used in this work, including cup designs that are associated with long-term clinical success and high incidence of early failure

can provide suitable benchmarks for future comparisons with prospective acetabular cup designs. Given the computational tool proposed in Section 7.1, examining the effect of interference fit on the primary stability of these cups in the subset of 12 subjects identified as representative of the cohort can provide a gross indication of the level of patient and surgical variability in the output metrics. Prospective acetabular designs can be directly compared to the cups with proven track records when analysed in the same set of models. Adding more patients to the cohort, including younger patients and those of differing races and ethnicities with varying hemipelvis morphology (Lavy et al., 2003), in order to broaden the range of individuals in the total hip arthroplasty population examined. Having a large database of acetabular cups and patients could make a substantial amount of comparative information available for new cup designs being tested.

Improvements can be made to the FE models for assessing primary stability in future versions of the computational tool. The main limitation in the model was the linear-elastic assumption for bone which produced high strain fields in the acetabulum upon cup insertion. Modelling permanent deformation with plastic behaviour (Janssen et al., 2010) or using a crushable foam plasticity model (Kelly et al., 2013) may simulate more accurate post-yield behaviour of bone in the hemipelvis models. Applying the joint reaction forces from one walking trial of a single patient in the present work does not capture inter-subject variability in loading. Preferably, kinematic and force data would be collected on OA patients before and after total hip arthroplasty in a gait laboratory to provide information on muscle and internal joint forces in each new patient. Future models may also consider loading conditions from other activities of daily living, particularly more demanding conditions such as stair climb, which may be better at discriminating between designs (Pancanti et al., 2003; Spears et al., 2000).

Similar to the development of software, implementing future changes in the model requires careful management of the computational tool. Currently, direct comparisons could be made between two designs using an initial version of the proposed computational tool. However, if

adjustments are made to the FE model, the resulting changes to predictions would mean data on designs simulated on a new version of the computational tool may not be compatible with data from the older version. Moreover, simulation of the full cohort and all surgical parameters would have to be repeated to re-establish benchmark data before comparisons can be made with prospective cup designs with a new version of the computational tool. Thus, each incremental change to the FE model in the evolution of the computational tool is likely have a major computational expense.

The lack of bone ingrowth may be a prime risk factor for aseptic loosening of the cup but long-term loosening is a consequence of a variety of potentially concurring failure scenarios. Successful design depends on the ability to predict the risk associated with a broad range of failure scenarios. Previously, in the assessment of an epiphyseal stem, various failure scenarios were examined under physiological loading including femoral neck fracture, prosthesis failure, cement fatigue failure, fretting wear of cement, fibrous tissue formation, and adverse bone remodelling with driving biomechanical parameters in FE models (Martelli et al., 2011). Future versions of the computational tool may consider additional failure scenarios such as peri-prosthetic damage and stress shielding to give an overall assessment of the risk of cup failure.

7.4 Conclusion

The work in this thesis is a foundation for the development of a reliable pre-clinical computational tool to support the development of new cup designs. By accounting for patient and surgical variability and demonstrating computationally efficient techniques that provide an approximation of the variability, this work allows for a broader range of conditions to be examined in a more thorough evaluation of cups prior to clinical trials. Incorporating such a tool into the design and development phase of a new cup design as a routine activity could help produce new prostheses with greater assurances of safety for patients.

References

A Workgroup of the American Association of Hip and Knee Surgeons Evidence Based Committee, 2013. Obesity and Total Joint Arthroplasty: A Literature Based Review. The Journal of Arthroplasty 28, 714-721.

Adler, E., Stuchin, S.A., Kummer, F.J., 1992. Stability of press-fit acetabular cups. The Journal of Arthroplasty 7, 295-301.

Ahmad, S., Irons, B.M., Zienkiewicz, O.C., 1970. Analysis of thick and thin shell structures by curved finite elements. International Journal for Numerical Methods in Engineering 2, 419-451.

AIHW, 2017. The burden of musculoskeletal conditions in Australia. Australian Burden of Disease Study series no 13. Cat. no. BOD 14. AIHW, Canberra.

Amirouche, F., Solitro, G., Broviak, S., Goldstein, W., Gonzalez, M., Barmada, R., 2015. Primary cup stability in THA with augmentation of acetabular defect. A comparison of healthy and osteoporotic bone. Orthopaedics and Traumatology: Surgery and Research 101, 667-673.

Anderson, A.E., Peters, C.L., Tuttle, B.D., Weiss, J.A., 2005. Subject-specific finite element model of the pelvis: Development, validation and sensitivity studies. Journal of Biomechanical Engineering 127, 364-373.

Antoniades, G., Smith, E., Deakin, A., Wearing, S.C., Sarungi, M., 2013. Primary stability of two uncemented acetabular components of different geometry: hemispherical or peripherally enhanced? Bone and Joint Research 2, 264-269.

Archbold, H.A.P., Mockford, B., Molloy, D., McConway, J., Ogonda, L., Beverland, D., 2006. The transverse acetabular ligament: An aid to orientation of the acetabular component during primary total hip replacement. A preliminary study of 1000 cases investigating post-operative stability. Journal of Bone and Joint Surgery - Series B 88, 883-886.

Aro, H.T., Alm, J.J., Moritz, N., Mäkinen, T.J., Lankinen, P., 2012. Low BMD affects initial stability and delays stem osseointegration in cementless total hip arthroplasty in women: A 2-year RSA study of 39 patients. Acta Orthopaedica 83, 107-114.

Asayama, I., Akiyoshi, Y., Naito, M., Ezoe, M., 2004. Intraoperative pelvic motion in total hip arthroplasty. The Journal of arthroplasty 19, 992-997.

Australian Orthopaedic Association National Joint Replacement Registry. 2016. Annual Report / Australian Orthopaedic Association, National Joint Replacement Registry.

Bah, M.T., Nair, P.B., Taylor, M., Browne, M., 2011. Efficient computational method for assessing the effects of implant positioning in cementless total hip replacements. J. Biomech. 44, 1417-1422.

Bah, M.T., Shi, J., Heller, M.O., Suchier, Y., Lefebvre, F., Young, P., King, L., Dunlop, D.G., Boettcher, M., Draper, E., Browne, M., 2015. Inter-subject variability effects on the primary stability of a short cementless femoral stem. J. Biomech. 48, 1032-1042.

Baleani, M., Fognani, R., Toni, A., 2001. Initial stability of a cementless acetabular cup design: Experimental investigation on the effect of adding fins to the rim of the cup. Artif. Organs 25, 664-669.

Bedard, N.A., Callaghan, J.J., Stefl, M.D., Willman, T.J., Liu, S.S., Goetz, D.D., 2014. Fixation and Wear With a Contemporary Acetabular Component and Cross-Linked Polyethylene at Minimum 10-Year Follow-Up. Journal of Arthroplasty 29, 1961-1969.

Bergmann, G., 2001. Hip contact forces and gait patterns from routine activities. J. Biomech. 34, 859.

Bergmann, G., Graichen, F., Rohlmann, A., 1993. Hip joint loading during walking and running, measured in two patients. J. Biomech. 26, 969-990.

Bertin, K.C., Freeman, M.A.R., Morscher, E., Oeri, A., Ring, P.A., 1985. Cementless acetabular replacement using a pegged polyethylene prosthesis. Archives of Orthopaedic and Traumatic Surgery 104, 251-261.

Bevill, S.L., Bevill, G.R., Penmetsa, J.R., Petrella, A.J., Rullkoetter, P.J., 2005. Finite element simulation of early creep and wear in total hip arthroplasty. J. Biomech. 38, 2365-2374.

Biedermann, R., Tonin, A., Krismer, M., Eibl, G., Stöckl, B., 2005. Reducing the risk of dislocation after total hip arthroplasty. Journal of Bone and Joint Surgery - Series B 87, 762-769.

Bishop, N.E., Waldow, F., Morlock, M.M., 2008. Friction moments of large metal-on-metal hip joint bearings and other modern designs. Med. Eng. Phys. 30, 1057-1064.

Bloebaum, R.D., Bachus, K.N., Momberger, N.G., Hofmann, A.A., 1994. Mineral apposition rates of human cancellous bone at the interface of porous coated implants. Journal of Biomedical Materials Research 28, 537-544.

Bloebaum, R.D., Mihalopoulus, N.L., Jensen, J.W., Dorr, L.D., 1997. Postmortem analysis of bone growth into porous-coated acetabular components. Journal of Bone and Joint Surgery - Series A 79, 1013-1022.

Bobyn, J.D., Pilliar, R.M., Cameron, H.U., Weatherly, G.C., 1980. The optimum pore size for the fixation of porous surfaced metal implants by the ingrowth of bone. Clin. Orthop. Relat. Res. NO. 150, 263-270.

Bobyn, J.D., Pilliar, R.M., Cameron, H.U., Weatherly, G.C., 1981. Osteogenic phenomena across endosteal bone-implant spaces with porous surfaced intramedullary implants. Acta Orthopaedica 52, 145-153.

Bobyn, J.D., Stackpool, G.J., Hacking, S.A., Tanzer, M., Krygier, J.J., 1999. Characteristics of bone ingrowth and interface mechanics of a new porous tantalum biomaterial. Journal of Bone and Joint Surgery - Series B 81, 907-914.

Bonnin, M.P., Archbold, P.H.A., Basiglini, L., Fessy, M.H., Beverl, D.E., 2012. Do we medialise the hip centre of rotation in total hip arthroplasty? Influence of acetabular offset and surgical technique. HIP International 22, 371-378.

Brekelmans, W.A.M., Poort, H.W., Slooff, T.J.J.H., 1972. A New Method to Analyse the Mechanical Behaviour of Skeletal Parts. Acta Orthopaedica Scandinavica 43, 301-317.

Brown, C.J., 2007. Arthritis and Allied Conditions, in: Callaghan, J.J., Rosenberg, A.G., Rubash, H. (Eds.), The Adult Hip, 2 ed. Lippincott, Williams & Wilkins, Philadelphia, USA, pp. 572 - 584.

Bruijn, J.D., Seelen, J.L., Feenstra, R.M., Hansen, B.E., Bernoski, F.P., 1995. Failure of the Mecring screw-ring acetabular component in total hip arthroplasty: A three to seven year follow-up study. Journal of Bone and Joint Surgery - Series A 77, 760-766.

Bryan, R., Nair, P.B., Taylor, M., 2012. Influence of femur size and morphology on load transfer in the resurfaced femoral head: A large scale, multi-subject finite element study. J. Biomech. 45, 1952-1958.

Bryan, R., Surya Mohan, P., Hopkins, A., Galloway, F., Taylor, M., Nair, P.B., 2010. Statistical modelling of the whole human femur incorporating geometric and material properties. Medical Engineering and Physics 32, 57-65.

Callaghan, J.J., Kim, Y.S., Pedersen, D.R., Brown, T.D., 1995. Acetabular preparation and insertion of cementless acetabular components. Operative Techniques in Orthopaedics 5, 325-330.

Canadian Joint Replacement Registry, 2015. Hip and Knee Replacements in Canada: Canadian Joint Replacement Registry 2015 Annual Report. Canadian Joint Replacement Registry, Toronta, Canada.

Canale, S.T., Beaty, J.H., 2012. Campbell's Operative Orthopaedics, 12 ed. Elsevier Health Sciences, Philadelphia, PA.

Chan, T.M., 1996. Optimal output-sensitive convex hull algorithms in two and three dimensions. Discrete and Computational Geometry 16, 361-368.

Charnley, J., 1979. Low Friction Arthroplasty of the Hip : Theory and Practice. Springer-Verlag, New York, USA.

Chen, P.Q., Turner, T.M., Ronnigen, H., Galante, J., Urban, R., Rostoker, W., 1983. A canine cementless total hip prosthesis model. Clin. Orthop. Relat. Res. No. 176, 24-33.

Cherian, J.J., Jauregui, J.J., Banerjee, S., Pierce, T., Mont, M.A., 2015. What Host Factors Affect Aseptic Loosening After THA and TKA? Clin. Orthop. Relat. Res. 473, 2700-2709.

Cilingir, A.C., 2010. Finite element analysis of the contact mechanics of ceramic-on-ceramic hip resurfacing prostheses. Journal of Bionic Engineering 7, 244-253.

Clarke, S.G., Phillips, A.T.M., Bull, A.M.J., 2012a. Validation of FE Micromotions and Strains Around a Press-Fit Cup: Introducing a New Micromotion Measuring Technique. Ann. Biomed. Eng. 40, 1586-1596.

Clarke, S.G., Phillips, A.T.M., Bull, A.M.J., 2013. Evaluating a suitable level of model complexity for finite element analysis of the intact acetabulum. Comput. Methods Biomech. Biomed. Eng. 16, 717-724.

Clarke, S.G., Phillips, A.T.M., Bull, A.M.J., Cobb, J.P., 2012b. A hierarchy of computationally derived surgical and patient influences on metal on metal press-fit acetabular cup failure. J. Biomech. 45, 1698-1704.

Clohisy, J.C., Harris, W.H., 1999. The Harris-Galante porous-coated acetabular component with screw fixation. An average ten-year follow-up study. Journal of Bone and Joint Surgery - Series A 81, 66-73.

Cohen, R., 2002. A porous tantalum trabecular metal: basic science. American journal of orthopedics (Belle Mead, N.J.) 31, 216-217.

Constantinou, M., Loureiro, A., Carty, C., Mills, P., Barrett, R., 2017. Hip joint mechanics during walking in individuals with mild-to-moderate hip osteoarthritis. Gait and Posture 53, 162-167.

Cook, S.D., Thomas, K.A., Delton, J.E., Volkman, T.K., Whitecloud, T.S., Key, J.F., 1992. Hydroxylapatite coating of porous implants improves bone ingrowth and interface attachment strength. Journal of Biomedical Materials Research 26, 989-1001.

Cook, S.D., Walsh, K.A., Haddad Jr, R.J., 1985. Interface mechanics and bone growth in porous Co-Cr-Mo alloy implants. Clin. Orthop. Relat. Res. NO. 193, 271-280.

Cornell, C.N., Salvati, E.A., Pellicci, P.M., 1985. Long-term follow-up of total hip replacement in patients with osteonecrosis. Orthopedic Clinics of North America 16, 757-769.

Corten, K., Au, K., Bourne, R.B., 2009. Acetabular options: Notes from the other side. Orthopedics 32, 664.

Cristofolini, L., 2015. Biomechanics: Applications in Orthopedics, in: Doblare, M., Merodio, J. (Eds.), Biomechanics. Eolss Publishers, United Kingdom.

Cristofolini, L., Conti, G., Juszczyk, M., Cremonini, S., Sint Jan, S.V., Viceconti, M., 2010a. Structural behaviour and strain distribution of the long bones of the human lower limbs. J. Biomech. 43, 826-835.

Cristofolini, L., Schileo, E., Juszczyk, M., Taddei, F., Martelli, S., Viceconti, M., 2010b. Mechanical testing of bones: the positive synergy of finite–element models and in vitro experiments. Philosophical Transactions of the Royal Society A: Mathematical, Physical and Engineering Sciences 368, 2725.

Cristofolini, L., Teutonico, A.S., Monti, L., Cappello, A., Toni, A., 2003. Comparative in vitro study on the long term performance of cemented hip stems: Validation of a protocol to discriminate between "good" and "bad" designs. J. Biomech. 36, 1603-1615.

Crosnier, E.A., Keogh, P.S., Miles, A.W., 2014. A novel method to assess primary stability of press-fit acetabular cups. Proceedings of the Institution of Mechanical Engineers, Part H: Journal of Engineering in Medicine 228, 1126-1134.

Culliford, D., Maskell, J., Judge, A., Cooper, C., Prieto-Alhambra, D., Arden, N.K., 2015. Future projections of total hip and knee arthroplasty in the UK: Results from the UK Clinical Practice Research Datalink. Osteoarthritis and Cartilage 23, 594-600.

Curtis, M.J., Jinnah, R.H., Wilson, V.D., Hungerford, D.S., 1992. The initial stability of uncemented acetabular components. Journal of Bone and Joint Surgery - Series B 74, 372-376.

Dalstra, M., Huiskes, R., 1991. The pelvic bone as a sandwich construction; A 3-D finite element study. J. Biomech. 24, 455.

Dalstra, M., Huiskes, R., 1995. Load transfer across the pelvic bone. J. Biomech. 28, 715-724.

Dalstra, M., Huiskes, R., Odgaard, A., van Erning, L., 1993. Mechanical and textural properties of pelvic trabecular bone. J. Biomech. 26, 523-535.

Dalstra, M., Huiskes, R., Van Erning, L., 1995. Development and validation of a three-dimensional finite element model of the pelvic bone. Journal of Biomechanical Engineering 117, 272-278.

Daniel, M., Iglič, A., Kralj-Iglič, V., 2005. The shape of acetabular cartilage optimizes hip contact stress distribution. J. Anat. 207, 85-91.

D'Antonio, J., Capello, W., Manley, M., Bierbaum, B., 2002. New experience with alumina-on-alumina ceramic bearings for total hip arthroplasty. The Journal of Arthroplasty 17, 390-397.

Dar, F.H., Meakin, J.R., Aspden, R.M., 2002. Statistical methods in finite element analysis. J. Biomech. 35, 1155-1161.

Della Valle, C.J., Mesko, N.W., Quigley, L., Rosenberg, A.G., Jacobs, J.J., Galante, J.O., 2009. Primary Total Hip Arthroplasty with a Porous-Coated Acetabular Component. The Journal of Bone & Joint Surgery 91, 1130.

Deville, S., Chevalier, J., Fantozzi, G., Bartolomé, J.F., Requena, J., Moya, J.S., Torrecillas, R., Díaz, L.A., 2003. Low-temperature ageing of zirconia-toughened alumina ceramics and its implication in biomedical implants. Journal of the European Ceramic Society 23, 2975-2982.

Dieppe, P.A., Lohmander, L.S., 2005. Pathogenesis and management of pain in osteoarthritis. Lancet 365, 965-973.

DiGioia III, A.M., Jaramaz, B., Plakseychuk, A.Y., Moody Jr, J.E., Nikou, C., LaBarca, R.S., Levison, T.J., Picard, F., 2002. Comparison of a mechanical acetabular alignment guide with computer placement of the socket. The Journal of Arthroplasty 17, 359-364.

DiGioia, A.M., Jaramaz, B., Blackwell, M., Simon, D.A., Morgan, F., Moody, J.E., Nikou, C., Colgan, B.D., Aston, C.A., Labarca, R.S., Kischell, E., Kanade, T., 1998. Image guided navigation system to measure intraoperatively acetabular implant alignment. Clin. Orthop. Relat. Res., 8-22.

Donaldson, F.E., Nyman Jr, E., Coburn, J.C., 2015. Prediction of contact mechanics in metal-on-metal Total Hip Replacement for parametrically comprehensive designs and loads. J. Biomech. 48, 1828-1835.

Dopico-González, C., New, A.M., Browne, M., 2010. Probabilistic finite element analysis of the uncemented hip replacement-effect of femur characteristics and implant design geometry. J. Biomech. 43, 512-520.

Drake, R., Vogl, A.W., Mitchell, A., 2014. Gray's Anatomy for Students 3rd ed. Churchill Livingstone, Philadelphia, PA.

Electricwala, A.J., Narkbunnam, R., Huddleston, J.I., Maloney, W.J., Goodman, S.B., Amanatullah, D.F., 2016. Obesity is Associated With Early Total Hip Revision for Aseptic Loosening. Journal of Arthroplasty.

Engh, C.A., Bobyn, J.D., Glassman, A.H., 1987. Porous-coated hip replacement. The factors governing bone ingrowth, stress shielding, and clinical results. Journal of Bone and Joint Surgery - Series B 69, 45-55.

Engh, C.A., Griffin, W.L., Marx, C.L., 1990. Cementless acetabular components. Journal of Bone and Joint Surgery - Series B 72, 53-59.

Engh, C.A., Hopper Jr, R.H., Engh Jr, C.A., 2004. Long-term porous-coated cup survivorship using spikes, screws, and press-fitting for initial fixation. Journal of Arthroplasty 19, 54-60.

Engh, C.A., Zettl-Schaffer, K.F., Kukita, Y., Sweet, D., Jasty, M., Bragdon, C., 1993. Histological and radiographic assessment of well functioning porous- coated acetabular components: A human postmortem retrieval study. Journal of Bone and Joint Surgery - Series A 75, 814-824.

Eskinazi, I., Fregly, B.J., 2015. Surrogate modeling of deformable joint contact using artificial neural networks. Med. Eng. Phys. 37, 885-891.

Espehaug, B., Havelin, L.I., Engesæter, L.B., Langeland, N., Vollset, S.E., 1998. Patient satisfaction and function after primary and revision total hip replacement. Clin. Orthop. Relat. Res., 135-148.

Esquenazi, A., Talaty, M., 2011. Gait Analysis: Technology and Clinical Applications, Physical Medicine and Rehabilitation, 4th Edition ed. Elsevier Saunders, Philadelphia, USA.

Fehring, K.A., Owen, J.R., Kurdin, A.A., Wayne, J.S., Jiranek, W.A., 2014. Initial stability of press-fit acetabular components under rotational forces. Journal of Arthroplasty 29, 1038-1042.

Felson, D.T., Lawrence, R.C., Hochberg, M.C., McAlindon, T., Dieppe, P.A., Minor, M.A., Blair, S.N., Berman, B.M., Fries, J.F., Weinberger, M., Lorig, K.R., Jacobs, J.J., Goldberg, V., 2000. Osteoarthritis: New insights. Part 2: Treatment approaches. Annals of Internal Medicine 133, 726-737.

Felson, D.T., Zhang, Y., 1998. An update on the epidemiology of knee and hip osteoarthritis with a view to prevention. Arthritis Rheum. 41, 1343-1355.

Fisher, J., Jin, Z., Tipper, J., Stone, M., Ingham, E., 2006. Tribology of alternative bearings. Clin. Orthop. Relat. Res., 25-34.

Fitzpatrick, C.K., Baldwin, M.A., Rullkoetter, P.J., Laz, P.J., 2011. Combined probabilistic and principal component analysis approach for multivariate sensitivity evaluation and application to implanted patellofemoral mechanics. J. Biomech. 44, 13-21.

Fitzpatrick, C.K., Clary, C.W., Laz, P.J., Rullkoetter, P.J., 2012. Relative contributions of design, alignment, and loading variability in knee replacement mechanics. J. Orth. Res. 30, 2015-2024.

Fitzpatrick, C.K., Hemelaar, P., Taylor, M., 2014. Computationally efficient prediction of bone-implant interface micromotion of a cementless tibial tray during gait. J. Biomech. 47, 1718-1726.

Forrester, A., Sobester, A., Keane, A., 2008. Engineering design via surrogate modelling: a practical guide. John Wiley & Sons.

Fox, G.M., McBeath, A.A., Heiner, J.P., 1994. Hip replacement with a threaded acetabular cup. A follow-up study. Journal of Bone and Joint Surgery - Series A 76, 195-201.

Freeman, M.A.R., McLeod, H.C., Levai, J.P., 1983. Cementless fixation of prosthetic components in total arthroplasty of the knee and hip. Clin. Orthop. Relat. Res. No. 176, 88-94.

Galloway, F., 2012. Large Scale Population Based Finite Element Analysis of Cementless Tibial Tray Fixation. UNiversity of Southampton, Southampton.

Galloway, F., Kahnt, M., Ramm, H., Worsley, P., Zachow, S., Nair, P., Taylor, M., 2013. A large scale finite element study of a cementless osseointegrated tibial tray. J. Biomech. 46, 1900-1906.

Ghosh, R., Pal, B., Ghosh, D., Gupta, S., 2015. Finite element analysis of a hemi-pelvis: the effect of inclusion of cartilage layer on acetabular stresses and strain. Comput. Methods Biomech. Biomed. Eng. 18, 697-710.

Gilbert, J.L., 2007. Metals, in: Callaghan, J.J., Rosenberg, A.G., Rubash, H. (Eds.), The Adult Hip, 2 ed. Lippincott, Williams & Wilkins, Philadelphia, USA, pp. 128 - 143.

Glasserman, P., 2003. Monte Carlo Methods in Financial Engineering. New York, NY : Springer New York : Imprint: Springer.

Goldstein, S.A., 1987. The mechanical properties of trabecular bone: Dependence on anatomic location and function. J. Biomech. 20, 1055-1061.

Gorissen, D., Couckuyt, I., Demeester, P., Dhaene, T., Crombecq, K., 2010. A surrogate modeling and adaptive sampling toolbox for computer based design. The Journal of Machine Learning Research 11, 2051-2055.

Greenwald, A.S., Garino, J.P., 2001. Alternative bearing surfaces: The good, the bad, and the ugly. Journal of Bone and Joint Surgery - Series A 83, 68-72.

Griss, P., Heimke, G., 1981. Five years experience with ceramic-metal-composite hip endoprostheses - I. Clinical evaluation. Archives of Orthopaedic and Traumatic Surgery 98, 157-164.

Grosso, A., Jamali, A.R.M.J.U., Locatelli, M., 2009. Finding maximin latin hypercube designs by Iterated Local Search heuristics. European Journal of Operational Research 197, 541-547.

Gruen, T.A., Poggie, R.A., Lewallen, D.G., Hanssen, A.D., Lewis, R.J., O'Keefe, T.J., Stulberg, S.D., Sutherland, C.J., 2005. Radiographic evaluation of a monoblock acetabular component: A multicenter study with 2- to 5-year results. Journal of Arthroplasty 20, 369-378.

Haddad, F.S., Thakrar, R.R., Hart, A.J., Skinner, J.A., Nargol, A.V.F., Nolan, J.F., Gill, H.S., Murray, D.W., Blom, A.W., Case, C.P., 2011. Metal-on-metal bearings: The evidence so far. Journal of Bone and Joint Surgery - Series B 93 B, 572-579.

Haidukewych, G.J., Jacofsky, D.J., Hanssen, A.D., Lewallen, D.G., 2006. Intraoperative fractures of the acetabulum during primary total hip arthroplasty. Journal of Bone and Joint Surgery - Series A 88, 1952-1956.

Hair, J.F., Black, W.C., Babin, B.J., Anderson, R.E., 2010. Multivariate Data Analysis, 7th Edition ed. Pearson Prentice Hall, Essex, UK.

Halloran, J.P., Erdemir, A., van den Bogert, A.J., 2008. Adaptive Surrogate Modeling for Efficient Coupling of Musculoskeletal Control and Tissue Deformation Models. Journal of Biomechanical Engineering 131, 011014-011014.

Harris, W.H., 2003. Results of Uncemented Cups: A Critical Appraisal at 15 Years. Clin. Orthop. Relat. Res., 121-125.

Havelin, L.I., Espehaug, B., Vollset, S.E., Engesaeter, L.B., 1994. Early failures among 14,009 cemented and 1,326 uncemented prostheses for primary coxarthrosis: the norwegian arthroplasty register, 1987-1992. Acta Orthopaedica 65, 1-6.

Havelin, L.I., Vollset, S.E., Engesæter, L.B., 1995. Revision for aseptic loosening of uncemented cups in 4,352 primary total hip prostheses: A report from the norwegian arthroplasty register. Acta Orthopaedica 66, 494-500.

Haverkamp, D., Klinkenbijl, M.N., Somford, M.P., Albers, G.H.R., Van Der Vis, H.M., 2011. Obesity in total hip arthroplasty: Does it really matter? Acta Orthopaedica 82, 417-422.

Helgason, B., Perilli, E., Schileo, E., Taddei, F., Brynjólfsson, S., Viceconti, M., 2008. Mathematical relationships between bone density and mechanical properties: A literature review. Clin. Biomech. 23, 135-146.

Holzwarth, U., Cotogno, G., 2012. Total hip arthroplasty : State of the Art, Challenges and Prospects EUR - Scientific and Technical Research Reports. European Union.

Hothi, H.S., Busfield, J.J.C., Shelton, J.C., 2011. Explicit finite element modelling of the impaction of metal press-fit acetabular components. Proceedings of the Institution of Mechanical Engineers, Part H: Journal of Engineering in Medicine 225, 303-314.

Howard, J.L., Kremers, H.M., Loechler, Y.A., Schleck, C.D., Harmsen, W.S., Berry, D.J., Cabanela, M.E., Hanssen, A.D., Pagnano, M.W., Trousdale, R.T., Lewallen, D.G., 2011. Comparative survival of uncemented acetabular components following primary total hip arthroplasty. Journal of Bone and Joint Surgery - Series A 93, 1597-1604.

Hsu, J.T., Chang, C.H., Huang, H.L., Zobitz, M.E., Chen, W.P., Lai, K.A., An, K.N., 2007. The number of screws, bone quality, and friction coefficient affect acetabular cup stability. Medical Engineering and Physics 29, 1089-1095.

Huiskes, R., 1993. Failed innovation in total hip replacement: Diagnosis and proposals for a cure. Acta Orthopaedica 64, 699-716.

Huiskes, R., Chao, E.Y.S., 1983. A survey of finite element analysis in orthopedic biomechanics: The first decade. J. Biomech. 16, 385-409.

Huiskes, R., Weinans, H., Grootenboer, H.J., Dalstra, M., Fudala, B., Slooff, T.J., 1987. Adaptive bone-remodeling theory applied to prosthetic-design analysis. J. Biomech. 20, 1135-1150.

Ihle, M., Mai, S., Pfluger, D., Siebert, W., 2008. The results of the titanium-coated RM acetabular component at 20 years: A long-term follow-up of an uncemented primary total hip replacement. Journal of Bone and Joint Surgery - Series B 90, 1284-1290.

Inacio, M.C.S., Ake, C.F., Paxton, E.W., Khatod, M., Wang, C., Gross, T.P., Kaczmarek, R.G., Marinac-Dabic, D., Sedrakyan, A., 2013. Sex and risk of hip implant failure: Assessing total hip arthroplasty outcomes in the United States. JAMA Internal Medicine 173, 435-441.

Incavo, S.J., DiFazio, F.A., Howe, J.G., 1993. Cementless hemispheric acetabular components. 2-4-year results. The Journal of Arthroplasty 8, 573-580.

Ingham, E., Fisher, J., 2005. The role of macrophages in osteolysis of total joint replacement. Biomaterials 26, 1271-1286.

Isaksson, H., van Donkelaar, C.C., Huiskes, R., Yao, J., Ito, K., 2008. Determining the most important cellular characteristics for fracture healing using design of experiments methods. J. Theor. Biol. 255, 26-39.

Isaksson, H., van Donkelaar, C.C., Ito, K., 2009. Sensitivity of tissue differentiation and bone healing predictions to tissue properties. J. Biomech. 42, 555-564.

Jaffe, W.L., Scott, D.F., 1996. Total hip arthroplasty with hydroxyapatite-coated prostheses. Journal of Bone and Joint Surgery - Series A 78, 1918-1934.

Janssen, D., Zwartelé, R.E., Doets, H.C., Verdonschot, N., 2010. Computational assessment of press-fit acetabular implant fixation: The effect of implant design, interference fit, bone quality, and frictional properties. Proceedings of the Institution of Mechanical Engineers, Part H: Journal of Engineering in Medicine 224, 67-75.

Jasty, M., Bragdon, C., Burke, D., O'Connor, D., Lowenstein, J., Harris, W.H., 1997. In vivo skeletal responses to porous-surfaced implants subjected to small induced motions. Journal of Bone and Joint Surgery - Series A 79, 707-714.

Jasty, M., Bragdon, C.R., Schutzer, S., Rubash, H., Haire, T., Harr is, W.H., 1989. Bone ingrowth into porous coated canine total hip replacements. Quantification by backscattered scanning electron microscopy and image analysis. Scanning Microscopy 3, 1051-1057.

Jasty, M., Kienapfel, H., Griss, P., 2007. Fixation by Ingrowth, in: Callaghan, J.J., Rosenberg, A.G., Rubash, H. (Eds.), The Adult Hip, 2 ed. Lippincott, Williams & Wilkins, Philadelphia, USA, pp. 195 - 206.

Jin, Z.M., Meakins, S., Morlock, M.M., Parsons, P., Hardaker, C., Flett, M., Isaac, G., 2006. Deformation of press-fitted metallic resurfacing cups. Part 1: Experimental simulation. Proceedings of the Institution of Mechanical Engineers, Part H: Journal of Engineering in Medicine 220, 299-309.

John, T.K., Ghosh, G., Ranawat, C.S., Ranawat, A.S., Meftah, M., 2015. Performance of Non-Cemented, Hemispherical, Rim-Fit, Hydroxyapatite Coated Acetabular Component. The Journal of Arthroplasty 30, 2233-2236.

Johnston, R.C., Crowninshield, R.D., 1983. Roentgenologic results of total hip arthroplasty. A ten-year follow-up study. Clin. Orthop. Relat. Res. NO. 181, 92-98.

Kadaba, M.P., Ramakrishnan, H.K., Wootten, M.E., 1990. Measurement of lower extremity kinematics during level walking. J. Orth. Res. 8, 383-392.

Kalteis, T.A., Handel, M., Herbst, B., Grifka, J., Renkawitz, T., 2009. In Vitro Investigation of the Influence of Pelvic Tilt on Acetabular Cup Alignment. Journal of Arthroplasty 24, 152-157.

Keating, E.M., Ritter, M.A., Faris, P.M., 1990. Structures at risk from medially placed acetabular screws. Journal of Bone and Joint Surgery - Series A 72, 509-511.

Keaveny, T.M., Morgan, E.F., Niebur, G.L., Yeh, O.C., 2001. Biomechanics of trabecular bone, Annu. Rev. Biomed. Eng., pp. 307-333.

Kelly, N., Cawley, D.T., Shannon, F.J., McGarry, J.P., 2013. An investigation of the inelastic behaviour of trabecular bone during the press-fit implantation of a tibial component in total knee arthroplasty. Medical Engineering and Physics 35, 1599-1606.

Kennedy, J.G., Rogers, W.B., Soffe, K.E., Sullivan, R.J., Griffen, D.G., Sheehan, L.J., 1998. Effect of acetabular component orientation on recurrent dislocation, pelvic osteolysis, polyethylene wear, and component migration. The Journal of Arthroplasty 13, 530-534.

Keyak, J.H., Meagher, J.M., Skinner, H.B., Mote Jr, C.D., 1990. Automated three-dimensional finite element modelling of bone: a new method. Journal of Biomedical Engineering 12, 389-397.

Kienapfel, H., Sprey, C., Wilke, A., Griss, P., 1999. Implant fixation by bone ingrowth. The Journal of Arthroplasty 14, 355-368.

Kim, Y.H., Kim, V.E.M., 1993. Uncemented porous-coated anatomic total hip replacement. Results at six years in a consecutive series. Journal of Bone and Joint Surgery - Series B 75, 6-13.

Kim, Y.S., Brown, T.D., Pedersen, D.R., Callaghan, J.J., 1995. Reamed surface topography and component seating in press-fit cementless acetabular fixation. The Journal of Arthroplasty 10.

Klaassen, M.A., Martínez-Villalobos, M., Pietrzak, W.S., Mangino, G.P., Guzman, D.C., 2009. Midterm Survivorship of a Press-Fit, Plasma-Sprayed, Tri-Spike Acetabular Component. Journal of Arthroplasty 24, 391-399.

Klika, A.K., Murray, T.G., Darwiche, H., Barsoum, W.K., 2007. Options for acetabular fixation surfaces. J. Long Term Effects Med. Implants 17, 187-192.

Knight, S.R., Aujla, R., Biswas, S.P., 2011. Total Hip Arthroplasty - over 100 years of operative history. Orthopedic Reviews 3, e16.

Kroeber, M., Ries, M.D., Suzuki, Y., Renowitzky, G., Ashford, F., Lotz, J., 2002. Impact biomechanics and pelvic deformation during insertion of press-fit acetabular cups. The Journal of Arthroplasty 17, 349-354.

Kroese, D.P., Taimre, T., Botev, Z.I., 2011. Handbook of Monte Carlo Methods. John Wiley and Sons, New York, USA.

Kurtz, S.M., Muratoglu, O.K., Evans, M., Edidin, A.A., 1999. Advances in the processing, sterilization, and crosslinking of ultra-high molecular weight polyethylene for total joint arthroplasty. Biomaterials 20, 1659-1688.

Kwong, L.M., O'Connor, D.O., Sedlacek, R.C., Krushell, R.J., Maloney, W.J., Harris, W.H., 1994. A quantitative in vitro assessment of fit and screw fixation on the stability of a cementless hemispherical acetabular component. The Journal of Arthroplasty 9, 163-170.

Lachiewicz, P.F., Kelley, S.S., 2002. The use of constrained components in total hip arthroplasty. The Journal of the American Academy of Orthopaedic Surgeons 10, 233-238.

Lachiewicz, P.F., Suh, P.B., Gilbert, J.A., 1989. In vitro initial fixation of porous-coated acetabular total hip components. A biomechanical comparative study. Journal of Arthroplasty 4, 201-205.

Langton, D.J., Jameson, S.S., Joyce, T.J., Hallab, N.J., Natu, S., Nargol, A.V.F., 2010. Early failure of metal-on-metal bearings in hip resurfacing and large-diameter total hip replacement: A consequence of excess wear. Journal of Bone and Joint Surgery - Series B 92, 38-46.

Lavy, C.B.D., Msamati, B.C., Igbigbi, P.S., 2003. Racial and gender variations in adult hip morphology. International Orthopaedics 27, 331-333.

Lee, G.-C., Bistolfi, A., 2015. Ceramic-on-ceramic total hip arthroplasty: A new standard. Seminars in Arthroplasty 26, 11-15.

Lee, J.M., Pilliar, R.M., Abdulla, D., Bobyn, J.D., Year In vitro mechanical testing of porous-coated orthopedic implant support in bone after 1 year: Differences between fibrous tissue support and bone ingrowth. In Transactions of the Annual Meeting of the Society for Biomaterials in conjunction with the International Biomaterials Symposium.

Lehman, D.E., Capello, W.N., Feinberg, J.R., 1994. Total hip arthroplasty without cement in obese patients. A minimum two- year clinical and radiographic follow-up study. Journal of Bone and Joint Surgery - Series A 76, 854-862.

Leung, A.S.O., Gordon, L.M., Skrinskas, T., Szwedowski, T., Whyne, C.M., 2009. Effects of bone density alterations on strain patterns in the pelvis: Application of a finite element model.

Proceedings of the Institution of Mechanical Engineers, Part H: Journal of Engineering in Medicine 223, 965-979.

Lewinnek, G.E., Lewis, J.L., Tarr, R., Compere, C.L., Zimmerman, J.R., 1978. Dislocations after total hip-replacement arthroplasties. Journal of Bone and Joint Surgery - Series A 60 A, 217-220.

Lin, Y.-C., Haftka, R.T., Queipo, N.V., Fregly, B.J., 2010. Surrogate articular contact models for computationally efficient multibody dynamic simulations. Med. Eng. Phys. 32, 584-594.

Lord, G., Bancel, P., 1983. The madreporic cementless total hip arthroplasty. New experimental data and a seven-year clinical follow-up study. Clin. Orthop. Relat. Res. No. 176, 67-76.

Lübbeke, A., Stern, R., Garavaglia, G., Zurcher, L., Hoffmeyer, P., 2007. Differences in outcomes of obese women and men undergoing primary total hip arthroplasty. Arthritis and rheumatism 57, 327-334.

Macdonald, W., Carlsson, L.V., Charnley, G.J., Jacobsson, C.M., Johansson, C.B., 1999. Inaccuracy of acetabular reaming under surgical conditions. Journal of Arthroplasty 14, 730-737.

MacKenzie, J.R., Callaghan, J.J., Pedersen, D.R., Brown, T.D., 1994. Areas of contact and extent of gaps with implantation of oversized acetabular components in total hip arthroplasty. Clin. Orthop. Relat. Res., 127-136.

Maher, S.A., Prendergast, P.J., 2002. Discriminating the loosening behaviour of cemented hip prostheses using measurements of migration and inducible displacement. J. Biomech. 35, 257-265.

Majumder, S., Roychowdhury, A., Pal, S., 2007. Simulation of hip fracture in sideways fall using a 3D finite element model of pelvis–femur–soft tissue complex with simplified representation of whole body. Med. Eng. Phys. 29, 1167-1178.

Mäkelä, K.T., Eskelinen, A., Pulkkinen, P., Paavolainen, P., Remes, V., 2008. Total hip arthroplasty for primary osteoarthritis in patients fifty-five years of age or older: An analysis of the Finnish Arthroplasty Registry. Journal of Bone and Joint Surgery - Series A 90, 2160-2170.

Malandrino, A., Planell, J.A., Lacroix, D., 2009. Statistical factorial analysis on the poroelastic material properties sensitivity of the lumbar intervertebral disc under compression, flexion and axial rotation. J. Biomech. 42, 2780-2788.

Malchau, H., Garellick, G., Eisler, T., Kärrholm, J., Herberts, P., 2005. Presidential guest address: The Swedish Hip Registry: Increasing the sensitivity by patient outcome data. Clin. Orthop. Relat. Res., 19-29.

Manley, M.T., Capello, W.N., D'Antonio, J.A., Edidin, A.A., Geesink, R.G.T., 1998. Fixation of acetabular cups without cement in total hip arthroplasty: A comparison of three different implant surfaces at a minimum duration of follow-up of five years. Journal of Bone and Joint Surgery - Series A 80, 1175-1185.

Manley, M.T., Ong, K.L., Kurtz, S.M., 2006. The potential for bone loss in acetabular structures following THA. Clin. Orthop. Relat. Res., 246-253.

Markel, D.C., Hora, N., Grimm, M., 2002. Press-fit stability of uncemented hemispheric acetabular components: A comparison of three porous coating systems. International Orthopaedics 26, 72-75.

Marom, S.A., Linden, M.J., 1990. Computer aided stress analysis of long bones utilizing computed tomography. J. Biomech. 23, 399-404.

Martelli, S., Taddei, F., Cristofolini, L., Gill, H.S., Viceconti, M., 2011. Extensive risk analysis of mechanical failure for an epiphyseal hip prothesis: A combined numerical-experimental

approach. Proceedings of the Institution of Mechanical Engineers, Part H: Journal of Engineering in Medicine 225, 126-140.

Martelli, S., Taddei, F., Schileo, E., Cristofolini, L., Rushton, N., Viceconti, M., 2012. Biomechanical robustness of a new proximal epiphyseal hip replacement to patient variability and surgical uncertainties: A FE study. Medical Engineering and Physics 34, 161-171.

Martini, F., Nath, J.L., Bartholomew, E.F., 2012. Fundamentals of anatomy & physiology. Benjamin Cummings, San Francisco.

Mason, R.L., Gunst, R.F., Hess, J.L., 2003. Statistical design and analysis of experiments: with applications to engineering and science. John Wiley & Sons.

Mathieu, V., Michel, A., Flouzat Lachaniette, C.H., Poignard, A., Hernigou, P., Allain, J., Haïat, G., 2013. Variation of the impact duration during the in vitro insertion of acetabular cup implants. Medical Engineering and Physics 35, 1558-1563.

McKay, M.D., Beckman, R.J., Conover, W.J., 1979. Comparison of three methods for selecting values of input variables in the analysis of output from a computer code. Technometrics 21, 239-245.

McKee, G.K., Watson-Farrar, J., 1966. Replacement of arthritic hips by the McKee-Farrar prosthesis. Journal of Bone and Joint Surgery - Series B 48, 245-259.

McKellop, H., Shen, F.W., Lu, B., Campbell, P., Salovey, R., 1999. Development of an extremely wear-resistant ultra high molecular weight polyethylene for total hip replacements. J. Orth. Res. 17, 157-167.

McLaughlin, J.R., Lee, K.R., 2006. The outcome of total hip replacement in obese and non-obese patients at 10- to 18-years. Journal of Bone and Joint Surgery - Series B 88, 1286-1292.

McMinn, D.J., Snell, K.I., Daniel, J., Treacy, R.B., Pynsent, P.B., Riley, R.D., 2012. Mortality and implant revision rates of hip arthroplasty in patients with osteoarthritis: registry based cohort study. BMJ (Clinical research ed.) 344.

Meneghini, R.M., Daluga, A., Soliman, M., 2011. Mechanical stability of cementless tibial components in normal and osteoporotic bone. The journal of knee surgery 24, 191-196.

Michel, A., Nguyen, V.H., Bosc, R., Vayron, R., Hernigou, P., Naili, S., Haiat, G., 2016. Finite element model of the impaction of a press-fitted acetabular cup. Medical and Biological Engineering and Computing, 1-11.

Morgan, E.F., Keaveny, T.M., 2001. Dependence of yield strain of human trabecular bone on anatomic site. J. Biomech. 34, 569-577.

Morlock, M., Schneider, E., Bluhm, A., Vollmer, M., Bergmann, G., Müller, V., Honl, M., 2001. Duration and frequency of every day activities in total hip patients. J. Biomech. 34, 873-881.

Morrey, B.F., Ilstrup, D., 1989. Size of the femoral head and acetabular revision in total hip-replacement arthroplasty. Journal of Bone and Joint Surgery - Series A 71, 50-55.

Morscher, E., Bereiter, H., Lampert, C., 1989. Cementless press-fit cup. Principles, experimental data, and three-year follow-up study. Clin. Orthop. Relat. Res., 12-20.

Morscher, E., Masar, Z., 1988. Development and first experience with an uncemented press-fit cup. Clin. Orthop. Relat. Res., 96-103.

Morscher, E.W., 1992. Current status of acetabular fixation in primary total hip arthroplasty. Clin. Orthop. Relat. Res., 172-193.

Moskal, J.T., Capps, S.G., Scanelli, J.A., 2013. Improving the accuracy of acetabular component orientation: Avoiding malpositioning: AAOS exhibit selection. Journal of Bone and Joint Surgery - Series A 95.

Mulroy Jr, R.D., Harris, W.H., 1990. The effect of improved cementing techniques on component loosening in total hip replacement. An 11-year radiographic review. Journal of Bone and Joint Surgery - Series B 72, 757-760.

Murray, D.W., 1993. The definition and measurement of acetabular orientation. Journal of Bone and Joint Surgery - Series B 75, 228-232.

Murtha, P.E., Hafez, M.A., Jaramaz, B., DiGioia Iii, A.M., 2008. Variations in acetabular anatomy with reference to total hip replacement. Journal of Bone and Joint Surgery - Series B 90, 308-313.

National Joint Registry for England, Wales, Northern Ireland and Isle of Man, 2015. 12th Annual Report.

Ochsner, P.E., Schweizer, A., 2003. Total Hip Replacement: Implantation Technique and Local Complications. Springer, New York, USA.

OECD, 2015. Health at a Glance 2015: OECD Indicators Paris.

Ong, K.L., Lehman, J., Notz, W.I., Santner, T.J., Bartel, D.L., 2006. Acetabular cup geometry and bone-implant interference have more influence on initial periprosthetic joint space than joint loading and surgical cup insertion. Journal of Biomechanical Engineering 128, 169-175.

Ong, K.L., Santner, T.J., Bartel, D.L., 2008. Robust design for acetabular cup stability accounting for patient and surgical variability. Journal of Biomechanical Engineering 130.

Pakvis, D., Janssen, D., Schreurs, B., Verdonschot, N., 2014. Acetabular Load-Transfer And Mechanical Stability: A Finite Element Analysis Comparing Different Cementless Sockets. J. Mech. Med. Biol. 14.

Pancanti, A., Bernakiewicz, M., Viceconti, M., 2003. The primary stability of a cementless stem varies between subjects as much as between activities. J. Biomech. 36, 777-785.

Pandit, H., Glyn-Jones, S., McLardy-Smith, P., Gundle, R., Whitwell, D., Gibbons, C.L.M., Ostlere, S., Athanasou, N., Gill, H.S., Murray, D.W., 2008. Pseudotumours associated with metal-on-metal hip resurfacings. Journal of Bone and Joint Surgery - Series B 90, 847-851.

Pandy, M.G., Berme, N., 1988. A numerical method for simulating the dynamics of human walking. J. Biomech. 21, 1043-1051.

Pant, S., Limbert, G., Curzen, N.P., Bressloff, N.W., 2011. Multiobjective design optimisation of coronary stents. Biomaterials 32, 7755-7773.

Paul, J.P., 1976. Force Actions Transmitted by Joints in the Human Body. Proceedings of the Royal Society of London. Series B. Biological Sciences 192, 163.

Pedersen, D.R., Crowninshield, R.D., Brand, R.A., Johnston, R.C., 1982. An axisymmetric model of acetabular components in total hip arthroplasty. J. Biomech. 15.

Perillo-Marcone, A., Alonso-Vazquez, A., Taylor, M., 2003. Assessment of the effect of mesh density on the material property discretisation within QCT based FE models: A practical example using the implanted proximal tibia. Comput. Methods Biomech. Biomed. Eng. 6, 17-26.

Perona, P.G., Lawrence, J., Paprosky, W.G., Patwardhan, A.G., Sartori, M., 1992. Acetabular micromotion as a measure of initial implant stability in primary hip arthroplasty: An in vitro comparison of different methods of initial acetabular component fixation. Journal of Arthroplasty 7, 537-547.

Peters, C.L., Miller, M.D., 2007. The Cementless Acetabular Component in: Callaghan, J.J., Rosenberg, A.G., Rubash, H. (Eds.), The Adult Hip, 2 ed. Lippincott, Williams & Wilkins, Philadelphia, USA, pp. 946 - 968.

Phillips, A.T.M., Pankaj, P., Howie, C.R., Usmani, A.S., Simpson, A.H.R.W., 2007. Finite element modelling of the pelvis: Inclusion of muscular and ligamentous boundary conditions. Medical Engineering and Physics 29, 739-748.

Picavet, H.S.J., Hoeymans, N., 2004. Health related quality of life in multiple musculoskeletal diseases: SF-36 and EQ-5D in the DMC3 study. Ann. Rheum. Dis. 63, 723-729.

Pilliar, R.M., Lee, J.M., Maniatopoulos, C., 1986. Observations on the effect of movement on bone ingrowth into porous-surfaced implants. Clin. Orthop. Relat. Res. NO. 208, 108-113.

Powers, C.C., Ho, H., Beykirch, S.E., Huynh, C., Hopper, R.H., Engh, C.A., Engh, C.A., 2010. A comparison of a second- and a third-generation modular cup design. Is new improved? Journal of Arthroplasty 25, 514-521.

Prendergast, P.J., 1997. Finite element models in tissue mechanics and orthopaedic implant design. Clin. Biomech. 12, 343-366.

Pupparo, F., Engh, C.A., 1991. Comparison of porous-threaded and smooth-threaded acetabular components of identical design: Two- to four-year results. Clin. Orthop. Relat. Res., 201-206.

Radcliffe, I.A.J., Prescott, P., Man, H.S., Taylor, M., 2007. Determination of suitable sample sizes for multi-patient based finite element studies. Medical Engineering and Physics 29, 1065-1072.

Rancourt D, Shirazi-Adl A, Drouin G, et al. 1990. Friction properties of the interface between porous-surfaced metals and tibial cancellous bone. Journal of Biomedical Materials Research 24:1503-1519.

Rapperport, D.J., Carter, D.R., Schurman, D.J., 1985. Contact finite element stress analysis of the hip joint. J. Orth. Res. 3, 435-446.

Reilly, D.T., Burstein, A.H., 1974. The mechanical properties of cortical bone. Journal of Bone and Joint Surgery - Series A 56, 1001-1022.

Reina, R.J., Rodriguez, J.A., Rasquinha, V.J., Ranawat, C.S., 2007. Fixation and Osteolysis in Plasma-Sprayed Hemispherical Cups With Hybrid Total Hip Arthroplasty. Journal of Arthroplasty 22, 531-534.

Rho, J.Y., Hobatho, M.C., Ashman, R.B., 1995. Relations of mechanical properties to density and CT numbers in human bone. Medical Engineering and Physics 17, 347-355.

Ries, M.D., Harbaugh, M., 1997. Acetabular strains produced by oversized press fit cups. Clin. Orthop. Relat. Res., 276-281.

Ries, M.D., Harbaugh, M., Shea, J., Lambert, R., 1997. Effect of cementless acetabular cup geometry on strain distribution and press-fit stability. Journal of Arthroplasty 12, 207-212.

Riggs, B.L., Melton Iii, L.J., Robb, R.A., Camp, J.J., Atkinson, E.J., Peterson, J.M., Rouleau, P.A., McCollough, C.H., Bouxsein, M.L., Khosla, S., 2004. Population-based study of age and sex differences in bone volumetric density, size, geometry, and structure at different skeletal sites. J. Bone Miner. Res. 19, 1945-1954.

Ring, P.A., 1983. Ring UPM total hip arthroplasty. Clin. Orthop. Relat. Res. No. 176, 115-123.

Röder, C., Bach, B., Berry, D.J., Eggli, S., Langenhahn, R., Busato, A., 2010. Obesity, age, sex, diagnosis, and fixation mode differently affect early cup failure in total hip arthroplasty: A matched case-control study of 4420 patients. Journal of Bone and Joint Surgery - Series A 92, 1954-1963.

Röder, C., Eggli, S., Münger, P., Melloh, M., Busato, A., 2008. Patient characteristics differently affect early cup and stem loosening in THA: A case-control study on 7,535 patients. International Orthopaedics 32, 33-38.

Roth, A., Winzer, T., Sander, K., Anders, J.O., Venbrocks, R.A., 2006. Press fit fixation of cementless cups: How much stability do we need indeed? Archives of Orthopaedic and Trauma Surgery 126, 77-81.

Saikko, V.O., Paavolainen, P.O., Slätis, P., 1993. Wear of the polyethylene acetabular cup: Metallic and ceramic heads compared in a hip simulator. Acta Orthopaedica 64, 391-402.

Sakellariou, V.I., Sculco, T., 2013. Acetabular options: Notes from the other side. Seminars in Arthroplasty 24, 76-82.

Salvati, E.A., Wilson Jr, P.D., Jolley, M.N., Vakili, F., Aglietti, P., Brown, G.C., 1981. A ten-year follow-up study of our first one hundred consecutive Charnley total hip replacements. Journal of Bone and Joint Surgery - Series A 63, 753-767.

Sandborn, P.M., Cook, S.D., Spires, W.P., Kester, M.A., 1988. Tissue response to porous-coated implants lacking initial bone apposition. Journal of Arthroplasty 3, 337-346.

Santaguida, P.L., Hawker, G.A., Hudak, P.L., Glazier, R., Mahomed, N.N., Kreder, H.J., Coyte, P.C., Wright, J.G., 2008. Patient characteristics affecting the prognosis of total hip and knee joint arthroplasty: A systematic review. Can. J. Surg. 51, 428-436.

Schmalzried, T.P., 2009. The Importance of Proper Acetabular Component Positioning and the Challenges to Achieving It. Operative Techniques in Orthopaedics 19, 132-136.

Schmalzried, T.P., Jasty, M., Harris, W.H., 1992a. Periprosthetic bone loss in total hip arthroplasty. Polyethylene wear debris and the concept of the effective joint space. Journal of Bone and Joint Surgery - Series A 74, 849-863.

Schmalzried, T.P., Kwong, L.M., Jasty, M., Sedlacek, R.C., Haire, T.C., O'Connor, D.O., Bragdon, C.R., Kabo, J.M., Malcolm, A.J., Harris, W.H., 1992b. The mechanism of loosening of cemented acetabular components in total hip arthroplasty: Analysis of specimens retrieved at autopsy. Clin. Orthop. Relat. Res., 60-78.

Schmalzried, T.P., Szuszczewicz, E.S., Northfield, M.R., Akizuki, K.H., Frankel, R.E., Belcher, G., Amstutz, H.C., 1998. Quantitative assessment of walking activity after total hip or knee replacement. Journal of Bone and Joint Surgery - Series A 80, 54-59.

Schmalzried, T.P., Wessinger, S.J., Hill, G.E., Harris, W.H., 1994. The Harris-Galante porous acetabular component press-fit without screw fixation. Five-year radiographic analysis of primary cases. The Journal of Arthroplasty 9, 235-242.

Schurman, D.J., Bloch, D.A., Segal, M.R., Tanner, C.M., 1989. Conventional cemented total hip arthroplasty: Assessment of clinical factors associated with revision for mechanical failure. Clin. Orthop. Relat. Res., 173-180.

Schwartz Jr, J.T., Engh, C.A., Forte, M.R., Kukita, Y., Grandia, S.K., 1993. Evaluation of initial surface apposition in porous-coated acetabular components. Clin. Orthop. Relat. Res., 174-187.

Schwartz, J.H., 2006. Skeleton Keys: An Introduction to Human Skeletal Morphology, Development, and Analysis, 2nd ed. Oxford University Press, New York, NY.

Seagrave, K.G., Troelsen, A., Malchau, H., Husted, H., Gromov, K., 2017. Acetabular cup position and risk of dislocation in primary total hip arthroplasty: A systematic review of the literature. Acta Orthopaedica 88, 10-17.

Shirazi-Adl A, Dammak M, Paiement G. 1993. Experimental determination of friction characteristics at the trabecular bone/porous-coated metal interface in cementless implants. Journal of Biomedical Materials Research 27:167-175.

Smith, A.J., Dieppe, P., Howard, P.W., Blom, A.W., 2012. Failure rates of metal-on-metal hip resurfacings: analysis of data from the National Joint Registry for England and Wales. The Lancet 380, 1759-1766.

Soballe, K., Hansen, E.S., Brockstedt-Rasmussen, H., Bunger, C., 1993. Hydroxyapatite coating converts fibrous tissue to bone around loaded implants. Journal of Bone and Joint Surgery - Series B 75, 270-278.

Spears, I.R., Morlock, M.M., Pfleiderer, M., Schneider, E., Hille, E., 1999. The influence of friction and interference on the seating of a hemispherical press-fit cup: A finite element investigation. J. Biomech. 32, 1183-1189.

Spears, I.R., Pfleiderer, M., Schneider, E., Hille, E., Bergmann, G., Morlock, M.M., 2000. Interfacial conditions between a press-fit acetabular cup and bone during daily activities: implications for achieving bone in-growth (how to measure micromotion). J. Biomech. 33, 1471-1477.

Spears, I.R., Pfleiderer, M., Schneider, E., Hille, E., Morlock, M., 2001. The effect of interfacial parameters on cup-bone relative micromotions: A finite element investigation. J. Biomech. 34, 113-120.

Stauffer, R.N., 1982. Ten-year follow-up study of total hip replacement. Journal of Bone and Joint Surgery - Series A 64, 983-990.

Stickles, B., Phillips, L., Brox, W.T., Owens, B., Lanzer, W.L., 2001. Defining the relationship between obesity and total joint arthroplasty. Obesity Res. 9, 219-223.

Stiehl, J.B., MacMillan, E., Skrade, D.A., 1991. Mechanical stability of porous-coated acetabular components in total hip arthroplasty. Journal of Arthroplasty 6, 295-300.

Sumner, D.R., Jasty, M., Jacobs, J.J., Urban, R.M., Bragdon, C.R., Harris, W.H., Galante, J.O., 1993. Histology of porous-coated acetabular components: 25 cementless cups retrieved after arthroplasty. Acta Orthopaedica 64, 619-626.

Sun, L., Berndt, C.C., Gross, K.A., Kucuk, A., 2001. Material fundamentals and clinical performance of plasma-sprayed hydroxyapatite coatings: A review. Journal of Biomedical Materials Research 58, 570-592.

Surin, V.V., Sundholm, K., 1983. Survival of patients and prostheses after total hip arthroplasty. Clin. Orthop. Relat. Res. No. 177, 148-153.

Sutherland, C.J., Wilde, A.H., Borden, L.S., Marks, K.E., 1982. A ten-year follow-up of one hundred consecutive Muller curved-stem total hip-replacement arthroplasties. Journal of Bone and Joint Surgery - Series A 64, 970-982.

Swarts, E., Bucher, T.A., Phillips, M., Yap, F.H.X., 2015. Does the ingrowth surface make a difference? A retrieval study of 423 cementless acetabular components. Journal of Arthroplasty 30, 706-712.

Szmukler-Moncler, S., Salama, H., Reingewirtz, Y., Dubruille, J., 1998. Timing of loading and effect of micromotion on bone-dental implant interface: review of experimental literature. Journal of biomedical materials research 43, 192-203.

Taddei, F., Martelli, S., Reggiani, B., Cristofolini, L., Viceconti, M., 2006. Finite-element modeling of bones from CT data: Sensitivity to geometry and material uncertainties. Biomedical Engineering, IEEE Transactions on 53, 2194-2200.

Taylor, M., Bryan, R., Galloway, F., 2013. Accounting for patient variability in finite element analysis of the intact and implanted hip and knee: A review. International Journal for Numerical Methods in Biomedical Engineering 29, 273-292.

Taylor, M., Prendergast, P.J., 2015. Four decades of finite element analysis of orthopaedic devices: Where are we now and what are the opportunities? J. Biomech. 48, 767-778.

Thompson, M.S., Northmore-Ball, M.D., Tanner, K.E., 2002. Effects of acetabular resurfacing component material and fixation on the strain distribution in the pelvis. Proceedings of the Institution of Mechanical Engineers, Part H: Journal of Engineering in Medicine 216, 237-245.

Traina, F., De Fine, M., Di Martino, A., Faldini, C., 2013. Fracture of ceramic bearing surfaces following total hip replacement: A systematic review. BioMed Research International 2013.

Udofia, I.J., Liu, F., Jin, Z., Roberts, P., Grigoris, P., 2007. The initial stability and contact mechanics of a press-fit resurfacing arthroplasty of the hip. Journal of Bone and Joint Surgery - Series B 89, 549-556.

Udomkiat, P., Dorr, L.D., Wan, Z., 2002. Cementless Hemispheric Porous-Coated Sockets Implanted with Press-Fit Technique without Screws: Average Ten-Year Follow-up. The Journal of Bone & Joint Surgery 84, 1195.

Vasu, R., Carter, D.R., Harris, W.H., 1982. Stress distributions in the acetabular region-I. Before and after total joint replacement. J. Biomech. 15, 155-157.

Verdonschot, N., Huiskes, R., 1997. The effects of cement-stem debonding in THA on the long-term failure probability of cement. J. Biomech. 30, 795-802.

Viceconti, M., Affatato, S., Baleani, M., Bordini, B., Cristofolini, L., Taddei, F., 2009. Pre-clinical validation of joint prostheses: A systematic approach. Journal of the Mechanical Behavior of Biomedical Materials 2, 120-127.

Viceconti, M., Brusi, G., Pancanti, A., Cristofolini, L., 2006. Primary stability of an anatomical cementless hip stem: A statistical analysis. J. Biomech. 39, 1169-1179.

Viceconti, M., Olsen, S., Nolte, L.P., Burton, K., 2005. Extracting clinically relevant data from finite element simulations. Clin. Biomech. 20, 451-454.

Wasielewski, R.C., Jacobs, J.J., Arthurs, B., Rubash, H.E., 2005. The acetabular insert-metal backing interface: An additional source of polyethylene wear debris. Journal of Arthroplasty 20, 914-922.

Williams, P.L., Warwick, R., 1973. Gray's Anatomy, 35th Edition ed. Churchill Livingstone, London, Uk.

Wilson-MacDonald, J., Morscher, E., Masar, Z., 1990. Cementless uncoated polyethylene acetabular components in total hip replacement. Review of five- to 10-year results. Journal of Bone and Joint Surgery - Series B 72, 423-430.

Won, C.H., Hearn, T.C., Tile, M., 1995. Micromotion of cementless hemispherical acetabular components. Journal of Bone and Joint Surgery - Series B 77, 484-489.

Wright, J.M., Pellicci, P.M., Salvati, E.A., Ghelman, B., Roberts, M.M., Koh, J.L., 2001. Bone density adjacent to press-fit acetabular components: A prospective analysis with quantitative computed tomography. Journal of Bone and Joint Surgery - Series A 83, 529-536.

Wright, J.M., Pellicci, P.M., Salvati, E.A., Ghelman, B., Roberts, M.M., Koh, J.L., 2001. Bone density adjacent to press-fit acetabular components: A prospective analysis with quantitative computed tomography. Journal of Bone and Joint Surgery - Series A 83, 529-536.

Wroblewski, B.M., Siney, P.D., Fleming, P.A., 2016. Charnley Low-Frictional Torque Arthroplasty of the Hip: Practice and Results. Springer, Switzerland.

Yao, J., Funkenbusch, P.D., Snibbe, J., Maloney, M., Lerner, A.L., 2005. Sensitivities of Medial Meniscal Motion and Deformation to Material Properties of Articular Cartilage, Meniscus and Meniscal Attachments Using Design of Experiments Methods. Journal of Biomechanical Engineering 128, 399-408.

Yew, A., Jin, Z.M., Donn, A., Morlock, M.M., Isaac, G., 2006. Deformation of press-fitted metallic resurfacing cups. Part 2: Finite element simulation. Proceedings of the Institution of Mechanical Engineers, Part H: Journal of Engineering in Medicine 220, 311-319.

Young, N.L., Cheah, D., Waddell, J.P., Wright, J.G., 1998. Patient characteristics that affect the outcome of total hip arthroplasty: A review. Can. J. Surg. 41, 188.

Young, P.G., Beresford-West, T.B.H., Coward, S.R.L., Notarberardino, B., Walker, B., Abdul-Aziz, A., 2008. An efficient approach to converting three-dimensional image data into highly accurate computational models. Philosophical Transactions of the Royal Society A: Mathematical, Physical and Engineering Sciences 366, 3155-3173.

Young, P.G., Beresford-West, T.B.H., Coward, S.R.L., Notarberardino, B., Walker, B., Abdul-Aziz, A., 2008. An efficient approach to converting three-dimensional image data into highly accurate computational models. Philosophical Transactions of the Royal Society A: Mathematical, Physical and Engineering Sciences 366, 3155-3173.

Zhang, J., 2013. Development of an Automated System for Building a Large Population-based Statistical Model of Femur Morphology. The University of Auckland.

Zhang, Q.H., Wang, J.Y., Lupton, C., Heaton-Adegbile, P., Guo, Z.X., Liu, Q., Tong, J., 2010. A subject-specific pelvic bone model and its application to cemented acetabular replacements. J. Biomech. 43, 2722-2727.

Zou, Z., Chávez Arreola, A., Mandal, P., Board, T., Alonso Rasgado, T., 2013. Optimization of the position of the acetabulum in a ganz periacetabular osteotomy by finite element analysis. J. Orth. Res. 31, 472-479.